



# **On surface electropolishing for the development of metallic stents**

**Mémoire**

**Jad Mousselli**

**Maîtrise en génie des matériaux et de la métallurgie - avec mémoire**  
Maître ès sciences (M. Sc.)

Québec, Canada

# **On surface electropolishing for the development of metallic stents.**

**Mémoire**

**Jad Mousselli**

Sous la direction de :

Diego Mantovani, directeur de recherche.

## Résumé

Les maladies cardiovasculaires sont responsables d'environ le tiers de tous les cas de décès au Canada. L'une des solutions utilisées pour résoudre ce problème consiste à utiliser un dispositif métallique constitué d'un maillage ayant une forme d'un filet et appelé stent.

Les stents sont de petits dispositifs implantés dans des vaisseaux sanguins rétrécis pour rétablir la circulation sanguine et éviter une crise cardiaque ou un accident vasculaire cérébral et pour traiter les anévrismes du cerveau. Un contrôle précis de la surface de ces stents est nécessaire pour assurer la compatibilité de l'alliage choisi avec le milieu biologique dont il va être en contact avec.

Les stents métalliques doivent satisfaire à des conditions précises définies en fonction de leur application finale. Ils doivent respecter des exigences strictes en termes de propriétés mécaniques, d'interaction électrochimique (corrosion) et de cytocompatibilité. Les alliages suivants sont traditionnellement utilisés dans les applications biomédicales et plus précisément pour les applications cardiovasculaires: l'alliage AISI316L est considéré comme une référence dans ce domaine, mais l'alliage L605, un alliage à base de Cobalt, prend de plus en plus d'importance grâce à ses propriétés mécaniques élevées (haute ductilité et haute résistance à la traction) et résistance élevée à la corrosion. L'utilisation d'alliages de titane est la nouvelle frontière pour les biomatériaux dans les applications cardiovasculaires, il est considéré comme un nouveau candidat potentiel pour les stents cardiovasculaires. Les alliages de titane présentent une combinaison unique de haute résistance et de grande ductilité (résistance à la traction et déformation uniforme supérieures à 1000 MPa et 30% respectivement).

L'électropolissage est une étape de prétraitement appliquée à ces alliages métalliques pour obtenir des surfaces chimiquement homogènes, recouvertes d'une couche d'oxyde uniforme et amorphe, généralement de rugosité très lisse. Ce processus permet non seulement de contrôler les propriétés physiques de la surface, mais également celles chimiques. Le processus d'électropolissage comporte certaines variables, telles que le courant, la tension, la solution électrolytique et la température de l'électrolyte. En les contrôlant, il est possible de

comprendre et d'améliorer les propriétés de la surface. Le but de ce projet est d'étudier les effets des différents variables d'électropolissage (courant, tension, solution électrolytique) sur les caractéristiques / propriétés de surface (morphologie, composition chimique et mouillabilité) des alliages utilisés pour la fabrication de stents.

## **Abstract**

Cardiovascular diseases (CVD) are responsible for about one-third of all death cases in Canada. One of the solutions used to solve this problem is using a metallic device made of a mesh and called a stent. Stents are small devices that are implanted in narrowed blood vessels to restore blood flow and to avoid a heart attack or stroke and to treat brain aneurysms. An accurate surface control is needed to assure the cytocompatibility of the chosen alloy with its biologic environment.

Metallic stents must satisfy precise conditions defined according to their final application. They need to respect strict requirements, in terms of mechanical properties, electrochemical interaction (corrosion) and cytocompatibility. The following alloys are traditionally used in biomedical applications and more precisely for cardiovascular applications: the alloy AISI316L is considered a reference in this field, but the alloy L605, a Co-based material, is gaining more and more importance, due to its high mechanical properties (high ductility and high ultimate tensile strength) and high corrosion resistance. The use of Titanium alloys is the new frontier for biomaterials in cardiovascular applications, it is considered as a new potential candidate for cardiovascular stents. Titanium alloys, shows a unique combination of high strength and high ductility (ultimate tensile strength and uniform deformation higher than 1000 MPa and 30%, respectively).

Electropolishing is a pre-treatment step applied to these alloys to obtain chemically homogeneous surfaces, covered with a uniform and amorphous oxide layer, generally with a very smooth roughness. This process not only makes it possible to control the physical properties of the surface, but also the chemical ones. The electropolishing process has some changeable variables, such as current, voltage, electrolytic solution and temperature of electrolyte. By controlling them, it is possible to understand and improve the surface properties.

This work is aimed at studying the effects of electropolishing changeable variables (current, voltage, electrolytic solution) on surface characteristics/properties (morphology, chemical composition and wettability) of those alloys used for the manufacture of stents.

## Table of Content:

|  |            |
|--|------------|
| <b>Résumé</b>  | <b>III</b> |
| <b>Abstract</b>  | <b>V</b>   |
| <b>Table of Content:</b>   | <b>VI</b>  |
| <b>List of Figures:</b>  | <b>IX</b>  |
| <b>List of Tables:</b>   | <b>X</b>   |
| <b>Acknowledgment</b>  | <b>XII</b> |
| <b>Introduction</b>  | <b>XIV</b> |
| <b>Chapter 1 From cardiovascular diseases to the clinical aspect of stenting</b> | <b>1</b>   |
| 1.1 The cardiovascular system  | 1          |
| 1.1.1 Description of the cardiovascular system                                   | 1          |
| 1.1.2 Vessel structure.  | 2          |
| 1.2 Occlusions in blood vessels  | 3          |
| 1.3 Cardiovascular diseases and associated treatments                            | 5          |
| 1.4 Cardiovascular disease treatment techniques                                  | 9          |
| 1.4.1 Pharmaceutical treatment   | 10         |
| 1.4.2 Angioplasty  | 10         |
| 1.4.3 Stenting   | 12         |
| 1.4.4 Coronary artery bypass grafting (CABG)                                     | 14         |
| 1.5 Framework of this research   | 14         |
| <b>Chapter 2 Engineering concept of stenting</b>                                 | <b>17</b>  |
| 2.1 Cardiovascular stents  | 17         |
| 2.2 Requirements for coronary stents   | 19         |
| 2.3 Stent surface treatment and surface modification                             | 24         |
| 2.3.1 Mechanical methods   | 25         |
| 2.3.2 Chemical methods   | 26         |
| 2.3.3 Physical methods   | 27         |
| 2.4 Biodegradable materials for stents   | 28         |
| 2.4.1 Iron and iron alloys   | 31         |
| 2.4.2 Magnesium and magnesium alloys   | 31         |
| 2.4.3 Zinc and zinc alloys   | 32         |

|  |   |           |
|--|---|-----------|
| 2.5  | Non-degradable alloys used for stent applications _____                   | 34        |
| 2.5.1  | Introduction _____  | 34        |
| 2.5.2  | AISI 316L stainless steel _____   | 34        |
| 2.5.3  | Co-Cr alloys _____  | 38        |
| 2.5.4  | Nitinol alloys _____  | 38        |
| 2.5.5  | Tantalum alloys _____   | 39        |
| 2.6  | Cobalt-based alloys _____   | 40        |
| 2.6.1  | Cobalt alloy metallurgy _____   | 40        |
| 2.7  | Titanium and its alloys _____   | 47        |
| 2.7.1  | Pure Titanium _____   | 47        |
| 2.7.2  | The use of Titanium in the biomedical fields _____                        | 48        |
| <b>Chapter 3 Electropolishing _____</b>      |   | <b>50</b> |
| 3.1  | Historical review about electropolishing _____                            | 50        |
| 3.2  | Fundamental of the electropolishing process _____                         | 51        |
| 3.2.1  | The salt films _____  | 54        |
| 3.2.2  | Nernst diffusion layer _____  | 54        |
| 3.3  | Polarization curves _____   | 56        |
| 3.4  | Mechanism of electropolishing _____                                       | 57        |
| 3.5  | Reactions occurring during electropolishing of Co-Cr _____                | 58        |
| 3.6  | Reactions occurring during electropolishing of Titanium _____             | 60        |
| 3.7  | Surface phenomena occurring during electropolishing _____                 | 62        |
| 3.8  | Pitting during electropolishing _____                                     | 63        |
| <b>Chapter 4 Materials and methods _____</b> |   | <b>65</b> |
| 4.1  | Materials _____   | 65        |
| 4.1.1  | L605 _____  | 65        |
| 4.1.2  | Pure Titanium _____   | 65        |
| 4.2  | Methods _____   | 65        |
| 4.2.1  | Cleaning of L605 and pure Ti samples (pre-electropolishing cleaning) ____ | 65        |
| 4.2.2  | Electropolishing processes _____  | 66        |
| 4.3  | Characterization _____  | 72        |
| 4.3.1  | Optical microscopy (OM) _____   | 72        |
| 4.3.2  | Scanning Electron Microscopy (SEM) _____                                  | 73        |

|  |   |            |
|--|---|------------|
| 4.3.3  | Atomic Forces Microscopy (AFM)  | 74         |
| 4.3.4  | Contact angle   | 75         |
| 4.3.5  | X-ray photoelectron spectroscopy (XPS)  | 76         |
| <b>Chapter 5 Electropolishing of L605: Results and discussion</b>          |   | <b>78</b>  |
| 5.1  | Effect of different amounts of acid addition  | 83         |
| 5.1.1  | Effect of hydrochloric acid   | 83         |
| 5.1.2  | Effect of perchloric acid   | 89         |
| 5.1.3  | Effect of hydrofluoric acid   | 94         |
| 5.2  | Roughness analysis by AFM   | 99         |
| 5.3  | Contact angle   | 104        |
| 5.4  | Mechanical polishing versus electropolishing  | 108        |
| 5.5  | Conclusions   | 111        |
| <b>Chapter 6 Electropolishing of pure Titanium: Results and discussion</b> |   | <b>112</b> |
| 6.1  | Introduction  | 112        |
| 6.2  | Preliminary investigations on the effect of the chemical composition of 5 different solutions                       | 115        |
| 6.3  | The effect on Ti of several electrolytes composed by CH <sub>3</sub> COOH, H <sub>2</sub> SO <sub>4</sub> , and HF. | 117        |
| 6.4  | Roughness analysis by AFM.  | 124        |
| 6.5  | Surface wettability.  | 126        |
| 6.6  | Chemical composition of the surface by XPS.   | 128        |
| 6.7  | Conclusions   | 129        |
| <b>General conclusions</b>   |   | <b>130</b> |
| <b>Bibliography:</b>   |   | <b>132</b> |



## List of Figures:

|   |     |
|---|-----|
| Figure 0.1 Distribution of major causes of death [1].   | XV  |
| Figure 1.1 Artery, vein and capillary structure [6].  | 3   |
| Figure 1.2 Main cardiovascular diseases sites [12].   | 6   |
| Figure 1.3 The proportion of global deaths from various cardiovascular diseases in 2002 [13].   | 7   |
| Figure 1.4 Schematic formation of arteriosclerotic and thrombotic vessels [14].   | 9   |
| Figure 1.5 Schematic of balloon coronary angioplasty [15].  | 11  |
| Figure 1.6 Schematic of stenting coronary angioplasty [20].   | 13  |
| Figure 2.1 Description of the procedure for the fabrication of a stent.   | 28  |
| Figure 3.1 Electropolishing systems [67].   | 53  |
| Figure 3.2 Nernst diffusion layer [73].   | 55  |
| Figure 3.3 Schematic of the polarization curve during electropolishing [70].  | 56  |
| Figure 3.4 Oxide growth on the titanium surface [77].   | 61  |
| Figure 4.1 Ultrasonic bath [85].  | 66  |
| Figure 4.2.C Shows the anode (positive potential in red) and cathode (negative potential in black).   | 67  |
| Figure 4.3 Olympus BX41M optical microscopy.  | 73  |
| Figure 4.4 Scanning Electron Microscopy.  | 74  |
| Figure 4.5 Atomic Forces Microscopy.  | 75  |
| Figure 4.6 Water contact angle.   | 76  |
| Figure 4.7 X-ray photoelectron spectroscopy.  | 77  |
| Figure 5.1 BSE images of Co-28Cr-9W-1Si-C alloys: (a) 0.03C and (b) 0.06C alloys and its phase diagram calculated using Thermocalc software.                      | 81  |
| Figure 5.2 EDS of As-received sample (b) chemical spectrum of alloy and (c) precipitated.   | 81  |
| Figure 5.3 EDS analysis of the after electropolishing sample using 3% of HCl.   | 88  |
| Figure 5.4 EDS analysis of the after electropolishing sample with 3% HClO <sub>4</sub> .  | 93  |
| Figure 5.5 Schematical comparison of surface vision between the as-received sample and the electropolished one.   | 97  |
| Figure 5.6 EDS analysis comparison between the as received and after Electropolishing with 3% HF using a film of Au and Pd as conductive coating over the sample. | 98  |
| Figure 5.7 The average of contact angle before and after electropolishing of L605 samples.  | 105 |
| Figure 5.8 XPS surveys describing the effect of different HF amounts on the surface chemical composition.   | 105 |
| Figure 5.9 XPS surveys describing the effect of different glycerol amounts on the surface chemical composition.   | 107 |
| Figure 5.10 XPS analysis and comparison between the mechanical polishing and the electropolishing from chemical point view.                                       | 110 |
| Figure 6.1 roughness analysis for as-received and electropolished pure Ti samples.  | 126 |
| Figure 6.2 Average contact angle for as received and electropolished Ti.  | 128 |
| Figure 6.3 Chemical composition of the surface before and after electropolishing.   | 128 |

## List of Tables:

|  |    |
|--|----|
| <i>Table 1.1 Comparison of risk factors and final outcome for arteriosclerosis and atherosclerosis [8].</i>  | 4  |
| <i>Table 1.2 Main risk factors for cardiovascular diseases [13].</i>   | 8  |
| <i>Table 1.3 Predictions of global cardiovascular disease deaths in the early twenty-first century [13].</i>   | 8  |
| <i>Table 2.1 Comparison of different properties of metals used for stents [27].</i>  | 18 |
| <i>Table 2.2 Mechanical properties of different alloys used for the fabrication of stents [28].</i>  | 19 |
| <i>Table 2.3 Ideal characteristics for coronary stent materials applications [28].</i>   | 20 |
| <i>Table 2.4 Comparison between different kinds of metallic stents used for the cardiovascular application.</i>  | 22 |
| <i>Table 2.5 Comparison of different bar metal stents [28].</i>  | 23 |
| <i>Table 2.6 Overview of mechanical methods used for surface modification of metals [37].</i>  | 26 |
| <i>Table 2.7 Overview of chemical methods used for surface modification of metals [37].</i>  | 27 |
| <i>Table 2.8 Overview of physical methods used for surface modification of metals [37].</i>  | 28 |
| <i>Table 2.9 Comparative properties of implanted degradable metals with SS316L [40].</i>   | 30 |
| <i>Table 2.10 Mechanical properties of some biomedical zinc alloys [46].</i>   | 33 |
| <i>Table 2.11 Implants classification and type of metals used [30].</i>  | 34 |
| <i>Table 2.12 General classification stainless steels structure [47].</i>  | 36 |
| <i>Table 2.14 Example of metals used for implants and their mechanical properties [47][31].</i>  | 37 |
| <i>Table 2.15 Mechanical properties of Ni-Ti alloys [45].</i>  | 39 |
| <i>Table 2.16 Mechanical properties for unalloyed tantalum [45].</i>   | 40 |
| <i>Table 2.17 Intermetallic compounds in cobalt-base superalloys [53].</i>   | 42 |
| <i>Table 2.18 Phases present in Haynes alloy 25 [53].</i>  | 42 |
| <i>Table 2.19 The effects of alloying elements on Cobalt base alloys [45].</i>   | 44 |
| <i>Table 2.20 International standards and chemical composition for metallic Co-base alloys used for medical application [54].</i>                                    | 45 |
| <i>Table 2.21 Physical and mechanical properties comparison between annealed Co-Cr alloys and 316L stent tubing [57].</i>  | 46 |
| <i>Table 2.22 Comparison of mechanical properties of biomedical titanium alloys[58].</i>   | 48 |
| <i>Table 4.1 Chemical analysis of Co-Cr alloy L605 from ``Rolled Alloy Canada`` [83].</i>  | 65 |
| <i>Table 4.2 Chemical analysis of pure Titanium alloy from ``Rolled Alloy Canada`` [84].</i>   | 65 |
| <i>Table 4.3 Electropolishing system [86].</i>   | 67 |
| <i>Table 4.4 The different amounts of HF and glycerol in the main electropolishing solutions. The given percentages are in volume.</i>                               | 68 |
| <i>Table 4.5 The different amounts of HCL and HCLO4 on the main electropolishing solutions. The given percentages are in volume.</i>                                 | 69 |
| <i>Table 4.6 The different solution used for electropolishing of L605 [87]. The given percentages are in volume.</i>   | 69 |
| <i>Table 4.7 The different solutions were tested on pure Ti samples.</i>   | 71 |
| <i>Table 4.8 The different concentration used from solution number 2 which as tested in Table 4.7. .</i>   | 72 |
| <i>Table 5.1 Optical microscopy images (a-c) as received sample, (d-f) represent respectively samples after electropolishing using the main based solution.</i>      | 78 |
| <i>Table 5.2 Electron secondary images S by SEM of (a-d) as received and (e-h) Electropolished samples using the main based solution at different magnification.</i> | 80 |

|  |     |
|--|-----|
| <i>Table 5.3 Optical microscopy using different addition of hydrochloric acid (a-c) with 1%, (d-f) with 3%, (g-i) with 5%, (j-l) with 10%.</i> | 85  |
| <i>Table 5.4 ES by SEM using different addition of hydrochloric acid (a-c) with 1%, (d-f) with 3%, (g-i) with 5%, (j-l) with 10%.</i>          | 87  |
| <i>Table 5.5 Optical microscopy using different addition of perchloric acid (a-c) with 1%, (d-f) with 3%, (g-i) with 5%, (j-l) with 10%.</i>   | 91  |
| <i>Table 5.6 SEM micrographs using different addition of perchloric acid (a-c) with 1%, (d-f) with 3%, (g-i) with 5%, (j-l) with 10%.</i>      | 92  |
| <i>Table 5.7 Optical microscopy using different addition of hydrofluoric acid (a-c) with 1%, (d-f) with 3%, (g-i) with 5%, (j-l) with 10%.</i> | 95  |
| <i>Table 5.8 ES by SEM using different addition of hydrofluoric acid (a-c) with 1%, (d-f) with 3%, (g-i) with 5%, (j-l) with 10%.</i>          | 96  |
| <i>Table 5.9 Roughness analysis using AFM for the received and electropolished samples, after using a different quantity of HF.</i>            | 101 |
| <i>Table 5.10 Comparison of surface features for electrolytes with 3 vol. % of HClO<sub>4</sub>, HF or HCl.</i>                                | 102 |
| <i>Table 5.11 Comparison of AFM analysis after adding 3% of each acid HClO<sub>4</sub>, HF, HCl using a scale of 1 x 1 μm.</i>                 | 103 |
| <i>Table 5.12 Water contact angle for L605 before and after electropolishing with the different addition of hydrofluoric acid.</i>             | 104 |
| <i>Table 5.13 Comparison between the mechanical polishing (1000 grit, Alumina) and the electropolishing using 3 vol. % of HF.</i>              | 109 |
| <i>Table 6.1 Chemical solutions used for electropolishing of pure Titanium. The percentages are in volume.</i>                                 | 112 |
| <i>Table 6.2 ES by SEM using different acid addition and solution for the electropolishing of pure Titanium.</i>                               | 114 |
| <i>Table 6.3 Chemical solutions used for electropolishing of pure Titanium with stable conditions.</i>   | 117 |
| <i>Table 6.4 ES by SEM using different acid addition and solution for the electropolishing of pure Titanium.</i>                               | 121 |
| <i>Table 6.5 Optical microscopy (a-d) as received sample, (e-h) sample after electropolishing using solution N° 10.</i>                        | 122 |
| <i>Table 6.6 ES by SEM (a-c) as received sample, (d-f) samples after electropolishing using solution N° 10.</i>                                | 123 |
| <i>Table 6.7 Roughness analysis using AFM.</i>   | 124 |
| <i>Table 6.8 Roughness for different samples before and after electropolishing.</i>  | 125 |
| <i>Table 6.9 water contact angle before and after electropolishing.</i>  | 127 |

## Acknowledgment

Je tiens sincèrement à remercier mon superviseur, Pr. Diego Mantovani, tout le groupe de recherche du LBB à l'hôpital st François d'Assise.

Pr. Mantovani, Merci pour m'avoir donné l'opportunité d'être parmi vos étudiants et dans votre groupe de recherche.

Merci pour votre supervision tout au long de ma maîtrise, tu m'as transmis beaucoup de leçons et de messages directement et indirectement, J'ai appris de vous la patience, la responsabilité et l'autonomie, j'ai aussi appris la recherche scientifique stricte suivant les conditions et les normes mondiales, dont, mon pays la Syrie, uniquement Université d'Alep, je n'ai pas eu la chance à apprendre sur le savoir-faire de la recherche scientifique. Une de vos leçons, dont j'y jamais l'oublié « arrêtes de penser à la Syrienne, ici c'est le Canada ».

Je remercie aussi les membres du jury qui ont évalué ce mémoire de maîtrise. Pr. Hendra Hermawan et Pr. Marta Multigner. Je remercie encore une fois Pr. Mantovani qui a lui aussi évalué ce mémoire.

Merci à Carlo Paternoster, notre professionnel de recherche dans le groupe de bio-métal, qui était comme mon grand frère, il était présent dans plusieurs moments difficiles durant ma maîtrise, dès le premier jour au laboratoire jusqu'à le dernier jour. Merci pour tous Carlo, ta présence et ta supervision durant les expériences et bien sûr pendant la rédaction de ma mémoire.

Je tiens également à remercier particulièrement les professionnels de recherche du LBB, sans votre disponibilité, qui aurait été difficile de présenter ce travail. Pascale Chevallier, Stéphane Turgeon, Lucie Lévesque, Rana Tolouei et Andrée-Anne Guay-Begin. Je vous remercie pour votre soutien technique et morale durant mes expériences au LBB.

J'ai eu la chance durant ces deux ans de faire la connaissance d'un magnifique groupe d'étudiants internationaux, de différentes cultures, différents ethniques, différentes religions, c'était une richesse humaine et culturelle, une expérience unique qui m'a appris l'ouverture sur l'autre, apprendre et accepter les différents points de vue. Des beaux moments qu'on a passé ensemble au laboratoire et à Québec cette belle ville.

Sergio D., Dimitria, Linda, Francesco, Vinicius, Ludivine, Carla, Max, Vanessa, Majid, Jean-François, Mahrokh, Nathalia, Fa, Chiara, Pedram, Gabriel, Saeideh, Emna, Souheila, Nawal, Melis, William, Miguel, Ibrahim, Morgane, Caroline R., Caroline L., Essowe, Stéphanie, Juliana, Clayton, Sergio L., Fernanda, Devi, Reza, Miame.

Beatrice, ma meilleure amie je suis très content qu'on a pu développer notre amitié, dont j'espère qu'elle restera pour toujours. Carolina, mon amie et ma collègue durant les expériences d'électropolissage, merci pour tous, tu étais avec moi dans les moments difficiles, Leticia, ma grande sœur, merci pour ton soutien durant la rédaction de cette mémoire, ton

sourire me donnera une énergie positif, Samira, content de faire ta connaissance, beaucoup de choses en commun entre nous, ça me fait toujours plaisir nos discussions infini, Arn, mon ami belge tu étais présent dans le laboratoire pour une petite période, mais c'était assez pour développer une amitié inoubliable, Ivàn, merci pour tes conseilles précieuses.

Je n'oublie jamais de remercier la présence de dieu, dans ma vie à Québec, représenter par l'œuvre de l'Opus Dei, et la fondation Haratan, qui m'ont aidé à s'intégrer au sein de la société Québécoise. Leurs présence spirituel et morale qui m'a aidé à dépasser tous la pression et l'angoisse que j'ai vécue au début. Je remercie les donateurs qui ont contribué par la bourse Syrie-Bois Gomin, dont j'ai profité durant mes premiers 6 mois à Québec, un aide qui a facilité ma vie au début de mon arrivé au Canada.

Merci notamment à Monsieur l'abbé Denis St Maurice, Patrick Duffley, Bruno Gagnon, Julio Quintero, Dominique Melançon.

Je tiens aussi à remercier Dr. Aida Bairam, qui m'a entouré durant mes études, merci pour ton aide morale et scientifique, tous tes conseils qui étaient vraiment précieuse, j'ai appris de ton expérience dans la vie et de tes études et tes recherches scientifiques entre la Syrie, la France et Canada. On te parlant j'ai pensé à mes parents, merci pour les belles soirées et les délicieux plats, qui me fait penser à la maison et la Syrie.

Bien sûr je voudrais aussi remercier ma famille, mes parents (Johnnie et Mouna), mes sœurs (Carine et Nadine), pour leurs présences dans ma vie, pour tous ce qu'ils m'ont donné et m'ont enseigné dès mon enfance jusqu'à maintenant et bien sûr dans le futur, j'espère qu'ils sont fiers de moi, dans le plaisir de se rencontrer prochainement, après 5 ans de séparation à cause de la guerre.

Je n'oublie pas mes amies et mes collègues Syriens, grâce aux technologies et les nouveaux moyens du media sociale, on est resté en contact malgré la distance, et les continents qui nous sépare.

Pierrot, Mays, Sina, Marc, Georgy, Toni, Carl, Cathy et Carla...

Baraa, Ghina, Mouina, Hrayer, Maher, et Marie...

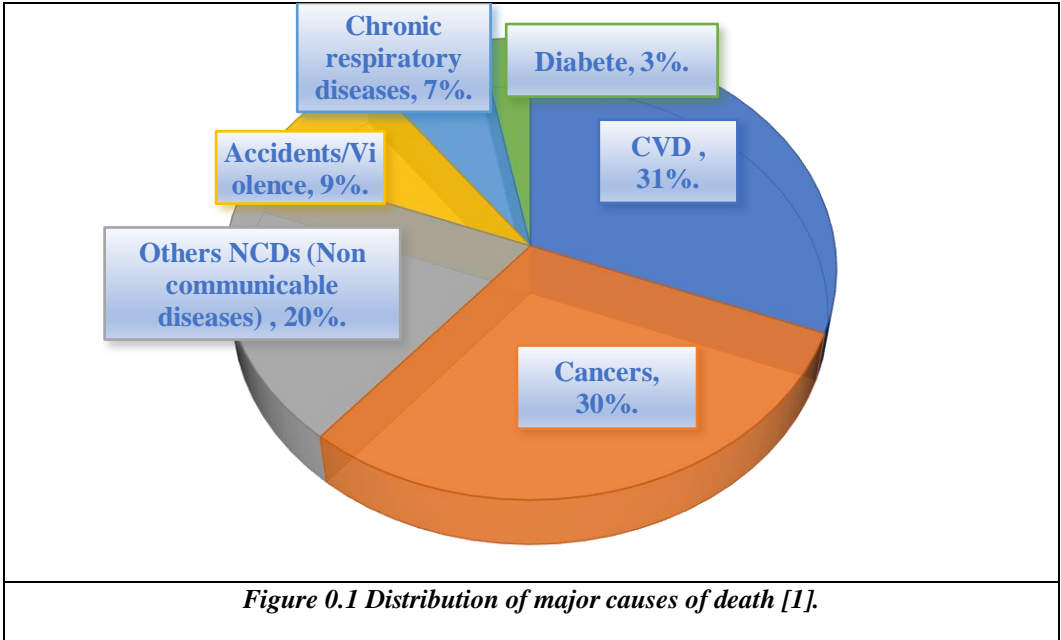
## **Introduction**

The term «cardiovascular diseases» includes all the pathologies touching the circulatory system including heart and blood vessels; A failure of the circulatory system can be catastrophic for the brain, kidneys, and other organs or body parts.

According to the World Health Organization, cardiovascular diseases are the first cause of death, globally. In 2015 more than 17.7 million people died from CVDs, representing 31% of all cases of death around the world [1].

Some of the main factors that increase the number of CVDs are high blood pressure, genetic factors, a high percentage of cholesterol in the blood, obesity, diabetes, age, and smoking. Other causes can also be responsible for the manifestation of this kind of pathologies, such as for example, a bad alimentation and the total absence of physical exercise.

The estimated risk of increasing these diseases in the man over 70 is 35 % while for women over 70 is 24% [2]. The risk of cardiovascular disease increases with age. In general half of the men and almost two-thirds of the women who die suddenly because of a coronary artery disease do not experience previous coronary artery disease warning signs. For this reason, there is a general interest in the development of advanced diagnostic systems, drugs and devices that could relieve the economic, social and psychological burden associated to this kind of diseases.



# Chapter 1 From cardiovascular diseases to the clinical aspect of stenting

## 1.1 The cardiovascular system

### 1.1.1 Description of the cardiovascular system

To better understand the causes and possible solution for cardiovascular diseases, it is important to take a closer look at the cardiovascular system, to its components and structure. The *heart* is a muscular organ that is responsible to pump the blood in the body vessel network. Blood is considered as a real connective tissue, containing several types of cells in an aqueous fluid called plasma.

Plasma represents the liquid part of the blood, which is composed by the red and white blood cells and platelets. Plasma contains some proteins such as albumin, fibrinogen, and globulins. Plasma is one of the main ingredients in the blood, it forms more than 55% of its volume, in the form of a yellow liquid. Blood is responsible for supplying oxygen to the other tissues and removing carbon dioxide, as a product of cellular metabolism. Plasma also is responsible for the creation of a protein reserve in the blood, and it had immune functions [3]. Three types of cells are presented in the blood, *red blood cells*, *white blood ones*, and *platelets*. They are responsible for transporting oxygen and nutrition into body tissues. In general, an adult human body contains 4 to 6 liters of blood. Other cells that can be found in the blood are for example monocytes, lymphocytes, eosinophils, basophils and neutrophil, each with specific and precise functions.

Blood is a complex tissue, which is the study object of the science called *hematology* (from the Greek word αἷμα, ατος, τό, *blood*).

The body has two kinds of circulatory systems:

The first one is the *pulmonary circulation system*: it is responsible for the transport of the deoxygenated blood, rich in CO<sub>2</sub>, from the right side of the heart to the lungs, where the blood takes O<sub>2</sub> and goes back to the left side of the heart.



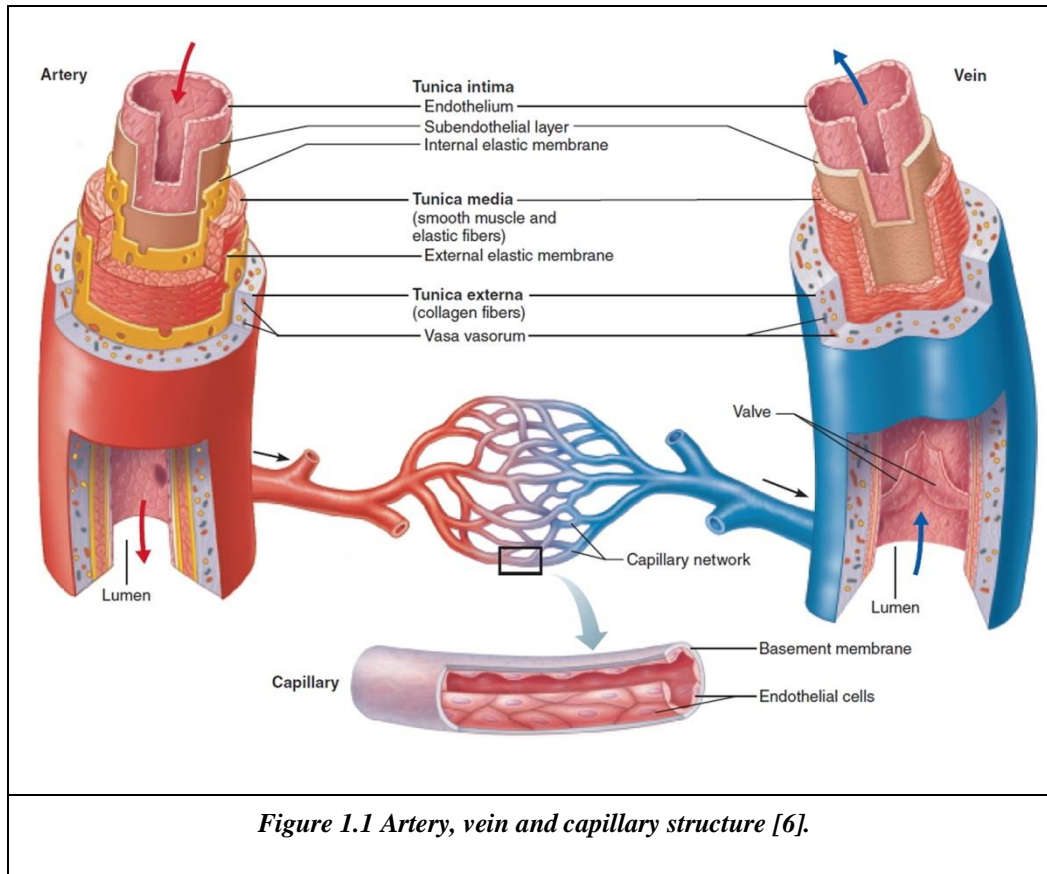
The second system is the *systemic circulation* one, which holds the oxygenated blood rich in O<sub>2</sub>, from the left side of the heart to all of the tissues of the body. The systemic circulation takes the metabolites from body tissues and brings back the deoxygenated blood to the right side of the heart. Blood vessels are of different types, they are classified in arteries, veins, and capillaries. The total length of the circulatory system in the human body extends over 100,000 km [4].

### **1.1.2 Vessel structure.**

The kinds of blood vessels present in the human body were already mentioned in the previous paragraph; here their structures will be described in detail.

An artery is composed of three layers, which are a *tunica externa*, a *tunica media*, and a *tunica intima*. The *tunica externa* is the outer layer of the artery that surrounds the other tissues. It is composed of a connective tissue, formed by fibroblasts, collagen and elastic fibers, which allow the stretching of the artery without permanent dilatation. The *tunica media* is the intermediate layer of the wall arteries and veins; it consists mainly of smooth muscle cells and elastic fibers. This layer is thicker in arteries than in the veins. The smooth muscle cells provide the movement of the cells by confronting or relaxing as a function of blood flow. The *tunica intima* is the internal layer of arteries, it contains a thin layer of connective tissue and endothelium. The endothelium is a monolayer of endothelium cells that are oriented in the direction of blood flow. These cells are in a direct contact with blood and they allow the exchange of nutrients with the surrounding tissues. They have the ability to migrate and proliferate at the site of injury when the endothelium is damaged [5].

Figure 1.1 shows the structure of a vein, composed by a *tunica externa* similar to that one of the artery, by a *tunica media* composed of smooth muscle cells and elastic fibers, and finally, a *tunica intima* formed by an endothelium and a sub-endothelial layer. The structure of a capillary is also shown in the same figure.



*Figure 1.1 Artery, vein and capillary structure [6].*

## 1.2 Occlusions in blood vessels

*Arteriosclerosis* is a general term to describe the thickening of the arteries. It can cause several vascular disorders and more generally vessel narrowing; the coronary artery, responsible for the supply of blood to the heart muscle, can be affected by this disease, too. When fatty residuals form a plaque, as they accumulate together with cholesterol, calcium, fibrin and cellular waste inside the vessels, the lumen is reduced, so that the affected vessel not only lose the ability to expand properly but also, they are not able anymore to deliver blood, oxygen and other nutrients to the tissues. This special form of arteriosclerosis is called *atherosclerosis*, and it means hardening of the arteries. The problem, as before mentioned, can affect also the heart artery (coronary artery). In fact, in general, the heart muscle needs blood to function, so when coronary arteries are blocked, they will no longer bring nutrients. The occurred damage can be so severe that not only the function of the organ itself is damaged, but also a generalized heart failure can lead to an acute pathology known as heart

attack. This phenomenon is often a consequence of the natural aging of the vessels, which causes the rigidity of the arterial walls [7].

| <b>Risk factors</b>   | <b>Disease process</b>             | <b>Outcome</b>   |
|---|------------------------------------|--|
| Fatigue fracture<br>Medical calcification<br>Elastin cross-linking  | Arteriosclerosis                   | Systolic hypertension<br>Heart failure<br>Coronary artery disease<br>Cerebrovascular disease |
| Hypertension<br>Inflammation<br>Diabetes mellitus   | Arteriosclerosis & atherosclerosis |  |
| Cholesterol<br>Smoking.<br>Intimal calcification.   | Atherosclerosis                    |  |
| <i>Table 1.1 Comparison of risk factors and final outcome for arteriosclerosis and atherosclerosis [8].</i> |                                    |  |

Some symptoms could be signs and indicators of a progressing arteriosclerotic disease, such as difficulty in speaking, partial loss of vision, chest pain, leg weakness during movement, high blood pressure, and kidney failure.

A *thrombosis* is due to the formation of a blood clot (or *thrombus*), a semi-solid or jelly-like occlusion formed by platelets in their aggregated state; red blood cells and a network of cross-linked fibrin, a protein that is involved in the hemostatic process and contributes to the formation of the final product of blood coagulation are involved in this process. The thrombus formation is triggered by a traumatic event, such as a blood leakage from a vessel, and it does not occur in a condition of normal circulation. Another factor playing a relevant role in the formation of a thrombus is the surface morphology of the affected artery, whose roughness attracts blood platelets. As already previously evidenced, a blood clot contains mainly platelets, red blood cells, and fibrin, all of them coagulated in correspondence of the arterial wall. Platelets play a primordial role in the formation of arterial thrombi, but their expansion

takes advantage of different biological mechanisms, such as inflammation and angiogenesis [9][10].

An atherosclerotic plaque can be more or less stable from the mechanical point of view, and it could be exposed to stresses depending on the blood flow in the artery. These stresses can break the fibrous layer encompassing the fatty material forming the plaque. This will allow the thrombogenic material, contained in the lipid core, to enter into contact with the bloodstream. This process leads to the coagulation of the blood, which finally results in thrombus formation [11].

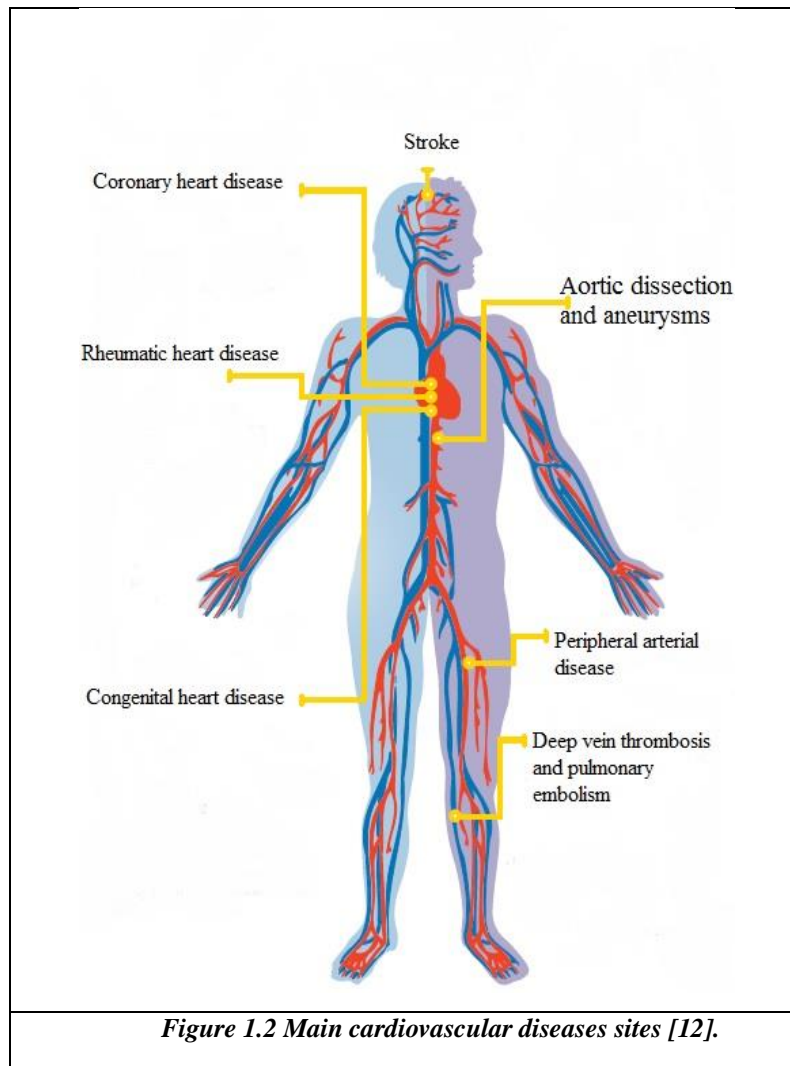
For this reason, a plaque can also be responsible for a clot formation and a vessel occlusion: In fact, at the site of the plaque rupture, the blood clot gets larger, while the amount of blood flowing through the vessel lumen decreases. If the blood clot completely blocks the artery, all tissues supplied by that artery begin to die not only in correspondence of the blocked section [7] but also further than the affected zone. The formation of a plaque is, in general, a long process that can also simultaneously affect many vessels; the formation of a clot is usually a rapid phenomenon, which can take place where a lesion has already occurred (for example, a broken plaque).

The understanding of interactions between blood components, such as leukocytes, platelets and red cells and tissues, such as the endothelium, can radically improve and prevent thrombus formation, as well it helps to identify patients with higher risk by controlling their cardiac events and reaction.

### **1.3 Cardiovascular diseases and associated treatments**

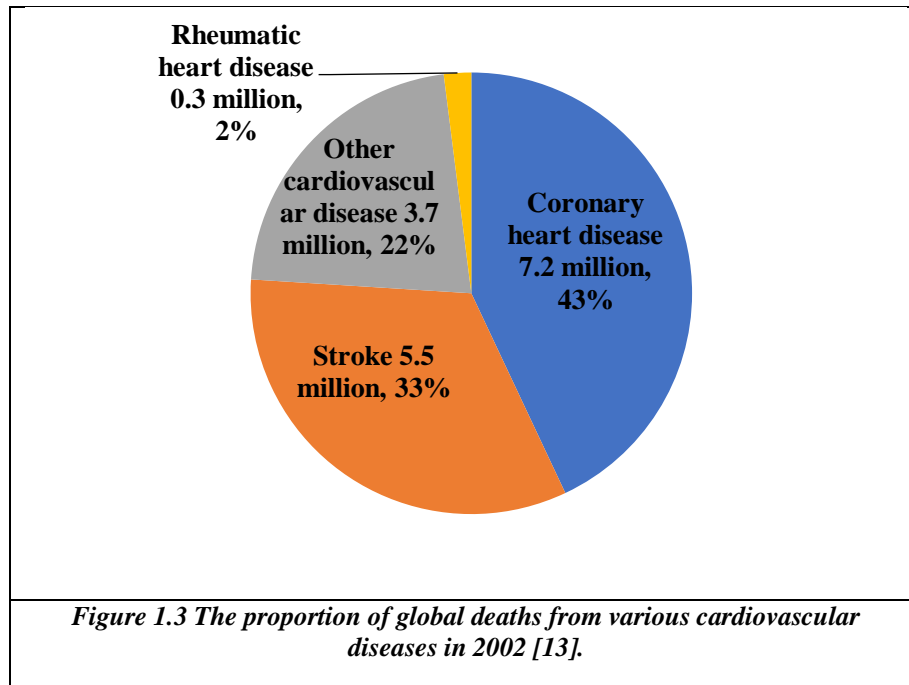
Cardiovascular diseases are a group of disorders affecting not only the heart but also blood vessels. Several pathologies are in this group, and they are classified depending on the kind of affected vessel, on the kind of affected tissue (vessel or muscle, for example) and on the type of blockage (clot or plaque, for example).

A list of the most common ones is proposed hereafter [1]:



- Coronary heart disease (a disease of the vessels that supply blood to the heart);
- Cerebrovascular diseases, stroke (affecting the blood vessels in the brain);
- Peripheral arterial diseases (the pathology involving the blood vessels that supply the arms and legs);
- Rheumatic heart disease (they involve the heart muscle and heart valves);
- Congenital heart malformations (they are related to the structure of the heart already present at birth);
- Deep vein thrombosis and pulmonary embolism (this disorder is responsible for the obstruction of the leg veins by blood clots; they may eventually migrate to the heart and lungs);

- Other cardiovascular diseases, (the heart tumors, disorders of the heart muscle, disorders of the lining of the heart) [12].



Several studies focused on the risks factors that increase cardiovascular diseases, by comparing the lifestyle of patients from different bag round and ethnicity. A healthy diet is an important factor to decrease cardiovascular accidents, as it is important for the control of other risk factors such as cholesterol, diabetes, obesity and blood pressure.

| <b>Biological risks factors<br/>(non-modifiable)</b>                 | <b>Biological risks factors<br/>(modifiable by treatment)</b> | <b>Lifestyle risk factors<br/>(modifiable)</b> |
|--|---|--|
| ageing   | high blood cholesterol  | smoking  |
| male   | high blood pressure   | unhealthy diet                                 |
| family genetic   | overweight and obesity  | inactivity                                     |
| race /ethnicity  | diabetes  | alcohol consumption                            |
| diabetes   | --  | --   |
| <i>Table 1.2 Main risk factors for cardiovascular diseases [13].</i> |   |  |

| <b>Cardiovascular disease<br/>(CVD) / Coronary heart<br/>disease (CHD) deaths</b>                            | <b>2010</b>  | <b>2020</b>  | <b>2030</b>  |
|--|--------------|--------------|--------------|
| annual number of CVD deaths.   | 18.1 million | 20.5 million | 24.2 million |
| CVD deaths as a percentage of<br>all deaths.   | 30.8%        | 31.5%        | 32.5%        |
| CHD deaths as a percentage of<br>all deaths for men.   | 13.1%        | 14.3%        | 14.9%        |
| CHD deaths as a percentage of<br>all deaths for women.   | 13.6%        | 13.0%        | 13.1%        |
| <i>Table 1.3 Predictions of global cardiovascular disease deaths in the early twenty-first century [13].</i> |              |              |              |

Two of the most widespread cardiovascular diseases are arteriosclerosis and thrombosis. Those diseases involve the heart and the circulatory system.

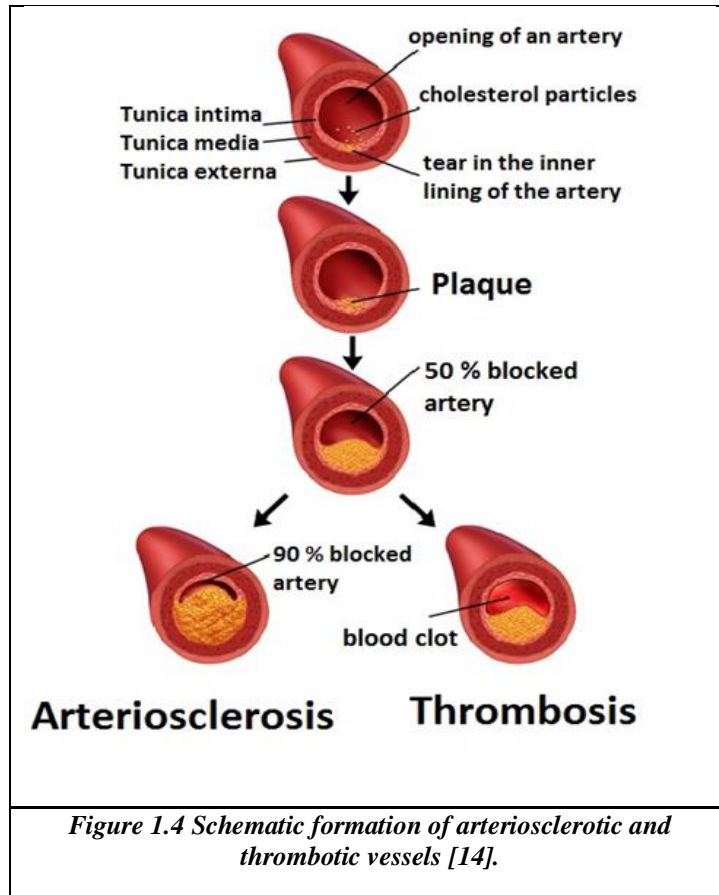


Figure 1.4 Schematic formation of arteriosclerotic and thrombotic vessels [14].

## 1.4 Cardiovascular disease treatment techniques

Depending on each case and level of risk in cardiovascular diseases, there are many types of treatments. Firstly, if the occlusion in the blood vessels is less than 30% it is preferable to treat it by drugs or by pharmaceutical treatment without using any type of catheter. If the occlusion reduces the vessel lumen in the range of 30% to 70%, then one of the most common practices that are used to treat cardiovascular diseases are based on balloon dilatation (angioplasty) or on the deployment of a balloon expandable stent (stenting). Both procedures have the aim of improving blood flow to the heart [15]. However, the results of angioplasty can be neutralized by re-narrowing of the coronary arteries due to elastic recoil and neointimal proliferation. This phenomenon of re-narrowing of the vessel is called *restenosis* [7]. In the advanced cases of cardiovascular diseases, where the level risk is very high, and



the occlusion of blood vessels is more than 75%, it is recommended to perform coronary artery bypass grafting or an open-heart surgery operation.

#### **1.4.1 Pharmaceutical treatment**

Generally, there are different type and groups of drugs that are used to treat cardiovascular diseases, depending on each situation. A doctor will decide which is the best solution. The proposed drugs could have some possible side effects on the patient so that it is important to understand the general situation of the patient before using them. The most common drugs that are used to treat cardiovascular diseases are presented in the following list:

- **ACE inhibitors.** They are used to decrease the blood pressure and enhance the blood flow to the heart;
- **Beta-blockers.** They are used to decrease the adrenaline amount and the blood pressure, but it has some side effect which it could make the beat of the heart slower;
- **Calcium channel blockers:** used to reduce the pain in the chest, and to decrease the high blood pressure. Its increase the blood flow and oxygen to the heart;
- **Warfarin:** its prevent and block the formation of clots in the blood;
- **Cholesterol-lowering drugs:** in general, cholesterol is active in the formation of new cells, in the production of hormones, and in the isolation of nerves. When inflammation phenomena take place, they cause a cholesterol build up on the wall arteries which causes heart attack and stroke [16].

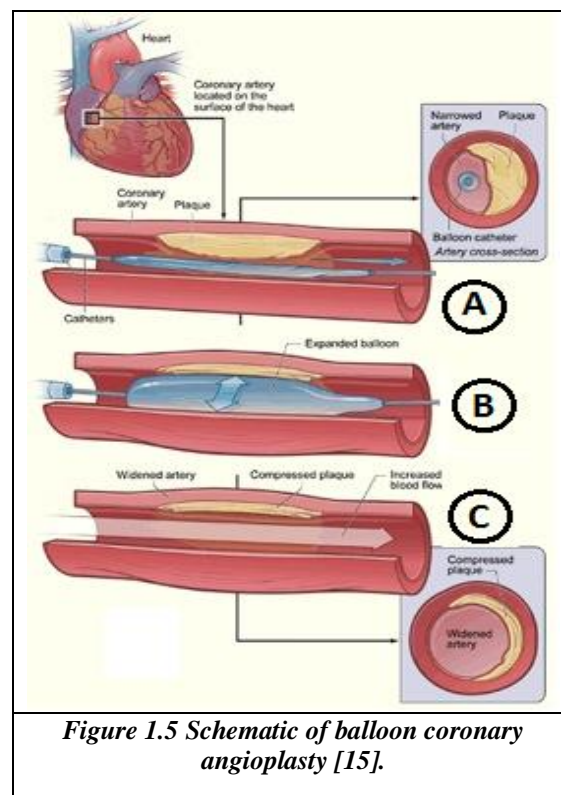
#### **1.4.2 Angioplasty**

Balloon angioplasty is a medical procedure in which a balloon is used to open a blockage in a coronary (heart) artery narrowed by atherosclerosis. A small tube called a catheter with a balloon at the end is put into a large blood vessel in the groin (upper thigh) or arm. The catheter is then threaded into the coronary arteries.

Geoffrey Hartzler was the first who did balloon angioplasty in 1979 [17]. Once the blocked segment in the artery is reached, the balloon is inflated, and it pushes the plaque outward against the artery wall. This improves the blood flow.

The illustration in Figure 1.5(A), shows firstly a cross-section of a coronary artery with a plaque build-up. The coronary artery is located on the surface of the heart. Then in Figure 1.5(B), the deflated balloon catheter inserted into the narrowed coronary artery. At the end, the Figure 1.5(C) show that the balloon is inflated, compressing the plaque and restoring the size of the artery. Generally, this procedure is considered as non-surgical because it is carried out through a tube or catheter inserted into a blood vessel, without surgery.

The balloon coronary angioplasty has some advantages like flexibility comparing to the stenting implantation, but it had the risk of elastic recoil, and it could cause dissection of the vessel [15].



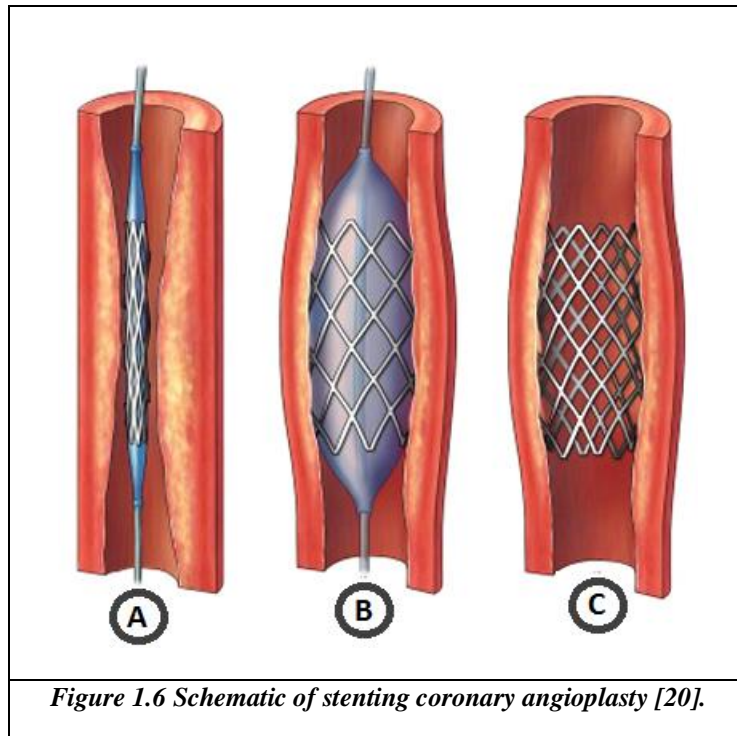
### 1.4.3 Stenting

Stenting is the practice of implantation of a tiny tubular-mesh-like device, which is a proven procedure for treating coronary artery occlusion. In 1986 Sigwat and Puel were the first to implant a stent in human coronary arteries. Since the first introduction, stent technology has progressively developed from conventional bare metal to the recent drug-eluting stents [17].

A stent is a small metallic mesh-like tubular scaffold and looks like small springs, which is placed and then expanded inside the newly widened part of the coronary artery to keep the lumen open [18].

The expansion of the stent pushes the device against the artery wall; when the balloon is deflated, the stent remains in place and holds the artery open, thus lowering the risk of the artery re-narrowing. Stenting can considerably reduce the risk of restenosis after the angioplasty, however, in about 25% of stenting cases, the problem of restenosis persists (in-stent restenosis, ISR) [19]. In general, an implanted stent needs to withstand high radial forces, but its flexibility is limited, with a higher risk of injury to the vessel due to excessive straightening. In some cases an overexpansion at the ends of the stent can occur, a bleeding from the blood vessel or some vessel damage [15].

Some stents, called drug-eluting stents, are coated with drugs that are slowly and continuously released into the artery. These drugs help prevent the artery from becoming blocked again from scar tissue that grows around the stent [17].



The illustration in Figure 1.6 shows the steps of the placement of a stent in a coronary artery with build-up plaque. Firstly, in Figure 1.6(A), a section of the blocked artery with a deflated balloon catheter is shown. A non-expanded stent in the narrowed coronary artery is also evident. Then in Figure 1.6(B) the inflated balloon deploys the stent and compresses the plaque to restore the size of the artery. Finally, Figure 1.6(C) shows the stent-widened artery and a cross-section of the compressed plaque [15].

A new combination of balloon dilatation, followed by the deployment of a self-expanding micro-stent used for the treatment of symptomatic intracranial arterial stenosis, combines the advantages of both techniques and allows a rapid, clinically effective and technically safe treatment of these frequently challenging lesions [17].

As any medical procedure, coronary angioplasty can have some complications, that is it could lead in rare cases to death. Less than two percent of people die during angioplasty.

#### **1.4.4 Coronary artery bypass grafting (CABG)**

This operation normally is used when an atherosclerotic plaque is too large, or when the lumen vessel is blocked more than 70%, and the artery is too much damaged. In this case, surgery is a mandatory step, and the use of bypass grants a solution for the blocked and narrowed artery. This operation is based on bypassing the blocked section of the coronary artery with a good and healthy part of another blood vessel, often taken from other parts of the human body [21] [22].

### **1.5 Framework of this research**

Cardiovascular diseases (CVD) are responsible for about one-third of all death cases in Canada. The incidence of heart diseases and their risk factors (hypertension, diabetes, and obesity) are increasing for all age categories. One of the solutions used to solve this problem is using a metallic device made of a mesh and called a stent. Stents are small devices that are implanted in narrowed blood vessels to restore blood flow and to avoid a heart attack or stroke and to treat brain aneurysms. This procedure shows a series of advantages when compared to the other techniques already mentioned.

One of the two important cause of stent failure is *stent thrombosis* (ST), and *in-stent restenosis* (ISR). The need to solve those two main problems is important, as they are related directly to the materials used for the stent fabrication: the progress in the manufacturing of the materials, their chemical composition and the technologies involved in the fabrication play a relevant role in the positive outcome of the disease. An accurate surface control is needed to assure the cytocompatibility of the chosen alloy: the surface modification method, useful in the real practice of stent and studied in the present work, is electropolishing, which is used to remove surface inhomogeneities, previous processing residuals and to have a surface more homogeneous from the chemical and topographical point of view. Electropolishing can also be used as a pre-treatment for other following surface treatments. This work is aimed at studying the influence of different electropolishing parameters on the final features of a Co-Cr alloy and on pure Ti, as a preliminary step for the optimization of the cytocompatibility and low-thrombogenicity of these materials.

Different approaches have been evaluated to reduce the restenosis rate and thinning of stent strut was shown to be the most satisfactory method. To be able to reduce strut thickness, while maintaining the required longitudinal and the radial strength of a stent, new alloys with superior mechanical properties are needed.

Metallic stents must satisfy precise conditions defined according to their final application. They need to respect strict requirements, in terms of mechanical properties, electrochemical interaction (corrosion) and cytocompatibility. The following alloys are traditionally used in biomedical applications and more precisely for cardiovascular applications: the alloy AISI316L is considered a reference in this field, but the alloy L605, a Co-based material, is gaining more and more importance, due to its high mechanical properties (high ductility and high ultimate tensile strength) and high corrosion resistance. The use of Titanium alloys is the new frontier for biomaterials in cardiovascular applications, it is considered as a new potential candidate for cardiovascular stents [23]. A recently developed family of Ti alloys are  $\beta$ -Titanium alloys, showing a unique combination of high strength and high ductility (ultimate tensile strength and uniform deformation higher than 1000 MPa and 30%, respectively)[24].

The chemical composition, the material working process, and its thermo-mechanical treatments affect not only the alloy structure but also the mechanical properties. The surface modification methods, therefore, make it possible to modify certain properties, while keeping the so-called "bulk" properties. Electrochemical behavior and cytocompatibility are influenced by surface characteristics. Electropolishing is a pre-treatment step applied to metallic materials to obtain a chemically homogeneous surface, covered with a uniform and amorphous oxide layer, generally with a very low roughness, or at least with a controlled one. Not only this process makes possible to control the surface chemical properties, but also it affects the physical ones, for example by modifying its surface morphology.

The electropolishing process is described by some parameters, for example, the current, the voltage, the composition of the electrolytic solution and the temperature of the electrolyte. By controlling those parameters led to understand the condition of electropolishing, which it will reflect positively on the surface properties of the metal itself.

The electropolishing mechanism was not fully studied or determined, still, need a lot of progress in different aspect especially from chemical point view. Different papers studied and compared the electropolishing parameters, such as the time of electropolishing, bath temperature, current-voltage curve.

It was found that the lower bath temperature, decrease the electropolishing rate proportionally. Increasing electropolishing time would decrease surface roughness of metals, with an increase in the contact angle. Other paper concludes that the increasing time of electropolishing increases the cell density (cells/ml).

The current study was engaged to investigate the acid concentration (which affect strongly the surface finish), and the effect of different strong acidic addition on the electrolytic bath and the surface characteristics and biocompatibility of electropolished Co-Cr alloy, and pure titanium alloy. Many acids were studied for both alloys such as phosphoric, sulfuric, acetic, hydrofluoric, perchloric, hydrochloric.

Controlled electropolishing was found at a lower quantity of hydrofluoric acid for Co-Cr alloy, and a higher one for pure titanium alloy, depending on each structure of metals.

## Chapter 2 Engineering concept of stenting

### 2.1 Cardiovascular stents

A stent is a small metallic mesh that is implanted inside narrowed blood vessels to restore blood flow and avoid heart attacks or strokes, and to treat brain aneurysms [25]. There are other kinds of stents, for example, are esophageal and also ureteral. Cardiovascular stenting is considered a resolutive intervention for patients suffering from high levels of atherosclerosis or thrombosis. Their design and performances improved since their first use by the French Jacques Puel from Toulouse, the first one that implanted the first human coronary stent in 1986 [26].

Nowadays coronary stents can be classified into four groups: (1) *permanent stents*, fabricated by alloys such as for example SS316L, Co-Cr, Nitinol, and other non-degradable alloys; (2) *biodegradable stents*, fabricated with degradable metals such as Fe-, Mg- and Zn based alloys or biodegradable polymers; (3) *bare metal stents (BMSs)*, a type of permanent stent, whose surface is metallic; the surface chemical composition is the same as the bulk material, but the surface can be treated; (4) *drug-eluting stents (DESs)* are another type of permanent stents; restenosis rates are decreased by the presence of medicaments embedded on the surface of the stent, for example, included in polymers; it represents the new generation of stents.

Stent angioplasty is considered as a rapid and safe process not requiring any surgery; it is deployed to maintain the vessel and the artery open and improve the blood circulation in the lesioned region. For this reason, some metallic alloys are the best candidates in the fabrication of stents, due to their mechanical properties, plasticity, hardness, and ability to be visible by X-ray imaging.

In the other hand, polymers possess a high flexibility but a very low strength and rigidity, which limit the use of these materials for cardiovascular grafting: the mechanical properties of polymers are usually lower than those ones of alloys.

The first stainless steel stent was made and tested in 1985 by Palmaz and his colleagues, later on, in the nineties, the stents were made also from cobalt base alloy for high corrosion resistance, and Ni-Ti alloys because of their super elasticity [27].



Generally, the most common metals used for manufacturing of coronary stents are stainless steel (316L SS), platinum-iridium (Pt–Ir) alloy, nitinol (Ni-Ti), Co–Cr alloys, titanium (Ti), pure iron (Fe), and magnesium (Mg) alloys [28]. Studies about the introduction of other alloys, such as for example Ta-based or Ti-based materials, or Fe-based alloys are currently being carried out. Table.1 shows the main and common metals known to be used in the fabrication of metallic stents.

| Material               | Mechanical property | Workability     |            |               | Corrosion resistance |
|------------------------|---------------------|-----------------|------------|---------------|----------------------|
|                        | Tensile strength    | Wear resistance | Plasticity | Machinability | Pitting              |
| Stainless steel 316L   | Good                | Good            | Excellent  | Excellent     | Excellent            |
| Co-Cr alloy            | Good                | Excellent       | Poor       | Poor          | Good                 |
| Cast annealed Ti alloy | Excellent           | Excellent       | Good       | Good          | Fair                 |
| Commercially pure Ti   | Excellent           | Good            | Fair       | Fair          | Excellent            |
| Ti-6Al-4V              | Excellent           | Good            | Fair       | Excellent     | Excellent            |

*Table 2.1 Comparison of different properties of metals used for stents [27].*

316L stainless steel is used as a reference material, as its use is well established in clinical use. Despite its weak radiopacity, it shows suitable mechanical properties and it is a corrosion resistant material.

Cobalt-based alloys show a higher density, elastic modulus, and tensile strength than the stainless steel, but a similar ductility. Generally, L605 has the highest mechanical and electrochemical properties if compared to other Co-Cr alloys.

Titanium-based alloys are not spread for coronary stents, but it has excellent properties as a biomaterial especially for its inertness and its cytocompatibility. Titanium-based alloys have a combination of high strength with a low elastic modulus, which affects its elastic range and

the recoil after deployment in the artery. The high strength and elastic range are useful for orthopedic applications.

Tantalum alloys are an interesting candidate for the coronary stents, as it has high radiopacity and good MRI visibility. Tantalum has a low elastic range, which could decrease the recoil after deployment in the artery.

| <b>Metal</b>  | <b>Elastic modulus (GPa)</b>                 | <b>Yield strength (MPa)</b>                     | <b>Tensile strength (MPa)</b> | <b>Density (g/cm<sup>3</sup>)</b> |
|---|--|---|-------------------------------|-----------------------------------|
| 316L stainless steel  | 190  | 331   | 586                           | 7.9                               |
| Tantalum  | 185  | 138   | 207                           | 16.6                              |
| Cp-Titanium   | 110  | 485   | 760                           | 4.5                               |
| Nitinol   | 83<br>(Austenite)<br>28 – 41<br>(Martensite) | 195-690<br>(Austenite)<br>70-40<br>(Martensite) | 895                           | 6.7                               |
| Cobalt-Chromium   | 210  | 448 – 648                                       | 951 – 1220                    | 9.2                               |
| Pure iron   | 211.4  | 120 – 150                                       | 180 – 210                     | 7.87                              |
| Mg alloy (WE43)   | 44   | 162   | 250                           | 1.84                              |
| <i>Table 2.2 Mechanical properties of different alloys used for the fabrication of stents [28].</i> |  |   |                               |                                   |

## 2.2 Requirements for coronary stents

Coronary stents materials must show desirable properties to be suitable for cardiovascular applications, for example, high mechanical and fatigue resistance, corrosion resistance, and visibility during the use of standard X-ray and MRI methodology. Moreover, it should

possess specific surface characteristics that could improve its permanence and interaction with the surrounding tissues after the implantation in the artery. Some of those features are:

- **Flexibility:** necessary characteristic for any coronary stent, it will facilitate the passage of the stent through the narrow and winding artery [29];
- **Biocompatibility:** an important factor that must be required in all the implant materials in the human body, it is expected from any implants to be highly non-toxic, without causing inflammatory or any other allergic reactions. Coronary stents should be also thrombus-resistance;

Some specific qualifications are required to increase the biocompatibility in the human body like minimal surface area, low surface potential, smooth surface with no contaminants or impurities, low profile [30];

- **Visibility:** density is reported to promote radiopacity. The mass attenuation coefficient  $\mu$  ( $\text{cm}^2/\text{g}$ ) is a measure of the absorption of x-rays of the material, and it is also dependent on the wavelength of the absorbed radiation;

| Property                          | Material             |
|-----------------------------------|----------------------|
| Elongation modulus                | 316L stainless steel |
| Tensile strength                  | Co–Cr                |
| Yield strength                    | Co–Cr                |
| Surface energy                    | PTFE                 |
| Biocompatibility                  | Ti                   |
| Surface potential                 | Ta                   |
| Surface texture                   | Electropolishing     |
| Stability of surface oxide layer  | Ta/Ti                |
| Therapeutics                      | Paclitaxel           |
| Radiopacity                       | Gold                 |
| MRI compatibility                 | Ta/Ti/Nitinol        |
| The preferred way of drug loading | Polymer-based        |

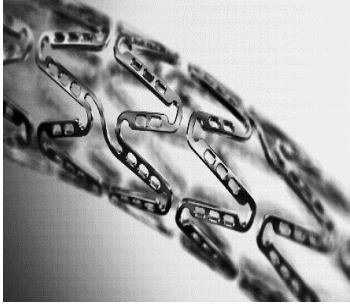




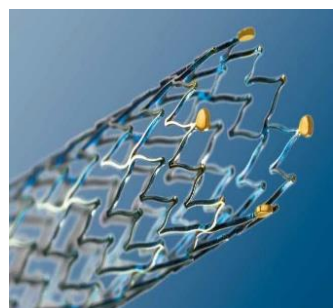
*Table 2.3 Ideal characteristics for coronary stent materials applications [28].*

Almost all the stents are laser cut from metallic tubes; The kind and the pureness of the material elements have a big impact on the homogeneity, porosity of the metallic alloys and its machinability [31]. Homogenous structure and small grains size are typically preferred for the stent, give a better polishing and resistance to fatigue and corrosion.

Small grain size intervenes with the mechanical properties and polishing, it increases the yield strength and affects the recoil during expansion.

The wall thickness is important for the deployment of the stent, especially during the laser cutting of the metal semi-finished product, that is a tube; the thickness has a relevant effect in the production of burrs, on the opposite side of the laser penetration. Cutting the stent is related to the machinability of the tube.

During cutting the stent it is preferred to keep an oxide layer on the surface because it will facilitate the laser removing of the slag on the metal surface [31].

|  |  |   |
|--|--|---|
|   |   |    |
| <p>The sirolimus-eluting stent in an open cell, Cobalt-Chromium stent. The struts contain a mixture of sirolimus and a bioabsorbable polymer which disappear in 90 days in vivo. The struts are connected by curved bridge elements and have ductile hinges [32].</p> <p>Size: <math>\phi</math> 2.3 – 3.5 mm, L: 8 – 28 mm.</p> | <p>Hybrid drug-eluting stents used as a bioabsorbable drug-carrier polymer that dissolves to leave behind a bare metal stent. The design is meant to eliminate the effects of late stent thrombosis, it is fabricated from L605 with a passive coating of Amorphous Silicon Carbide [33].</p> <p>Size: <math>\phi</math> 2.25 – 3 mm, L: 60 – 80 <math>\mu</math>m</p> | <p>Biodegradable polymeric, iron-based, and magnesium-based stent materials. The bioabsorbable coronary stents will corrode and be absorbed by the artery after completing their task as vascular scaffolding [34].</p> <p>Size: <math>\phi</math> 3 m, L: 10 mm.</p> |
|   |   |    |
| <p>Magnesium stents have potential advantages over polymeric stents in terms of higher radial strength [35].</p> <p>Size: <math>\phi</math> 3 mm, L: 12 – 14 mm.</p>   | <p>Angio-Sculpt scoring balloon catheter. It precise and predict dilatation across a wide range of lesion types. Compatible with 6F guiding catheters [33].</p> <p>Size: <math>\phi</math> 2 – 3.50 mm, L: 8 – 20 mm.</p>  | <p>Astron: Self-expanding stent. Used for atherosclerotic disease of iliac and femoral arteries. It pull-back delivery system for simple stent deployment [33].</p> <p>Size: <math>\phi</math> 7 - 10 mm, L: 30 - 80 mm.</p>  |
| <p><b><i>Table 2.4 Comparison between different kinds of metallic stents used for the cardiovascular application.</i></b></p>  |  |   |

| <b>Stent name</b>   | <b>Manufacturer</b>                        | <b>Bare stent material</b>        | <b>Coating</b>   | <b>FDA approval date</b> |
|---|--|-----------------------------------|--|--------------------------|
| BiodivYio™<br>AS  | Biocompatible<br>Cardiovascular Inc.<br>CA | 316L<br>stainless steel           | Cross-linked<br>phosphorylcholine  | September<br>2000        |
| BeStent™ 2  | Medtronic, Inc.,<br>Minnesota              | 316L<br>stainless steel           | Nil  | October 2000             |
| CYPHER™   | Cordis Corporation,<br>FL                  | 316L<br>stainless steel           | a mixture of<br>polyethylene vinyl<br>acetate, poly-butyl<br>methacrylate, and<br>Sirolimus          | April 2003               |
| MULTI-<br>LINK<br>VISION™                                       | Guidant Corporation                        | L-605 cobalt<br>chromium<br>alloy | Nil  | July 2003                |
| NIRflex™  | Medinol Ltd., Israel                       | 316L<br>stainless steel           | Nil  | October 2003             |
| TAXUS™<br>Express <sup>2</sup> ™                                | Boston Scientific<br>Corporation           | 316L<br>stainless steel           | Mixture of poly<br>(styrene-b-<br>isobutylene-b-<br>styrene) triblock<br>copolymer and<br>paclitaxel | March 2004               |
| Liberté™<br>Monorail™   | Boston Scientific<br>Corporation           | 316L<br>stainless steel           | Nil  | April 2005               |
| Rithron-XR  | Biotronik GmbH,<br>Germany                 | 316L<br>stainless steel           | Amorphous silicon-<br>carbide  | April 2005               |
| <i>Table 2.5 Comparison of different bar metal stents [28].</i> |  |                                   |  |                          |

### **2.3 Stent surface treatment and surface modification**

The surface properties of any metals are the object of modification to obtain a better appearance, to improve some surface features or to enhance the corrosion resistance. The surface treatment is performed between the initial treatment and the final stage of production.

The selection of suitable surface treatments is always based on acquiring a complete set of requirements on the part surface with respect to intended operating conditions. Generally, the surface of metals is responsible for all mechanical, thermal, chemical, and electrochemical interactions with the environment [36].

A biomaterial is a material used in the medical field to interact with biological systems to evaluate, treat, replace any tissue, organ or other function of the body [37].

The surface of any material is the outside part of the uppermost layer, often used when describing its texture, form, or extent. For this reason, the difference between a material and its surface related to the difference in the structure of the material. A surface could be defined by its roughness, wettability, charge, chemical composition and other features. Surface modification of a material is to import a new physical, chemical, mechanical, and biological properties of the material which are different from those that it could be found in the original surface.

The first contact between a biomaterial and the biological system inside the human body is first with the blood and any other biological liquids, secondly with the proteins, then it will be the contacts with the cells and tissues [38]. From this first contact, the proteins will form a layer on the surface. The interaction between a surface and a biomaterial can take place in different ways, for example by:

- Proteins adsorption.
- Inflammatory reaction.
- Thrombus formation.
- The release of ions/molecules.
- Corrosion of metals.
- Biological integration.

The adsorption of proteins is a phenomenon which describes the aggregation of molecules outside of the material. The ability of proteins to be attached to the material surface is highly depending on the surface properties of the materials. The more the proteins are bigger, the higher is their ability to adsorption and being attached to the surface [38].

Some factors affect the adsorption of the proteins (the adhesion to the biomaterials) such as surface energy or tension, surface hydrophobicity (wettability), and surface charge.

Many different factors about the interaction of a foreign material with the body should be taken into consideration, depending on the application and location of the implant biomedical device. As an example, the blood compatibility will be an important factor if the biomedical device will be in contact with blood (catheter, stent, and graft), or osseointegration could be the main parameter if the biomedical device will be used for the bone application. The host response for both kinds of applications is highly related to the surface properties of the biomedical device.

When a biomedical device will be in contact with blood, it should not activate the blood coagulation cascade, nor change or attract platelets or white blood cells. So, it is important to obtain a biomedical device with a finely tuned roughness, often in the range of nanometers, especially considering the fact that the surface roughness has an effect on-cell attachment.

There are several methods to modify the surface of metallic materials (including nanophase materials) that enhance their cellular activities when compared with traditional micro-rough materials.

### **2.3.1 Mechanical methods**

The object of mechanical modification is to produce a specific topography, to clean or roughen the surface, while leading to improved enhanced adhesion. These methods involve external action by the application of physical forces to modify the surface characteristics.

Sometimes during the machining of the metallic materials, structure deformations (disappearing of crystalline grains) can occur. They change the surface properties and increase surface hardness.



| <b>Mechanical methods</b>   | <b>Modified layer</b>   | <b>Objective</b>   |
|---|---|--|
| Grinding<br>Polishing<br>Machining<br>Blasting  | A rough or smooth surface formed by the subtraction process.  | Produce specific surface topography.<br><br>Clean and rough surface improves bonding adhesion.                       |
| Attrition   | Fabrication of a nanophase surface layer on the metal, which improve the tensile properties and the surface hardness. | Produce material with nanometer size grains (1- 1000 nm).<br><br>Produce rough morphology and higher hydrophilicity. |
| <i>Table 2.6 Overview of mechanical methods used for surface modification of metals [37].</i> |   |  |

### 2.3.2 Chemical methods

Chemical methods are used to enhance biocompatibility, bioactivity and bone conductivity, corrosion resistance and removal of contamination. They are based on the chemical reactions which happen at the interface between the metal and the solution. Among the chemical methods some of them are presented here, such as for example chemical treatments consisting of soaking in NaOH followed by heat treatment, etching in HCl, electrochemical treatment (anodic oxidation), sol-gel deposition, hydrogen peroxide treatment, chemical vapor deposition, and biochemical modification. Often a *pre-treatment* is required, to remove the surface contamination before the treatment, and to induce some controlled surface modifications, such as for example a controlled chemical composition.

| <b>Chemical methods</b>   | <b>Objective</b>   |
|---|--|
| Acidic treatment  | Remove oxide scales and contamination  |
| Alkaline treatment  | Improve biocompatibility and bone conductivity.  |
| Hydrogen peroxide treatment   | Improve biocompatibility and bone conductivity.  |
| Sol-gel   | Improve biocompatibility and bone conductivity.  |
| CVD   | Improve wear resistance, corrosion resistance, and blood compatibility.  |
| Anodic oxidation  | Produce specific surface topographies, improve corrosion resistance, improve biocompatibility, bioactivity or bone conductivity. |
| Biochemical methods   | Induce specific cell and tissue response by means of surface- immobilized peptides, proteins, or growth factors                  |
| <i>Table 2.7 Overview of chemical methods used for surface modification of metals [37].</i> |  |

### 2.3.3 Physical methods

Physical surface modification methods include processes which do not have any chemical reaction, such as thermal spraying, physical vapor deposition, ion implantation, and glow discharge plasma treatment.

During spraying methods, the coating materials are thermally melted into liquid droplets than it is sprayed onto the substrate at high speed. As an example of application newly introduced, a plasma gas spray is used for deposition of the metal coating. Physical vapor deposition consists of evaporating the target materials in a vacuum to form clusters, molecules or ions

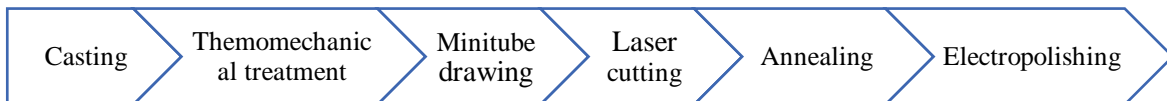
that are then transported to the surface of the substrate where film growth takes place by condensation [37].

| Physical methods   | Objective  |
|--|--|
| Thermal spray, flame spray, plasma spray.                        | Improve wear resistance, corrosion resistance and biological properties.       |
| Physical vapor deposition, evaporation, ion plating, sputtering. | Improve wear resistance, corrosion resistance, and blood compatibility.        |
| Ion implantation and deposition.                                 | Modify surface composition, improve corrosion resistance and biocompatibility. |
| Glow discharge plasma treatment.                                 | Cleaning, sterilizing, and removing the native surface layer.                  |

*Table 2.8 Overview of physical methods used for surface modification of metals [37].*

## 2.4 Biodegradable materials for stents

Biodegradable stents are more and more an alternative instead of the permanent stents. The materials used for biodegradable devices could be identified as material that degrades in the human body after an established time, and precisely after their support is no longer needed: they provide a temporary solution for specific clinical problems and progressively degrade thereafter. Metallic biodegradable stents have been used to treat diseases in pediatric patients [39]. The degradation is affected by the structure of the materials, which is a function of the fabrication method. Semi-finished product for stents (mini-tubes) can be fabricated by different steps, which are illustrated above:



*Figure 2.1 Description of the procedure for the fabrication of a stent.*

The fabrication method firstly starts with the production of the metallic ingot from which the stent will be fabricated. Casting is considered as essential fabrication method, then another method like forming or thermomechanical treatments are used for obtaining the required shape and mechanical properties of the alloy. Melting processes affect homogeneity, and porosity of the cast alloy. After hot working, metals are cold worked, and heat treated to obtain the final desired shape and physical and mechanical properties. Afterward, the fabrication of a mini tube follows, by either weld-redrawn or seamless forming. The next step is laser cutting which allows the obtainment of the stent design. Annealing reduces the residual stresses produced during tube drawing and laser cutting. The final step is the electropolishing to achieve a brilliant smoother metal surface, with no chemical residue and create a new protective oxide layer.

Three kinds of metals and their relative alloys have been utilized to fabricate biodegradable stents that is magnesium-, iron- and zinc-based. These alloys have their mechanical and cytocompatibility properties compared with those of stainless steel 316L (SS316L), the gold standard for metals used in cardiovascular applications. Because of their degradation, not only the interaction of the material with the tissue is studied, but also the release effects of several kinds of ions in the bloodstream is important [40]. Fe ions are useful for the body because it is an essential element. Implanted iron in the human body did not show any inflammatory reaction or the formation of any toxic element during dissolution. Iron can keep its mechanical properties during the implantation of stents without any failure. Zn ions play a role as an activator of some enzymes in the human body: many human cells secrete Zn ions and the presence of Zn is considered a requirement for a healthy body. Mg shows a low thrombogenicity and well-known biocompatibility. Other elements, used as alloy elements, play a role in the formation of proteins, for example, Mn, Ca, Al, Sr.

| <b>Metals</b>  | <b>Density<br/>(g/cm<sup>3</sup>)</b> | <b>Yield<br/>strength<br/>(MPa)</b> | <b>Ultimate<br/>tensile<br/>strength<br/>(MPa)</b> | <b>Young's<br/>modulus<br/>(GPa)</b> | <b>Maximum<br/>elongation<br/>(%)</b> | <b>Degradation<br/>rate<br/>(mm/year)</b> |
|--|---------------------------------------|-------------------------------------|--|--------------------------------------|---------------------------------------|---|
| <b>SS 316L</b>   | 8.00                                  | 190                                 | 490  | 193                                  | 40                                    | -   |
| <b>Pure<br/>Iron</b>   | 7.87                                  | 150                                 | 210  | 200                                  | 40                                    | 0.19                                      |
| <b>Fe-Mn<br/>steel<br/>(Hadfield<br/>steel)</b>  | 7.44                                  | 230                                 | 430  | 210                                  | 30                                    | 0.44                                      |
| <b>Pure Mg</b>   | 1.74                                  | 20                                  | 86   | 45                                   | 13                                    | 4.07                                      |
| <b>WE 43<br/>Mg alloy</b>  | 1.84                                  | 150                                 | 250  | 44                                   | 4                                     | 1.35                                      |
| <b>Pure Zn</b>   | 6.6                                   | 35                                  | 97   | 87                                   | 38                                    | 0.14                                      |
| <b>Zn-Mg<br/>alloy</b>   | 5.01                                  | 180                                 | 140  | 87                                   | 63                                    | 0.32                                      |
| <i>Table 2.9 Comparative properties of implanted degradable metals with SS316L [40].</i> |                                       |                                     |  |                                      |                                       |   |

### **2.4.1 Iron and iron alloys**

Pure iron is considered one of the best candidates to produce biodegradable stents due to its mechanical properties and biocompatibility. Iron has a high elastic modulus, comparable to that of stainless steel. Its high yielding and ultimate tensile strength are relevant in making stents with thinner struts. Iron has also high ductility which can be a positive point during the implantation of the stent when the device is plastically deformed.

The first biodegradable metallic stent was fabricated from Armco<sup>®</sup> pure Iron and it was implanted in the descending aorta of New Zealand white rabbits in 2001 [41]. The results from the implantation showed no significant evidence of either an inflammatory response or neo-intimal proliferation, and organ examination did not reveal any systemic toxicity [39]. Fluoroscopy was applied to view these stents (strut thickness varied from 100 to 120  $\mu\text{m}$ ). The biodegradation includes the oxidation of Iron into ferrous and ferric ions and these ions were dispersed into biological media. Ferrous ions reduce the proliferation of smooth muscle cells in in-vitro conditions and thus may inhibit neointimal hyperplasia [40]. It was noticed that the grain size of electroformed Iron stents was bigger than the one that found for SS316L so that it could have an effect on mechanical properties. [42].

Fe-Mn steels are considered as superplastic alloys, they have studied because of their manifest high ductility without a crack at a temperature over its melting point [43].

### **2.4.2 Magnesium and magnesium alloys**

Magnesium and its alloys have been used recently for biodegradable orthopedic implants. Mg alloys are considered the second choice for biodegradable metals used for implants or stents, because of its recognized biocompatibility and low thrombogenicity. It is an essential trace element and has a toxic level of about 7 to 10 millimoles per liter of serum [41].

The first uses of magnesium as a biodegradable stent in the human body was done by Zartner et al. It was implanted in the left pulmonary artery of a preterm baby with a congenital heart disease in 2005. This first use rescued a child from a highly severe clinical problem, this case gives confidence that stent technology could be more widely applicable in babies and children with different stent diameters and lengths [44].

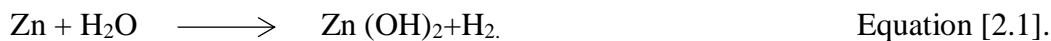
In general, magnesium alloys have faster degradation and lower mechanical properties than iron-based alloys, as Magnesium has a lower elastic modulus than AISI316L. Mg alloy stents may fracture because of their low ductility. Another disadvantage is that Mg stents are less radiopaque than iron alloys, so they can hardly be imaged by X-rays. One of the solutions used to solve this problem is the new intravascular ultrasound and MRI techniques which could detect Mg stents.

Mg stent struts should be thicker to supply an appropriate vessel wall support, but in this situation, the interaction area between metals and artery will be more extended; this in some cases could cause some allergic reaction [40].

### 2.4.3 Zinc and zinc alloys

Recently zinc and zinc alloys have been selected as a new choice for degradable materials used in biomaterials fields. Zinc is a brilliant metal, with a bluish-white color, exist naturally in the environment, known for its very low melting point, used as alloying elements with lead and Tin for making a solder. The use of zinc as metal dates to the old Romans empires.

As an alloying element zinc has the possibility to remove hydrogen ions from the solution, in the magnesium-zinc alloys the following reaction happens [45]:



Magnesium ions could also remove zinc ions from solution:



During the reaction, the evolution of hydrogen can be highly reduced.

Pure zinc has limited mechanical properties, and insufficient for bone and arterial device applications; for this reason, the use of pure zinc in the biomedical field is limited, but adding non-toxic and biocompatible alloying elements had given high mechanical properties, such as Mg which it improves the ultimate tensile strength and the elongation fracture.

Generally, zinc alloys show a high strength, a superior elongation for a strong design, good flexibility, with the ability to cold form and high finishing characteristics. Zinc alloys offer a high degradation rate more than iron but less than magnesium alloys, with a low melting point which makes it cast [46].

| <b>Alloy</b>                          | <b>Yield strength (YS) (MPa)</b> | <b>Ultimate Tensile Strength (UTS) (MPa)</b> | <b>Elongation (%)</b> | <b>Hardness (HV)</b> |
|---------------------------------------|----------------------------------|--|-----------------------|----------------------|
| Zn - 0.15 wt. %<br>Mg                 | 114                              | 250  | 22                    | 52                   |
| Zn - 1 wt. % Mg                       | 175                              | 250  | 12                    | -                    |
| Zn - 3 wt. % Mg                       | 291                              | 399  | 1                     | 117                  |
| Zn - 1.5 wt. %<br>Mg, 0.1 wt. %<br>Ca | 173                              | 241  | 1.72                  | 150                  |
| Zn - 1.5 wt. %<br>Mg, 0.1 wt. %<br>Mn | 115                              | 122  | 149                   | 0.77                 |

*Table 2.10 Mechanical properties of some biomedical zinc alloys [46].*



## 2.5 Non-degradable alloys used for stent applications

### 2.5.1 Introduction

The materials used for stents should provide a series of properties, satisfying strict needs from the mechanical, electrochemical and cytocompatibility point of view. Some materials, such as for example stainless steel, Co-Cr alloys and Nitinol, even if they are immersed in a corrosive environment such as the body one, present a very low degradation rate, so that they are known as nondegradable alloys.

In the twentieth century, several metallic alloys have been used in different biomedical fields, such as for example for implants for bone fracture fixation, cardiovascular applications, orthopedic devices, and dental equipment. These metallic alloys have been used depending on their specific features or properties such as flexibility, tensile strength, inertness, toxicity, corrosion resistance, and blood compatibilities. An example of several metallic materials used for a wide range of applications is shown in Table 2.11; some of them will be treated more in detail in the following sections.

| <b>Application</b>  | <b>Example of implants</b>         | <b>Types of metal</b>                               |
|---|------------------------------------|---|
| Cardiovascular  | Stent<br>Artificial valve          | 316 SS; CoCr;Ti<br>Ti6Al4V                          |
| Orthopedic  | Bone fixation<br>Artificial joints | 316L SS; Ti; Ti6Al4V<br>CoCrMo; Ti6Al4V; Ti6Al7Nb   |
| Dentistry   | Orthodontic wire<br>Filling        | 316L SS; CoCrMo; TiNi; TiMo<br>AgSn(Cu) amalgam, Au |
| Craniofacial  | Plate and screw                    | 316L SS; CoCrMo; Ti; Ti6Al4V                        |
| Otorhinology  | Artificial eardrum                 | 316L SS   |
| <i>Table 2.11 Implants classification and type of metals used [30].</i> |                                    |   |

### 2.5.2 AISI 316L stainless steel

Stainless steel was one of the first ferrous alloy used for biomedical applications. This alloy is composed of 50 wt. % Fe, 18 wt. % Cr and 8 wt. % Ni [30]. The addition of chromium is

responsible for the formation of a surface oxide passive layer, mainly composed of chromium oxide ( $\text{Cr}_2\text{O}_3$ ); it has effective results on increasing the corrosion resistance of the material, as this adherent oxide protects the surface from the external environment corrosion [47]. The addition of nickel makes the alloy tougher than pure Fe; moreover, it stabilizes the austenitic phase at room temperature, while increasing its resistance to corrosion [47]. Newer formulations of this alloys included some amounts of molybdenum; the addition of this element improved mainly the corrosion resistance and the resistance to pitting. Many efforts were made to reduce the content of C from 0,08 to 0,03 wt. % to improve the alloy corrosion resistance. In fact, C forms carbides at the grain boundaries, decreasing the amount of available Cr in the metallic matrix in that region; adding Mo plays a role in the resistance to corrosion, as they also form carbides, avoiding Cr consumption at grain boundaries [30]. Stainless steel alloys are divided into three main groups depending on their crystalline structure: they can be ferritic (Fe-Cr system), martensitic (Fe-Cr-C system) or austenitic (Fe-Cr-Ni system) [27].

In general, stainless steel is less corroded in an environment containing oxygen, but in chloride solutions, it could be affected by corrosion and form pits.

The most famous and common used alloy of stainless steel for biomedical applications is commercially known as AISI316L. It has a non-magnetic nature and it was developed by adding 2.0-3.0 W% of Mo, increasing the content of Nickel already present in the base one, AISI 304, and decreasing the content of Carbon to be less than 0,03 wt. % [48].

AISI316L is even actually now used in the biomedical application, due to its high mechanical properties, especially in the fabrication of stents, as it combines strength and ductility, and it is still considered the «gold standard» and the reference material for these applications.

Stainless steel has enough plasticity that could help the balloon expansion during the inserting of the stents in the human body [48].

|   |             |          |            |           |                         |
|---|-------------|----------|------------|-----------|-------------------------|
| <b>Structure</b>  | Martensitic | Ferritic | Austenitic | Duplex    | Precipitation hardening |
| <b>Base Composition</b>   | Fe12Cr0.1C  | Fe12Cr   | Fe18Cr8Ni  | Fe22Cr5Ni | Fe17Cr7Ni               |
| <i>Table 2.12 General classification stainless steels structure [47].</i> |             |          |            |           |                         |

| Metals  | Chemical composition (wt. %)   | Mechanical properties |           |                       |                    |
|---|--|-----------------------|-----------|-----------------------|--------------------|
|   |  | YS (MPa)              | UTS (MPa) | Young's modulus (GPa) | Max elongation (%) |
| <ul style="list-style-type: none"> <li>Stainless Steel 316L type ASTM A240</li> </ul> | 16-18.5 wt. % Cr, 10-14 wt. % Ni, 2-3 wt. % Mo; < 2 wt. % Mn; < 1 wt. % Si, < 0.003 wt. % C, Fe bal. | 190                   | 490       | 193                   | 40                 |
| <ul style="list-style-type: none"> <li>Stainless steel 316 L VM ASTM F138</li> </ul>  | 18 wt. % Cr, 14 wt. % Ni, 2.5 wt. % Mo, Fe bal.  | 340                   | 670       | 193                   | 48                 |
| Stainless steel ASTM F1314  | 22 wt. % Cr, 13 wt. % Ni, 5 wt. %, Fe bal.   | 448                   | 827       | 193                   | 45                 |
| Co-Cr alloys: Co-Cr-W-Ni (F90) (ASTM 2007a)   | 19-21 wt. % Cr<br>14-16 wt. % W, 19-11 wt.% Ni, Co bal.  | 310                   | 860       | 210                   | 20                 |
| Co-Ni-Cr-Mo (F 562) (ASTM, 2007b)   | 33-37 wt. % Ni, 19-21 wt. % Cr, 9-10.5 wt. % Mo, Co bal.   | 241                   | 793       | 232                   | 50                 |
| Co-Cr-Ni-Fe (Phynox) ASTM F 1058  | 20 wt. % Cr, 16 wt. % Ni, 16 wt. % Fe, 7 wt. % Mo, Co bal.   | 450                   | 950       | 221                   | 45                 |
| Pure Ti grade 4 (F67) (ASTM, 2006).   | 0.05 wt. % N, 0.1 wt. % C, 0.5 wt. % Fe, 0.015 wt. % H, Ti bal.                                      | 485                   | 550       | 110                   | 15                 |
| Ti6Al4V (F136) (ASTM, 2008)   | 5.5-6.75 wt. % Al, 3.5-4.5 wt. % V, 0.08 wt. % C, Ti bal.  | 795                   | 860       | 116                   | 10                 |

*Table 2.13 Example of metals used for implants and their mechanical properties [47][31].*

### 2.5.3 Co-Cr alloys

These alloys were developed for high resistance applications, such as for example where resistance to oxidation, resistance to corrosion and high mechanical properties are required all at once, (energy applications, such as turbines, etc.). Several formulations of these kinds of alloys have been proposed in time; they are usually rich in Ni (Ni superalloys), or in Co and Cr (Co-Cr alloys, also known as stellites). They are also resistant to wear, and they have attracted the attention of the scientific community for the possible use in biomedical applications mainly in the cardiovascular and prosthesis domains.

A more detailed discussion of the features, physical, mechanical and electrochemical properties of these alloys will be carried out in section 2.6. *Co-Cr alloys*, as they constitute one of the major groups of materials studied in the present work.

### 2.5.4 Nitinol alloys

Ti and its alloys are a wide group of metallic materials that are developing for a wide range of applications. Ti is a light element, like Al, and it can show a wide range of properties according to the alloying elements. Ti and its alloys are used in structural and corrosion-resistant material, for the construction of aircraft and automotive parts, or for other uses, such as in electric power plants, seawater desalination plants, and heat exchangers. As for Co-Cr alloys, Ti and its alloys will be better described in the section 2.7 *Ti and its alloys*, as for Co-Cr alloys, they are a relevant part of the present work.

Another alloy used for biomedical applications, composed mainly by Ti and for this reason considered as a Ti alloy, is Nitinol. It is formed by nickel and titanium, in the proportion of around ~50 at. % Ni and ~50 at. % Ti. This alloy is known for its excellent properties such as biocompatibility due to the formation of a passive TiO<sub>2</sub> layer on the surface. This layer acts as a diffusion barrier between the alloy and the human body, as it blocks the Nickel release, thus improving the corrosion resistance of the alloy. When removed, the surface layer is promptly reformed, due to the strong affinity of Ti for oxygen. Nitinol alloys have an excellent fatigue resistance. Nitinol alloys are known as shape memory alloys; this definition is related to the ability to return to its preformed shape after being heated to the transition

temperature. The solid-state phase transformation takes place between an original phase (austenite) and the new phase (martensite) [49].

Nitinol austenite has a body-centered cubic phase (bcc) while Nitinol martensite presents a monoclinic lattice. When Nitinol shows a martensitic phase, the plastic deformation is allocated by twinning. During Nitinol cooling, a big change occurs in its crystal structure from the austenite to a twinned martensite phase. On the other hand, heating the Nitinol to a temperature higher than the austenite formation one allows the restoration of the original austenitic structure [50].

| <b>Alloys</b>     | <b>Young's modulus (GPa)</b> | <b>Yield stress (MPa)</b> | <b>Maximal elastic strain %</b> | <b>UTS</b> | <b>Elongation at rupture</b> | <b>Fracture toughness (<math>MPa^{1/2}</math>)</b> |
|-------------------|------------------------------|---------------------------|---------------------------------|------------|------------------------------|--|
| Ni-Ti (Austenite) | 50 – 80                      | 200 – 700                 | 10                              | 900-1355   | 14.3                         | 30 - 60  |

*Table 2.14 Mechanical properties of Ni-Ti alloys [45].*

A disadvantage possibility in the Nitinol use is the Nickel release, in fact, Nickel is known to be an allergic and toxic element for the human body. Nickel ions could change the protein absorption, inducing a variation in cell morphology, favoring apoptosis, metal accumulation in tissues or erroneous gene expression [51].

### 2.5.5 Tantalum alloys

Tantalum was discovered in 1802. Tantalum belongs to the periodic table VB group, near to hafnium and tungsten. Tantalum is a very dense material ( $16,6 \text{ g/cm}^3$ ), and it has very high melting and boiling points, respectively  $T_f = 3100^\circ\text{C}$  and  $T_b = 5425^\circ\text{C}$ . Tantalum is considered as interesting material for biomedical applications due to its excellent corrosion resistance, high radiopacity, and high melting temperature. It is one of the most biocompatible metals because of its absence of toxic compounds [51].

The high corrosion resistance of Tantalum is due to its ability to form a passive and non-porous layer of  $\text{Ta}_2\text{O}_5$ . Tantalum has a high affinity for oxygen, hydrogen, nitrogen, and

carbon. Tantalum shows a high passivation tendency even in the highest aggressive environments: it can resist the attack of hydrofluoric acid at a temperature below 150 °C, which makes it an interesting choice for equipment to be used in aggressive chemical environments [52]. Tantalum has been used to coat other metals such as titanium and carbon foam used in biomedical applications concerning the spinal column. Ta coating of a porous material (70-80% porosity) was beneficial for the application above mentioned; it has, in fact, a similar structure to the cancellous bone, making this material suitable for bone regeneration applications.

| <b>Processing conditions</b>   | <b>Hardness (HV)</b> | <b>Young's modulus (GPa)</b> | <b>Yield strength (MPa)</b> | <b>UTS (MPa)</b> | <b>Elongation (%)</b> |
|--|----------------------|------------------------------|-----------------------------|------------------|-----------------------|
| Annealed   | 80 – 110             | 186 – 191                    | 140 ± 20                    | 205 ± 30         | 20 -30                |
| Cold-worked  | 120 - 300            | 186 - 191                    | 345 ± 50                    | 480 ± 70         | 1 - 25                |
| <i>Table 2.15 Mechanical properties for unalloyed tantalum [45].</i> |                      |                              |                             |                  |                       |

## **2.6 Cobalt-based alloys**

Cobalt-base alloys are a group of alloys with some specific features; they may generally identify as wear resistant, corrosion resistant and heat resistant. They can be grouped into two groups, respectively composed by Co-Cr-W or Co-Cr-Mo. These three elements, that is Cr, W, and Mo, are mainly responsible for the formation of carbides in the alloy [53]. The abrasion resistance of cobalt-based alloys, like other wear-resistant alloys, generally depends on the hardness of the carbide phases and the metal matrix [54].

### **2.6.1 Cobalt alloy metallurgy**

Cobalt provides a unique alloy base because of its allotropic face-centered cubic (fcc) to hexagonal close-packed (hcp) phase transformation, which occurs at a temperature of approximately 422 °C (792 °F) [54].

Alloying elements such as iron, manganese, nickel, and carbon tend to stabilize the fcc structure and increase stacking-fault energy, whereas elements such as chromium, molybdenum, tungsten, and silicon tend to stabilize the hcp structure and decrease stacking-fault energy [45]. In addition to chromium, small amounts of elements such as manganese,

silicon, and rare-earth elements (e.g., lanthanum) can be used to enhance the formation of protective oxide scales at elevated temperatures.

The solid-solution alloying decreases the stacking-fault energy, thereby making the cross-slip and climb of glide dislocations more difficult. Carbide precipitation (especially  $M_{23}C_6$  carbides) also can be quite effective in pinning glide dislocations, and both wrought and cast alloys strength depend on the dispersion of complex carbides. However, the use of high levels of carbon will limit manufacturing operations to hot-working processes.

The various carbide phases depend on chemical composition, heat treatment, and cooling during the thermo-mechanical treatment. The carbides also may be different in size and shape, even for the same phase. Subsequent heat treatments (intentional or from service exposure), and in general the thermomechanical treatments undergone by the alloy modify the morphology, the amounts and the types of carbides found inside the material. Some secondary carbides within grains can be formed by precipitation on dislocations located near large primary carbides. The carbides are seldom composed by two elements, as sometimes more elements are involved in their formation; chromium, tungsten, tantalum, silicon, zirconium, nickel and cobalt may all be present in a single particle or carbide. Molybdenum and tungsten form  $M_6C$  in the Co-Cr-C alloys when the content of either element is great enough so that it will no longer substitute for chromium in  $M_{23}C_6$ .

However, corrosion-resistant grades of cobalt alloys rely on molybdenum instead of tungsten for corrosion resistance. In addition, molybdenum has been found to enhance wear resistance in cobalt-base wear resistant alloys [55]. Another important aspect in the physical metallurgy of cobalt-based alloys is the occurrence of intermetallic compounds such as  $\sigma$ ,  $\mu$ , and Laves phases. These phases are deleterious in high-temperature applications, but Laves-phase alloys are used for wear-resistance applications (see the section “Laves-Phase Alloys” in this article).

The Laves phase is formed mainly based on atomic size factors. Some examples of these compounds in terms of general composition and crystal structure are given in Table 2.16.



| Compound   | Structure                       |
|--|---------------------------------|
| Co <sub>2</sub> (Mo, W, Ta, Nb)  | Hexagonal Laves phase           |
| Co <sub>2</sub> (Mo, W) <sub>6</sub>                                       | Rhombohedral, hexagonal μ phase |
| Co <sub>2</sub> (Ta, Nb, Ti)   | Cubic Laves phase               |
| Co <sub>2</sub> (Mo, W) <sub>3</sub>                                       | σ phase                         |
| <i>Table 2.16 Intermetallic compounds in cobalt-base superalloys [53].</i> |                                 |

Specific data for Haynes alloy 25 (an alternative commercial name for L605, such as UNS R30605, F90 or Stellite<sup>®</sup> 25) are listed in Table 2. The precipitation of these intermetallic phases can cause embrittlement, especially at low temperatures. On the other hand, precipitation of Laves phase can impart wear resistance, especially at high temperatures.

| Phase   | Crystal structure        | Lattice parameters, nm                |
|---|--------------------------|---------------------------------------|
| M <sub>7</sub> C <sub>3</sub>                             | Hexagonal (trigonal)     | a = 1.398, c = 0.053, c/a = 0.0324.   |
| M <sub>23</sub> C <sub>6</sub>                            | Fcc                      | α = 1.055 to 1.068.                   |
| M <sub>6</sub> C  | Fcc                      | α = 1.099 to 1.102.                   |
| Co <sub>2</sub> W   | Hexagonal                | α = 0.4730, c = 0.7700, c/α = 0.1628. |
| α-Co <sub>3</sub> W                                       | Ordered Fcc              | α = 0.3569.                           |
| β-Co <sub>3</sub> W                                       | Ordered hexagonal        | α = 0.5569, c = 0.410, c/α = 0.0802.  |
| Co <sub>7</sub> W <sub>6</sub>                            | Hexagonal (rhombohedral) | α = 0.473, c = 2.55, c/α = 0.539.     |
| Matrix  | Fcc                      | α = 0.3569.                           |
|   | hcp                      | α = 0.2524, c = 0.4099, c/α = 0.1624. |
| <i>Table 2.17 Phases present in Haynes alloy 25 [53].</i> |                          |                                       |

Cobalt-chromium-molybdenum alloy with moderately low carbon content was developed to satisfy the need for a suitable investment cast dental material. Carbon content influences hardness, ductility, and resistance to abrasive wear. The resistance of this group of alloys at higher temperatures is advantageous for high-temperature applications such as in gas-turbine vanes and buckets, but its versatility made this material useful for biomedical applications. This biocompatible material, which has the trade name Vitallium, it is now accepted in the biomedical industry as a high-strength alloy that can be used in implants. Abrasion resistance is highly affected by the size and shape of the hard phase precipitates within the microstructure and the size and shape of the abrading species [53]. Generally, in cobalt base alloys, chromium is responsible for the corrosion resistance.

It was seen that the dust containing cobalt caused several lung diseases, especially for the people who are working in the metallurgical industry [45]. Cobalt could induce a natural sensitivity or allergic reaction in tissues close to the metallic implants or prosthesis; nevertheless, a killer dose of soluble cobalt salts in contact with the human body is between 150 and 500 mg/kg.

| <b>Elements</b>  | <b>On corrosion resistance</b>                         | <b>On microstructure</b>                                       | <b>On mechanical properties</b>   |
|--|--|--|---|
| <b>Cr</b>  | Cr <sub>2</sub> O <sub>3</sub> to corrosion resistance | Form Cr <sub>23</sub> C <sub>6</sub>                           | Enhance wear resistance   |
| <b>Mo</b>  | Increase corrosion resistance                          | Refine grain size  | Enhance solid-solution strengthening  |
| <b>Ni</b>  | Increase corrosion resistance                          | --   | Enhance solid-solution strengthening. Increase castability.                             |
| <b>C</b>   | --   | Form Cr <sub>23</sub> C <sub>6</sub>                           | Enhance wear resistance. Increase castability   |
| <b>W</b>   | decrease corrosion resistance                          | Reduce cavity, gas attack hole and grain boundary separations. | Enhance solid solution strengthening.<br>Decrease corrosion fatigue strength stainless. |
| <i>Table 2.18 The effects of alloying elements on Cobalt base alloys [45].</i> |  |  |   |

Some Co-base alloys, for example, MP35N (Co-Ni-Cr-Mo, ASTM F562), contain more nickel. The presence of this element has relevant consequences from the corrosion and mechanical point of view, for example, it induces an improvement in the resistance to stress-corrosion cracking in aqueous solution. These alloys are not excellent for orthopedic applications due to the increased possibility of nickel allergic reactions. The biocompatibility of produced wear particles is also a reason for concern because their high surface to volume ratio is responsible for a relevant release of toxic ions in the body environment. In the work hardened and aged conditions, this alloy has elevated tensile properties which are considered suitable for implant applications [54].

| Alloy               | ISO     | Cr %      | Mo%       | Ni %     | Fe %      | Mn %      | W %     | Ti %      | Co %    |
|---------------------|---------|-----------|-----------|----------|-----------|-----------|---------|-----------|---------|
| <b>CoCrMo</b>       | 5832-4  | 26.5-30   | 4.5 - 7.0 | Max. 1.0 | Max. 1.0  | Max. 1.0  | --      | --        | Bal.    |
| <b>CoCrWNi</b>      | 5832-5  | 19-21     | --        | 9-11     | Max. 3.0  | Max. 2.0  | 14 - 16 | --        | Bal.    |
| <b>CoNiCrMo</b>     | 5832-6  | 19-21     | 9-10.5    | 33 - 37  | Max. 1.0  | Max. 0.15 | --      | Max. 1.0  | Bal.    |
| <b>CoCrNiMo Fe</b>  | 5832-7  | 18.5-21.5 | 6.5-8     | 14 - 18  | Bal.      | 1 - 2.5   | --      | --        | 39 - 42 |
| <b>CoNiCrMo WFe</b> | 5832-8  | 18-22     | 3 - 4     | 15 - 25  | 4 - 6     | Max. 1.0  | 3 - 4   | 0.5 - 3.5 | Bal.    |
| <b>CoCrMo</b>       | 5832-12 | 26-30     | 5 - 7     | Max. 1.0 | Max. 0.75 | Max. 1.0  | --      | --        | Bal.    |

*Table 2.19 International standards and chemical composition for metallic Co-base alloys used for medical application [54].*

L605 was above introduced; it is one of the cobalt-based alloys with Cr, W, and Ni as the main alloying elements.

This alloy contains up to 10 wt. % Ni; the amount of Ni in this alloy, needed to stabilize the FCC structure of the Co matrix, is lower compared to the AISI316L one, but it may still be responsible for nickel sensitivity reactions [54]. Tungsten is added as a solid solution strengthener and it is involved in the formation of carbides, to control their distribution and size [53]. Chromium improves corrosion and sulfide resistance; during alloy solidification chromium can form carbides, especially of the type  $M_7C_3$  and  $M_{23}C_6$  ( $M = Co, Cr$  or  $Mo$ ). It is also responsible for an increase in hardness.

The structure of these alloys is different if in the cast or in the wrought form. For example, after the casting process, the structure of L605 is mainly dendritic and rich of grain boundary precipitates, responsible for lower mechanical properties and corrosion resistance [54]. Hot working procedures allow a homogeneous structure with finer grains, improving the

chemical homogeneity, the ductility and the distribution and size of the alloy carbides [54]. Due to the excellent resistance to corrosion against body fluids, in recent years Co-based alloys have been used for orthopedic, cardiac and dental implants, heart valves and coronary stents. The first medical use of cobalt-based alloys was in the cast of dental implants [56].

| <b>Common name</b> | <b>ASTM Material designation</b> | <b>Specific Mass (g/cm<sup>3</sup>)</b> | <b>Elastic Modulus (GPa)</b> | <b>UTS (MPa)</b> | <b>Yield Strength (MPa)</b> | <b>Tensile Elongation (%)</b> |
|--------------------|----------------------------------|---|------------------------------|------------------|-----------------------------|-------------------------------|
| <b>Elgiloy</b>     | 40Co-20Cr-16Fe-15Ni-7Mo          | 8.30                                    | 221                          | 950              | 450                         | 45                            |
| <b>Phynox</b>      | 40Co-20Cr-16Fe-15Ni-7Mo          | 8.30                                    | 221                          | 950              | 450                         | 45                            |
| <b>MP35N</b>       | 35Co-35Ni-20Cr-10Mo              | 8.43                                    | 233                          | 930              | 414                         | 45                            |
| <b>L605</b>        | Co-20Cr-15W-10Ni                 | 9.1                                     | 243                          | 1000             | 500                         | 50                            |
| <b>316 L</b>       | Fe-18Cr-14Ni-3Mo-2Mn             | 7.95                                    | 193                          | 670              | 340                         | 48                            |

*Table 2.20 Physical and mechanical properties comparison between annealed Co-Cr alloys and 316L stent tubing [57].*

L605 has a higher elastic modulus, definitive tensile strength (UTS), yield strength and an excellent radial strength [57]. As evident from Table 2.20, L605 has higher mechanical properties than AISI 316L [57]. Furthermore, it shows a higher radiopacity and higher visibility under fluoroscopy during stent deployment, due to his high relative specific mass density, compared to AISI 316L [57].

## 2.7 Titanium and its alloys

### 2.7.1 Pure Titanium

Titanium is one of the most abundant metals on the planet. It has been recognized as an element in the early 19 century, but only during the last forty years ago, the metal acquired importance in different applications [53]. One of the reasons that facilitate the rapid growth in the use of Titanium is its good metal characteristics such as corrosion resistance and high strength.

Titanium corrosion resistance based on the structure and the formation of a protective oxide layer, which is in any case not stable for low pH levels and high fluoride concentration. This passive layer makes the metal advantageous in some applications like chemical equipment, surgical implants, prosthetic devices, sports equipment, and marine application.

Generally, Titanium exists in two crystallographic forms, that is the alpha ( $\alpha$ ) phase and the beta ( $\beta$ ) phase. Alpha phase has a hexagonal close-packed (hcp) crystal structure, while beta has a body-centered cubic phase (bcc) structure [53]. At 883 °C, the  $\alpha$  phase transforms to the  $\beta$  phase, this temperature called the transformation temperature and it depends on the nature of the used alloying elements, like aluminum, oxygen, nitrogen, and others. The alloying elements responsible for the stabilization of the alpha phase are called *alpha stabilizers* and they increase the alpha transformation temperature.

Some other elements such as Vanadium, Molybdenum, Iron, Chromium, and Niobium are responsible for the stabilization of the beta phase (*beta stabilizers*); compared to the other elements, they decrease the beta transformation temperature. The presence of the  $\alpha$  or  $\beta$  phase in a Ti alloy allows the classification of the material into a specific group; these alloys are in fact grouped in  $\alpha$  alloys,  $\beta$  alloys, and  $\alpha + \beta$  alloys [53], as described in the following table (table ). The mechanical properties are influenced by the presence of phases and their distribution; also, the thermomechanical processes needed to shape the alloys into semi-finished products have to take into account the alloy structure and the high affinity of this material for oxygen.

| Material   | Standard   | Modulus (GPa) | Tensile strength | Alloy type         |
|--|------------|---------------|------------------|--------------------|
| <b>First generation biomaterials (1950-1990)</b>   |            |               |                  |                    |
| Commercially pure Ti (cp grade 1- 4)   | ASTM 1341  | 100           | 240-550          | $\alpha$           |
| Ti-6Al-4V ELI wrought  | ASTM F136  | 110           | 860-965          | $\alpha+\beta$     |
| Ti-6Al-4V ELI Standard grade   | ASTM F1472 | 112           | 895-930          | $\alpha+\beta$     |
| Ti-6Al-7Nb Wrought   | ASTM F1295 | 110           | 900-1050         | $\alpha+\beta$     |
| Ti-5Al-2.5Fe   | --         | 110           | 1020             | $\alpha+\beta$     |
| <b>Second generation biomaterials (1900-till date)</b>                                   |            |               |                  |                    |
| Ti-13Nb-13Zr Wrought   | ASTM F1713 | 79 - 84       | 973-1037         | Metastable $\beta$ |
| Ti-12Mo-6Zr-2Fe (TMZF)   | ASTM F1813 | 74 - 85       | 1060-1100        | $\beta$            |
| Ti-35Nb-7Zr-5Ta (TNZT)   | --         | 55            | 596              | $\beta$            |
| Ti-29Nb-13Ta-4.6Zr   | --         | 65            | 911              | $\beta$            |
| Ti-35Nb-5Ta-7Zr-0.40 (TNZTO)   | --         | 66            | 1010             | $\beta$            |
| Ti-15Mo-5Zr-3Al  | --         | 82            | --               | $\beta$            |
| Ti-Mo  | ASTM F2066 | --            | --               | $\beta$            |
| <i>Table 2.21 Comparison of mechanical properties of biomedical titanium alloys[58].</i> |            |               |                  |                    |

### 2.7.2 The use of Titanium in the biomedical fields

Titanium does not have any biological role in the human body; it is known for its inertness, and it has high corrosion resistance when in contact with body fluids. Titanium is generally considered as a non-toxic element.

In the last two decades, the use of the titanium implant increased, if compared to the use of both stainless steel and Co-Cr-Mo alloys. This increase can be attributed to the low elastic modulus (around half that one of stainless steel and cobalt base alloys), and to the lower density of Ti alloys, that makes these materials useful especially for applications in which a low weight is required. On the other hand, titanium alloys have higher strength and high corrosion resistance, due to the stable oxide layer formed on its surface, which is formed

when the alloys are in contact with oxygen, and it can promptly be formed again at body temperature and in contact with biological fluids.

Generally, titanium implants are not refused by the human body; they have the ability to make a good connection with the biological host without anybody reaction. This is useful especially for orthopedic applications: once the implant is in contact with the bone, an appropriate geometry of the scaffold (appropriate pore size, etc.) allows the migration and activation of osteoblasts, responsible for the formation of the new bone. The process occurs without the formation of fibrous tissue around the implant [45]. Titanium is used for different biomedical domain, fabricate dentures, heart valve, stents, prostheses for hip and knee, wheelchairs, and bone plates because of its porous surface which helps ingrowth of bone, performing a powerful and longer permanent bond between implant and bone [58].



## Chapter 3 Electropolishing

### 3.1 Historical review about electropolishing

Electropolishing was first mentioned in 1907 by Buetel, when he noticed a satin-like finish on gold in an acid bath [59]. Later, in 1910, the German chemist Spitalsky understood the potential significance of such a brightening process. He published a patent about cyanide brightening process for gold, silver, and other metals. One of his electrolytic solutions was composed by a silver nitrate-potassium cyanide solution. This solution is still used today commercially for silver [60]. The first electropolishing mechanism was explained by Madsen in 1925 during the production of high-quality electrodeposition [60]. In 1928, Burns and Warner applied for a patent for an electro-cleaning process using 70 - 100 % (v/v) phosphoric acid and a current density of 100 amp/ft<sup>2</sup> [60]. They noticed a brightening finish on a steel surface after the experiment.

The real development of the electropolishing process that is famous nowadays, is referred to the French engineer, Pierre A. Jacquet. Jacquet in 1929 had observed that very soft copper filament anodes were polished when electrolyzed in a solution of phosphoric and perchloric acids in organic solvents [61]. In 1935 Jacquet tested the effect of surface brightening by electropolishing copper in an electrolyte composed of acetic and perchloric acid with different concentrations [61]. In 1952 J. Edwards explored the mechanism of copper smoothing in phosphoric acid solutions [55]. In the sixties, the increased commercial relevance of stainless steel was the cause for an important increase and progresses in electropolishing procedures for these alloys [62].

Later in the seventies and the eighties, the development of more effective and secure electrolytes continued, so that the new-found solutions allowed the development of processes at lower temperatures than the previous ones. This development enabled the realization of a highly reflective and bright polished surface [62].

### 3.2 Fundamental of the electropolishing process

Electropolishing is an electrochemical surface finishing process, used to change some surface characteristics such as roughness, chemical composition, and other physical properties, providing the alloy a good final appearance.[55]

During the electropolishing process, the metallic material is subjected to anodic dissolution: a thin surface layer in contact with the electrolyte is removed uniformly, and the surface becomes smoother. This electrochemical treatment must be performed in a certain range of temperatures, voltages, and currents, as a not controlled procedure can lead to damage to the sample, for example, a discriminatory chemical etching of the grain boundaries or other microstructural features can take place. By this method, the original surface will be covered by a new oxide layer: this phenomenon is called passivation and it can be achieved by a special procedure, with the aim of protecting the metallic surface from oxidation. Electropolishing procedures are used also in biomedical applications for a series of reasons, for example, because they were proven to reduce bacterial growth [63].

During the electropolishing process, the metallic workpiece is immersed in an electrolyte that is often composed of different solvents and acids. The electrolytic cell is composed of two metallic electrodes, a container, a power source, an electrolyte, and electrical connection. The electrodes are the *anode* or working electrode, (positive electrode) whose surface is electropolished. The metal of the anode is subjected to electrochemical dissolution, so that metallic ions are released into the electrolyte. Gaseous oxygen is produced at the anode. The other electrode is the *cathode* (negative electrode) where the metallic ions are deposited produces gaseous hydrogen. The metallic electrodes, the power supply, and the electrolyte form a circuit, in which the anode is the positive pole and the cathode is the negative one [55].

When an appropriate voltage and current are applied to the circuit, the anodic dissolution of the metallic material takes place. The process is so efficient that it can remove any kind of contamination from the surface [64], The electropolishing, applied to pre-strained metallic materials, can decrease the amount of residual stress [65]. The electropolishing process is highly dependent on the grain orientation, which could affect the homogeneity of the final surface [62]. The parameter control during the anodic dissolution process is fundamental to

obtain a suitable final product: for example, increasing the ion current increases the dissolution rate, thus decreasing the surface roughness [55]. In fact, several parameters affect the electropolishing process; the most relevant ones are current density, electrolyte temperature, the chemical composition of the used electrolyte, the time of treatment, and the presence of stirring. By modifying these variables, the final surface finishing could obtain a better result [55]. The chemical and physical changes of the electropolished surfaces are often evidenced by a more brilliant and flat surface [62].

The principles used in electropolishing are the same as those used in electroplating, even if the attained outcome is different. Electroplating is a way to deposit a coating, usually metallic, on an electrode. The process takes place by exploiting the redox chemical reactions occurring in the electrolyte. The anode is made of the material to be coated on the cathode; the electrolyte contains a certain concentration of cations of the same element which makes up the anode. In the latter, the element to be deposited is in a metallic state. Negative charges are pumped by a power supply toward the anode (the workpiece surface). The cations in solution are reduced on the surface of the cathode, where they form a metallic deposit. In fact, in electroplating the wished effect is the deposition of metallic ions on the cathode (cation reduction), while in electropolishing the anodic dissolution is the desired objective, taking place on the metallic workpiece (anode), which dissolves in the electrolyte [55].

One of the common use of electropolishing was in the field of aesthetic demand, consumer goods to produce cookware, or in the production of luxury goods, such as for example fountain pens. In recent years, the industry was more prone to use electropolishing for engineering applications, especially in the food, medical, pharmaceutical and semiconductor fields. In these domains, the need for clean and smooth surfaces is desirable [63]. Numerous studies show, for example, that bacteriological contamination levels are less on the electropolished surfaces used in the vascular, dental and orthopedic implants [66].

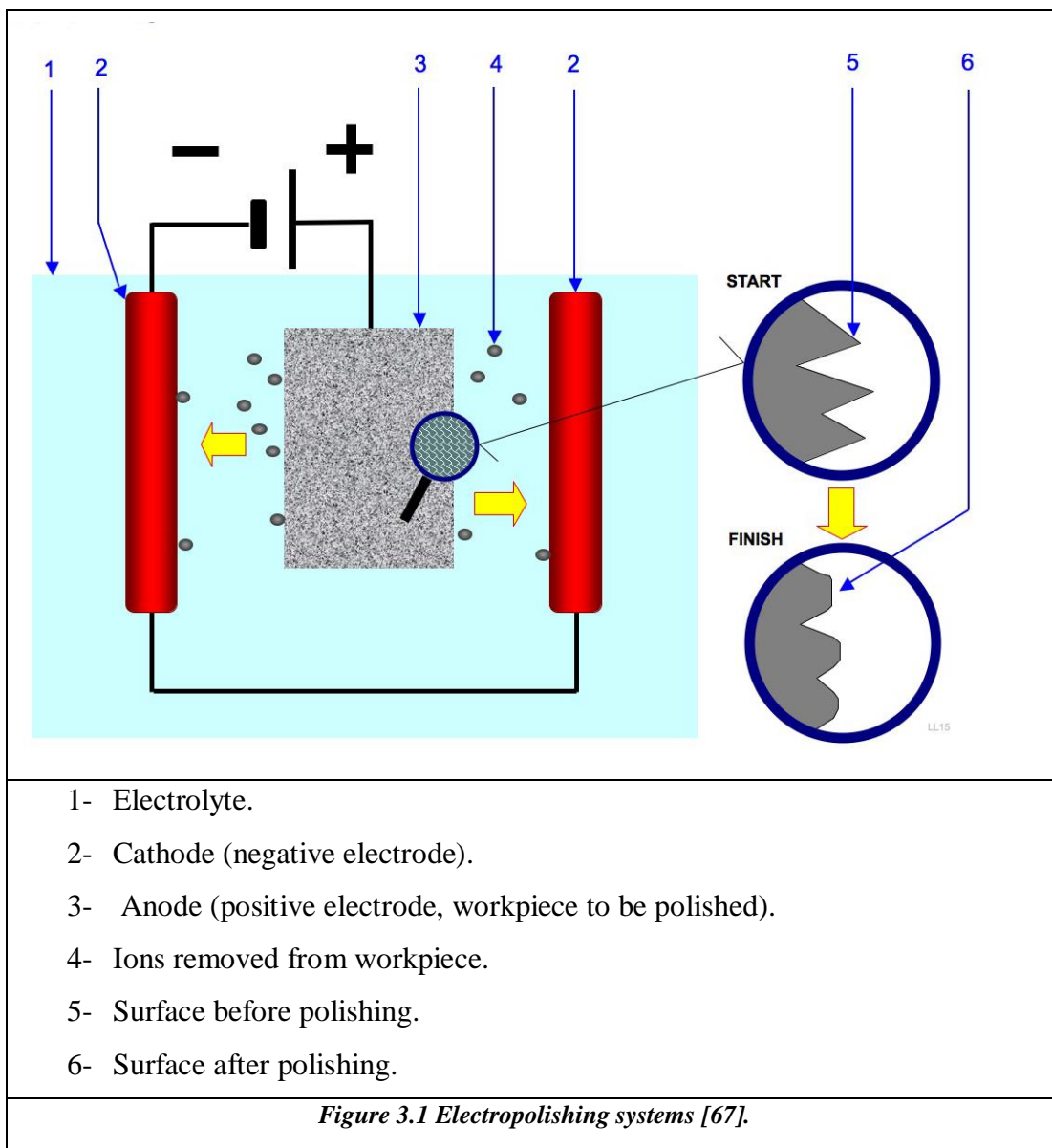


Figure 3.1 shows a scheme of the electropolishing setup: the work-piece is immersed in the electrolyte (a mixture of different concentrated acids), the anode (the positive electrode, the workpiece to be polished) and the cathode (the negative electrode) are connected to a DC power supply. A current will pass from the anode where metal is dissolved to the cathode where hydrogen evolves. The release of metal ions occurs at the anode. The surface finish is characterized by smoothing and brightening [68].

The voltage is related to the mass transport control which is characterized by current density ( $i_L$ ) which is given by the following relation [69]:

$$i_L = \frac{nFD(C_s - C_b)}{\delta} \quad \text{Equation [3.1]}$$

$n$  = charge of the ion involved. (q/e)

$F$  = Faraday constant, equal to 96485.33289(59) C mol<sup>-1</sup>.

$D$  = Diffusion coefficient of the rate-limiting species (m<sup>2</sup>/s).

$C_s$  = Surface concentration (saturation concentration of metal ions in the solution when a salt film mechanism is taking place or zero when an acceptor mechanism is taking place). (mm<sup>2</sup>)

$C_b$  = Bulk concentration (which is approximately zero when a salt film mechanism is formed, or it is the bulk concentration of the acceptor species when an acceptor mechanism is involved) (mm<sup>2</sup>/s).

$\delta$  = Thickness of the Nernst diffusion layer (mm).

### 3.2.1 The salt films

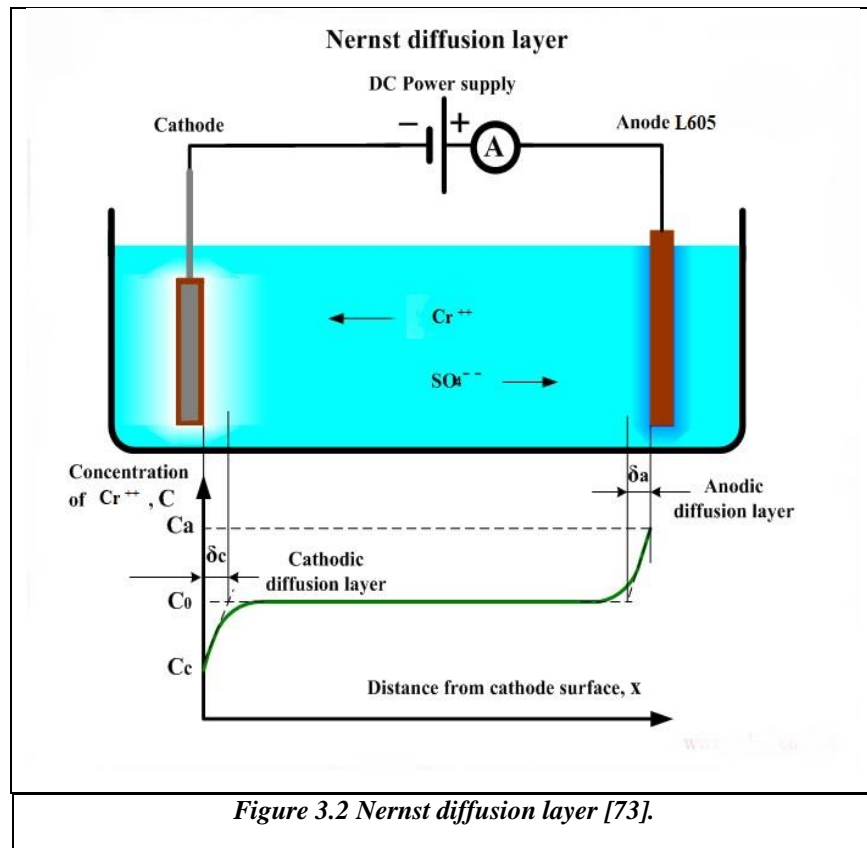
During the dissolution of the metallic ions from the anode, a salt film is formed on the surface of the anode. This block any further gas development on the anode, as this film which is non-conductive [70]. The formed salt film makes the concentration of the metallic ions at the anode equal to the saturation concentration [69]. It could be either compact, porous or present the two features at the same time. The formation of the salt layer starts from the bottom of the pits with an ionic transport when a high electric current is applied [70]. The deposition of this layer has an effect on the thickness, chemical composition and the final properties of the surface (for example on its quality as expressed by the brightening and final finishing). The deposited salts dissolve quickly dissolve once that the power supply is switched off [71].

### 3.2.2 Nernst diffusion layer

During electropolishing, the processes of ions dissolution from the anode and transfer in the electrolyte take place within a thin electrolyte region that is called diffusion layers. Diffusion layers are the regions near the metallic electrodes, where the concentration of ions is different

from the one assumed in the bulk solution; the bulk concentration is also supposed to be constant, depending on the distance from the electrodes. In general, at the anode surface, the metallic ions concentration is higher than the bulk concentration [72].

The Nernst diffusion layer, where the concentration of ions is constant and similar to the bulk concentration near the metallic electrode. The Nernst diffusion layer plays an important role in the reckoning mass transfer in the electro dialysis system. The thickness of the Nernst diffusion layer calculated by the ion concentration Vs its distance from the electrode surface. The Nernst layer could expand from the metallic electrode surface to reach the point of crossing levels between the horizontal line representing the bulk concentration and the tangent to the curve at the interface as is shown at Figure 3.2. Usually, the Nernst thickness layer is in the range of (0.1 - 0.001) mm, depending on the density of heating transportation formed by the reaction of the electrodes and electrolyte [72].



### 3.3 Polarization curves

The relation between the current density and the applied voltage is an important parameter to understand the electropolishing process; it is also of a practical use, as this voltammetry diagram allows the choice of the most advantageous conditions to do electropolishing. Figure 3.3 shows the polarization curve which is formed by four important regions. In the first region, etching phenomena occur; in this region, there is the direct dissolution of the anode metal, and it is characterized by an increase in current and a relative increase in voltage. In this region, the Butler-Volmer kinetic model, described by the following equation, is used [3.2]:

$$i = i_0 \left[ \exp\left(\frac{\beta n F \eta}{RT}\right) - \exp\left(-\frac{(1-\beta)n F \eta}{RT}\right) \right] \quad \text{Equation [3.2]}$$

where  $i$  and  $i_0$  are respectively the electrode current density and the exchange current density, in  $A/m^2$ .

$\eta$  is the overpotential defined as  $\eta = E - E_{eq}$ ,  $E$  is the electrode potential (V),  $E_{eq}$  the equilibrium potential (V),  $n$  the number of electrons involved in the electrode reaction,  $\beta$  is the symmetry factor,  $R$  is the gas constant equal to  $8.3144598(48) \text{ J}\cdot\text{mol}^{-1}\cdot\text{K}^{-1}$ , and  $T$  is the absolute temperature (K),  $n$ , and  $F$  is the faraday constant mentioned in equation [3.1].

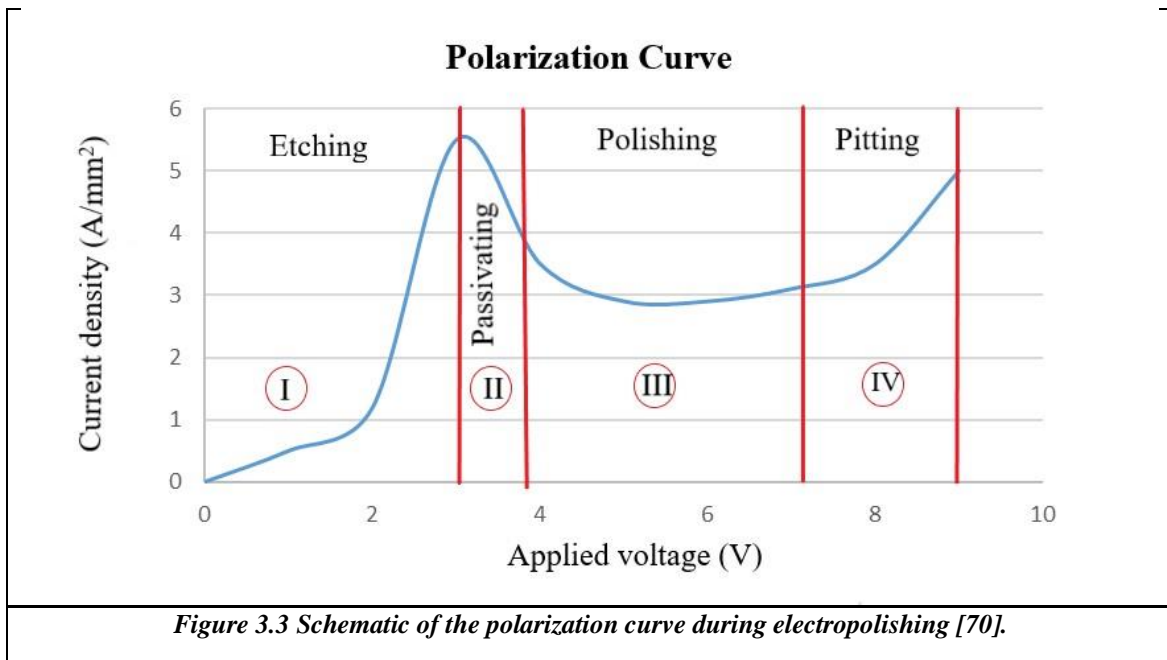


Figure 3.3 Schematic of the polarization curve during electropolishing [70].

The second region is the passivation region, where a small decrease in the current density while the voltage is increasing: This indicates the formation of the oxide layer on the anode after the ionic metal dissolution in the electrolyte. The third region is characterized by the stabilization of current density and it continues to increase for increasing voltage; this behavior is related to the stabilization of the passive oxide layer, and this region is characterized by the best electropolishing conditions. The oxygen bubbles which are formed for these conditions of voltage and current nucleate and grow in special points of the surface; they can attach to the same surface where they are formed and create zones of different electrical conductivity: this mechanism is responsible for different rates of dissolution of the metal at the anode.

The last region of the V-I diagram is the one connected to the pits formation; these phenomena are related to the increment of the voltage, and it occurs after electropolishing during the cooling and cleaning by water, due to a difference in temperature between the electrolyte which is characterized by its elevated temperature. The pits occur near the sub-boundaries or grain boundaries, its attributed to the concentration of vacuum at specific sites in the free surface. In the last region of V-I curve, the formation of pitting is due to the high-speed rate of oxygen formation and to the rapid oxygen bubble movement from the surface, causing pitting [74].

### **3.4 Mechanism of electropolishing**

Electropolishing is based on three mains mechanisms (the dissolution of metals ions, interaction with acceptor ions, and effect of water molecules in the electrolyte) related to the current distribution on the surface of the samples. This current distribution is based on the potential difference between the anode and the cathode [74].

The first mechanism occurs after the salts film had some precipitate on the anodic metal surface, during the reaction between the dissolved metallic ions and the electrolyte anions. The second mechanism based on the diffusion of acceptor anions (as chromium and cobalt), into the metal surface. The acceptor anions collect the dissolved metallic ions and create a sticky layer on the surface. The concentration of the metallic ions on the surface is fixed to



zero, to be consumed when it reaches the surface. The water molecules as considered the third mechanism of electropolishing, they are conjoined with the dissolved metallic ions when they reach the surface [69]. The presence of water molecules leads to the anodic dissolution which could cause pitting formation on the anode because of its increase the stability of the passive oxide film on the anode surface [75].

### **3.5 Reactions occurring during electropolishing of Co-Cr**

As was mention firstly, the electropolishing process is divided into two processes, the anodic dissolution (the metallic ions are dissolved from the anode) and the cathodic deposition (the metallic will be dissolved in the chemical electrolyte)[59].

During the oxidation time of cobalt and chromium, the metal surface also is oxidized resulting in dissolution for mass transfer through the aqueous medium, as shown in equations [3.3] and [3.4].

The rate of electropolishing is greatly dependents on the ability of the metal ions to dissolve from the anode into the medium, so if the current density was high, the dissolving tendency of the metallic ions will be increased [55]. Therefore, the higher the current density, the more ability the metal ions dissolve from the anode, where it is happening the oxygen gas formation during electropolishing, is shown in equations [3.5] and [3.6]. In the equations [3.7] and [3.8] it is shown the formation of the oxide layer which occurs on the anode. The anode passivation has a role in decreasing the rate of corrosion and protect the surface of the material from any further oxidation [55]. The electrochemical reactions are as follows:

#### **Anode Dissolution:**

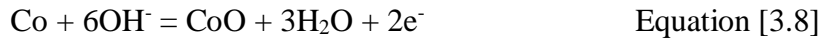
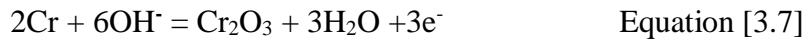


#### **Oxygen Formation:**





**Oxide Layer Formation:**



The material removal from electropolishing can be explained using Faraday's law of electrolysis, as shown in Equation [3.9].

$$W_{loss} = \frac{ItM}{nF} \quad \text{Equation [3.9]}$$

where  $W_{loss}$  is the total material loss (g),  $n$  is the valence of the metal ion,  $F$  is Faraday's constant (96485.33289(59) C mol<sup>-1</sup>),  $M$  is the molecular weight of the anode (g/mol),  $I$  is the process current (Ampère), and ( $t$ ) is the polishing time (sec.).  $M$ ,  $n$ , and  $F$  are constants. The two variables that affect the total material loss during electropolishing procedure are current ( $I$ ) and electropolishing time ( $t$ ).

During electropolishing, the old oxide layer is replaced by a new uniform oxide film while the metal surface is polished. The newly formed oxide layer plays an important role to enhance and increase the corrosion resistance. Many variables influence the formation of this oxide layer such as the time and the duration of each electropolishing cycle, the process current, the bath temperature and the chemical concentration of the electrolyte [74].

The Standard Gibbs Free Energy of Formation help to detect the main oxides that will be formed on the workpiece (anode) [55]:

$$\Delta G = \Delta G_f^\circ + RT \ln Q \quad \text{Equation [3.10]}$$

$Q$  is the reaction quotient and  $R$  is the universal gas constant. (8.31451 J/ (k. mol)).

$T$  represents the temperature in Kelvin.  $\Delta G$  is the specific free energy difference between reactants and products (J/mol).  $\Delta G_f^\circ$  is the standard free energy of formation (J/mol). At equilibrium,  $\Delta G$  equals zero because there is no tendency for the reaction to proceed in either direction, resulting in equation [7].

$$\Delta G^{\circ}_f = -RT \ln K \quad \text{Equation [3.11]}$$

K is the equilibrium constant for the reaction. When  $\Delta G^{\circ}_f < 0$ , the reaction is spontaneous and favors the product. When  $\Delta G^{\circ}_f > 0$ , the reaction is not spontaneous.

Generally, electropolishing rates calculated by the following equation:

$$EP \text{ rate} = \frac{\left[ \frac{\text{Weight before EP} - \text{weight after EP}}{\text{Area}} \right]}{\text{time}} \quad \text{Equation [3.12]}$$

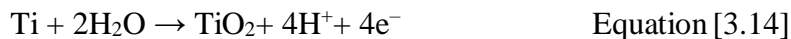
where (Weight before EP) is the weight of the test material workpiece before electropolishing and after surface preparation and (Weight after EP) is the weight of the material workpiece after electropolishing and post cleaning. The area is the total area of the material workpiece, and Time is the electropolishing time. The units of the EP rate were gram/ (cm<sup>2</sup>. min).

### 3.6 Reactions occurring during electropolishing of Titanium

Electropolished Titanium alloys are generally covered by a thin (about 3 nm) oxide film layer which is chargeable for increasing the corrosion resistance and bio-compatibility of Ti based alloys. This oxide layer is unstable for low pH levels and high concentrations of fluorine, which has even a stronger affinity for titanium atoms more than oxygen [76].

The oxide layer of titanium participates in the protection of the surface from any oxidation, it also acts as a diffusion barrier, by decreasing the presence of some toxic elements that could be present in titanium alloys; for example in Nitinol, there is a nickel which is considered toxic for the human body by creating this homogeneous oxide layer [55].

A titanium oxide layer (TiO<sub>2</sub>) quickly covers the metals, especially after being exposed to ambient air or water; this gives the metals his inertness nature, by following those reactions [77]:

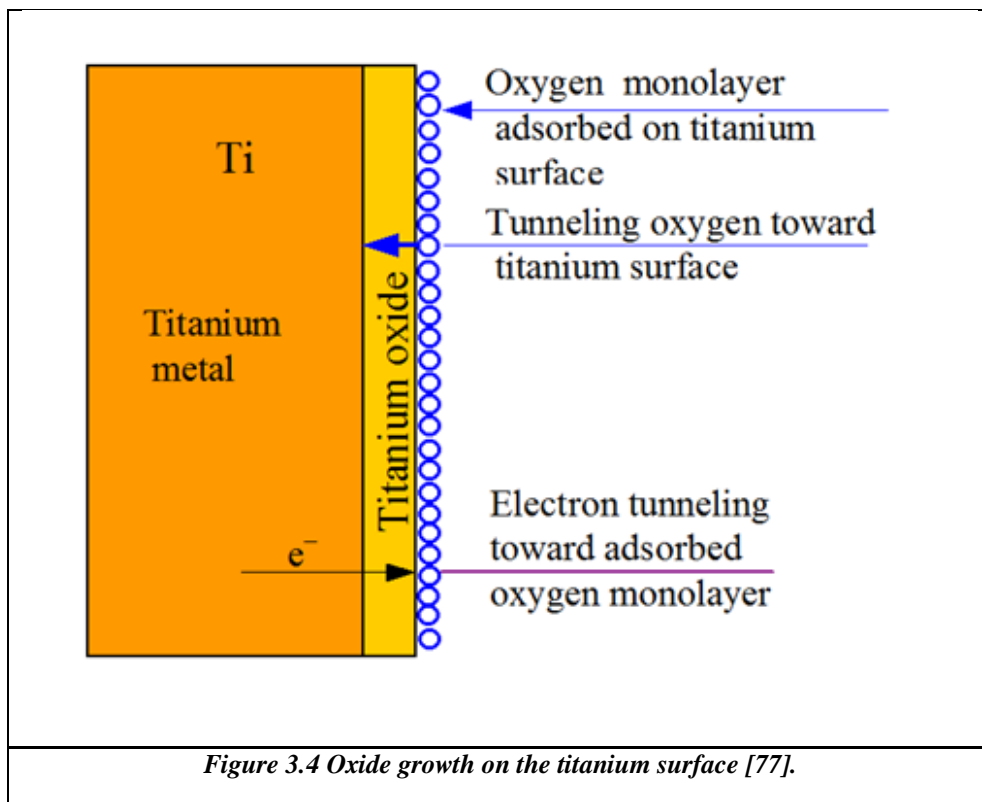


The stability of TiO<sub>2</sub> can be affected only by the presence of some media in which HF or H<sub>2</sub>O<sub>2</sub> are present: they can effectively drive to the dissolution of the oxide layer on the

surface. Normally without the influence of adverse environmental conditions, the oxide is quite stable in a wide range of pH between ~2 – 12 [77].

The protectiveness of the passive film on titanium depends on several parameters associated with the treatment process, such as thickness, morphology, homogeneity, type, and volume of chemicals species combined in its surface.

The oxide of titanium is considered a semiconductor, which means that the transport of anions is controlling the growth of the film and it is linked to the activity of oxygen ions through the titanium metals. Anyway, the activity of oxygen ions is linked to the thickening of oxide film layer [77]. Oxide of titanium could be found in three main forms which are: 1- rutile (tetragonal lattice), 2- anatase (tetragonal lattice), 3- brookite (orthorhombic) [77].

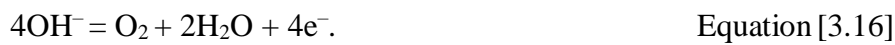


During electropolishing of titanium, the natural oxides already present on the surface will be dissolved, and a new fresh and homogeneous oxide layer is created during the process; this oxide layer has an important role as, already evidenced, it has an influence on the electrochemical properties of the base material. The following reactions occur in the electrolyte, describing the electropolishing process at the anode and the cathode.

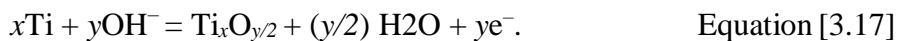
**1. A dissolution and transferring of titanium ions from the anode into solution.**



**2. Evolution of the oxygen from the anode surface.**



**3. Formation of the passive film on the anode surface.**



The oxide layer created by the electropolishing method is very homogeneous, even if some imperfections are created, such as holes. This oxide layer is very stable, as already anticipated, and it resists to the aggression of many different ambient media; the different thicknesses of oxide create also interference effects, giving the Ti oxide layer its characteristic colors, the electropolished samples could maintain their color, because of their stability, without changes for long periods of time. On the other hand, the naturally formed oxide layer on a non-electropolish sample is less chemically stable and less resistant to oxidation in ambient air [78].

### **3.7 Surface phenomena occurring during electropolishing**

Understanding the phenomena which occur on the metal surface during electropolishing helps to optimize the electropolishing procedure. Generally, electropolishing is limited by mass transport phenomena. The precipitates which are formed on the surface of the metal are caused by the presence of diffusion-limited species. The high electrical resistance of the salt film, formed during electropolishing, is due to its low porosity and its large thickness. The

buildup of a large thickness film is caused by the low mobility of ions during state transport process [79]. The salt film that is formed on the surface subjecting dissolution is a result of a polluted oxide that has integrated anions from the electrolytic solution. The salt film due to the fact that gas bubble evolution does not happen on the surface even if the potential was high, its related to the non-electron conducting nature of the film [69].

The cations which are formed by the metal oxidation will be removed from the surface by the acceptor ions.

### **3.8 Pitting during electropolishing**

Pitting is a type of corrosion, considered one of the main problems affecting the electropolished surface. Generally pitting appears in several metals and alloys after immersion in acid solutions. The evolution of oxygen on the anode or the formation of hydrogen on the cathode could be responsible for the formation of pitting; this problem could be solved by decreasing the oxygen bubble formation and adhesion to the cathode surface, and by increasing the potential. For what concerns the hydrogen formation at the anode surface, the pitting should be avoided by decreasing its production at the anode and preserving the ionic conductivity of the electrolytic solution.

Others factors causing pitting are stresses on the surface, the surplus stirring in the electrolyte bath, different treatment on the surface [80].

The presence of residual stresses could cause pitting on the surface, as shown by Frankenthal [81]; a relevant pit growth was found more for mechanically polished Fe-Cr alloys than for the electropolished one, due to the surface plastic deformation induced during the mechanical polishing.

Other reasons related to the presence of pitting are the presence of inclusions; during electropolishing, all the sites with inclusions would not have the protective film layer. The lack of this protective film would result in a higher local chemical etching, and enhance the pitting in correspondence of the inclusion site [82]. An improved stirring of the electrolyte is used to maintain the viscous film as thin as possible, as well to obtain a higher dissolution rate by increasing the current, with the objective of decreasing the pitting formation [82].

Three important factors are to be considered to control the corrosion rate and to obtain a pit-free surface, that is the current density, the mass transfer and the applied voltage on the polishing plateau. The pitting occurs when a high current density develops on a passivated metal surface, due to a breakdown of the passive layer in the presence of high acid concentration.

The precipitation of the salt film affects the stability of the pits due to the absence of the oxide layer in the precipitation site. The salt film is important to keep the potential of the metal in the active region, while the rest of the metal surface is in the passive region [69].

## Chapter 4 Materials and methods

### 4.1 Materials

#### 4.1.1 L605

Samples of the alloy L-605 (also referred to as HAYNES® 25) are manufactured by Rolled Alloys-Canada. The nominal composition of the alloy is reported in the following Table 4.1.

|            | <b>Cr</b> | <b>Ni</b> | <b>Co</b> | <b>W</b> | <b>C</b> | <b>Fe</b> | <b>Mn</b> | <b>Si</b> | <b>P</b> | <b>S</b> |
|------------|-----------|-----------|-----------|----------|----------|-----------|-----------|-----------|----------|----------|
| <b>MIN</b> | 19.0      | 9.0       | -         | 14.0     | 0.05     | -         | 1.0       | -         | -        | -        |
| <b>MAX</b> | 21.0      | 11.0      | Balance   | 16.0     | 0.15     | 3.0       | 2.0       | 0.4       | 0.04     | 0.03     |

*Table 4.1 Chemical analysis of Co-Cr alloy L605 from ``Rolled Alloy Canada`` [83].*

#### 4.1.2 Pure Titanium

Pure Titanium samples of the alloy CP-3GR 2 known as CP Titanium grade 2, manufactured by Rolled Alloys-Canada. The nominal chemical composition is reported in the following Table 4.2.

|            | <b>C</b> | <b>N</b> | <b>O</b> | <b>H</b> | <b>Fe</b> | <b>Others, total</b> | <b>Ti</b> |
|------------|----------|----------|----------|----------|-----------|----------------------|-----------|
| <b>Max</b> | 0.08     | 0.05     | 0.2      | 0.015    | 0.1       | 0.30                 | Balance   |

*Table 4.2 Chemical analysis of pure Titanium alloy from ``Rolled Alloy Canada`` [84].*

### 4.2 Methods

#### 4.2.1 Cleaning of L605 and pure Ti samples (pre-electropolishing cleaning)

Samples of L605 and pure Ti (10 mm x 10 mm), as received were thoroughly cleaned with different solvents before any further treatment. Firstly, the samples were cleaned with soap and water to remove oil, lubricant form residual thermomechanical treatments, dust particles or other impurities found on the surface of the metal after the preliminary manipulation (stocking, cutting, rolling, etc.). They were then placed successively in a 50 mL acetone beaker (99.5%, Fisher Science, Fair Lawn, New Jersey), and then subjected to ultrasounds





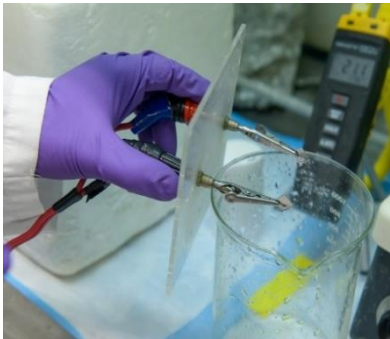
cleaning for 10 minutes. The samples were extracted, rinsed with deionized water and then dried with compressed air. The same cleaning step was repeated twice again, using a different solvent each time, that is deionized water after acetone and finally methanol (99.8%, J. T. Baker, California). The temperature of the solvents was in the range 22,5 – 25,0°C.



#### 4.2.2 Electropolishing processes

A 400 mL beaker, of a diameter of around ~10 cm, was used as an electrolyte cell (100 mm diameter and 70 mm height). For L605 electropolishing, another 10 mm x 10 mm piece of L605 was used as a cathode; for pure Ti electropolishing, another 10 mm x 10 mm piece of pure Ti was used as a cathode. Samples to be treated were used as an anode (positive potential). The two samples were kept in place by a metallic stainless-steel crocodile holder, connected to a power supply (AMETEK, SORENSEN, XHR 100-10); the potential that the machine could apply was in the range of 0 - 100 Volt, while the electric current was in the range 0 - 10 A. When the electric current passes through the anode, an oxidation process

takes place, and metallic ions go into the electrolytic solution. At the cathode (the negative electrode) the production of hydrogen was evident, while at the anode some oxygen was produced. The distance between the two electrodes was fixed at 60 mm. A more precise explanation of the mechanisms involved in the electropolishing processes is given in chapter 3.

|   |  |   |
|---|--|---|
|    |   |                                 |
| <p><i>Figure 4.2. A Show power supply composed of current and voltage, they are connected to the cathode and anode.</i></p> | <p><i>Figure 4.2. B Shows the electrolytic cell which occurs the acidic solution that used for electropolishing.</i></p> | <p><i>Figure 4.2.C Shows the anode (positive potential in red) and cathode (negative potential in black).</i></p> |
| <p><b>Table 4.3 Electropolishing system [86].</b></p>   |  |   |

#### 4.2.2.1 Electrolytic solutions for L605 samples

A 200 mL amount of fresh electrolyte was used every three electropolished samples; the dissolved ions in solution from the anode modifies the concentration of the electrolyte salts so that the electrolyte composition is modified. The electropolishing was conducted by cycles of around 2 minutes each. After each cycle, the samples were extracted, rinsed by deionized water, dried by compressed air, and then returned in the electrolyte for another 2 cycles. At the end of each cycle, the sample was always cleaned as previously described.

A current source was used with a fixed current in the range of 2.8 – 3.0 A; consequently, the voltage was oscillating in the range 23 – 14 V depending on the temperature of the solution. The electrolyte was placed in an ice box to decrease the temperature and keep it stable during the electropolishing; for a temperature between 2°C and 10°C, the measured voltage was around 23 – 25 V, decreasing down to 12 – 14 for temperatures as high as ~40°C. For higher

temperatures, the deposition of salts, probably Co phosphates and sulfates, take place, covering the electrodes with a red-brownish deposit. These salts can be easily removed by a fresh electrolyte solution and/or by cleaning with deionized water.

The main electropolishing solution was composed by 60 vol. % H<sub>3</sub>PO<sub>4</sub>, 27 vol. % H<sub>2</sub>SO<sub>4</sub>, 10 vol. % deionized H<sub>2</sub>O. Some other acids or chemicals in different quantities were added to this «base recipe» or «base electrolyte», such as hydrofluoric acid (HF), hydrochloride acid (HCl), and perchloric acid (HClO<sub>4</sub>), or viscous agents as glycerol, to investigate the effects of these components on the efficiency and efficacy of this electrolyte.

| Solutions  | H <sub>3</sub> PO <sub>4</sub> | H <sub>2</sub> SO <sub>4</sub> | H <sub>2</sub> O | HF  | Glycerol |
|--|--------------------------------|--------------------------------|------------------|-----|----------|
| <b>1</b>   | 68,38 %                        | 20,42%                         | 10,20%           | 1%  | 10 drops |
|  | 67%                            | 20%                            | 10%              | 3%  | 10 drops |
|  | 65,61%                         | 19,58%                         | 9,97%            | 5%  | 10 drops |
|  | 64,23%                         | 19,17%                         | 9,58%            | 7%  | 10 drops |
|  | 62.16%                         | 18,55%                         | 9,27%            | 10% | 10 drops |
| <b>2</b>   | 66,30%                         | 19,79%                         | 9,89%            | 3%  | 1%       |
|  | 64,92%                         | 19,38%                         | 9,96%            | 3%  | 3%       |
|  | 63,54%                         | 18,96%                         | 9,48%            | 3%  | 5%       |
| <b>3</b>   | 64,92%                         | 19,38%                         | 9,96%            | 5%  | 1%       |
|  | 63,54%                         | 18,96%                         | 9,48%            | 5%  | 3%       |
|  | 62,08%                         | 18,55%                         | 9,27%            | 5%  | 5%       |
| <b>4</b>   | 63,54%                         | 18,96%                         | 9,48%            | 7%  | 1%       |
|  | 62,08%                         | 18,55%                         | 9,27%            | 7%  | 3%       |
|  | 60,78%                         | 36,28%                         | 9,07%            | 7%  | 5%       |
| <b>Table 4.4 The different amounts of HF and glycerol in the main electropolishing solutions. The given percentages are in volume.</b> |                                |                                |                  |     |          |

| Solutions | H <sub>3</sub> PO <sub>4</sub> | H <sub>2</sub> SO <sub>4</sub> | H <sub>2</sub> O | HCl | HClO <sub>4</sub> | Glycerol |
|-----------|--------------------------------|--------------------------------|------------------|-----|-------------------|----------|
| 5         | 68,38 %                        | 20,42%                         | 10,20%           | 1%  | --                | 10 drops |
|           | 67%                            | 20%                            | 10%              | 3%  | --                | 10 drops |
|           | 65,61%                         | 19,58%                         | 9,97%            | 5%  | --                | 10 drops |
|           | 62.16%                         | 18,55%                         | 9,27%            | 10% | --                | 10 drops |
| 6         | 68,38 %                        | 20,42%                         | 10,20%           | --  | 1%                | 10 drops |
|           | 67%                            | 20%                            | 10%              | --  | 3%                | 10 drops |
|           | 65,61%                         | 19,58%                         | 9,97%            | --  | 5%                | 10 drops |
|           | 62.16%                         | 18,55%                         | 9,27%            | --  | 10%               | 10 drops |

*Table 4.5 The different amounts of HCL and HCLO4 on the main electropolishing solutions. The given percentages are in volume.*

Table 4.6 shows some solutions whose chemical composition is different from the groups shown in Table 4.4 and Table 4.5, from reference [87] [88]. The presence of pitting fond mainly on the periphery of the sample will be discussed in chapter 5.

| Solutions | CH <sub>3</sub> COOH | HClO <sub>4</sub> | H <sub>2</sub> O | Glycerol |
|-----------|----------------------|-------------------|------------------|----------|
| 7         | 70 %                 | 20%               | 10%              | --       |
|           | 60%                  | 10%               | 10%              | 20%      |
|           | 60%                  | 15%               | 20%              | 5%       |
|           | 75%                  | 15%               | --               | 10%      |

*Table 4.6 The different solution used for electropolishing of L605 [87]. The given percentages are in volume.*

#### **4.2.2.2 Rinsing (post-electropolishing treatment)**

At the end of the electropolishing phase, that is after the 2<sup>nd</sup> or 3<sup>rd</sup> electropolishing cycle, another step of the whole pre-treatment procedure was carried out to remove acidic remains from electropolishing. Electropolished samples were at first immersed in a 20 mL beaker deionized water ultrasound bath, rinsed with deionized water and dried by compressed air; secondly they were immersed in a 20 mL NaOH 1 N (Sigma-Aldrich) ultrasound bath, rinsed with deionized water and dried by compressed air; and finally samples were again immersed in a 20 mL beaker deionized water ultrasound bath, rinsed with deionized water and dried by compressed air.

The effect of the duration and/or presence of the previously described steps was investigated in the present work, and the outcomes are described in chapter 5.

#### **4.2.2.3 Electrolytic solution for Titanium**

Even in this case, A 200 mL amount of fresh electrolyte was used every three electropolished samples, as already evidenced by L605 samples. The electropolishing process was one minute for just one time without repetition, and then the samples were dried.

The power source delivered a 6 A-fixed current; a voltage in the range of 50 – 80 Volts was obtained for the considered currents. The used electrolyte volume was 200 mL. The electrolyte was placed in the ice to decrease the temperature and keep it stable during the electropolishing. The electrolyte temperature during the process was between 20°C and 30°C, and after each cycle of electropolishing (duration of one minute) of pure Ti, the temperature increased up in the range 70 °C – 80 °C.

| Number  | Solutions   | Voltage (V) | Current (A) | Time (sec.) | Temperature (°C) |
|---|---|-------------|-------------|-------------|------------------|
| N° 1  | 70% (H <sub>2</sub> SO <sub>4</sub> )<br>5% (HNO <sub>3</sub> )<br>5% (HF)<br>20% water | 30          | 2,5         | 60          | 5 - 30           |
| N° 2  | 90% (H <sub>2</sub> SO <sub>4</sub> )<br>5% (HNO <sub>3</sub> )<br>5% HF                | 50 - 40     | 5.5         | 120         | 20 - 40          |
| N° 3  | 10% methanol<br>70% ethanol<br>20% (HClO <sub>4</sub> )                                 | 30 - 60     | 1.5         | 60          | 0 - 5            |
| N° 4  | 80% (CH <sub>3</sub> COOH)<br>20% (HClO <sub>4</sub> )                                  | ~ 60        | 0.8         | 30          | 0 - 10           |
| N° 5  | 60 % ethanol<br>30% H <sub>2</sub> SO <sub>4</sub><br>10% methanol                      | ~70         | 1.1         | 60          | 0 - 5            |
| <b><i>Table 4.7 The different solutions were tested on pure Ti samples.</i></b> |   |             |             |             |                  |

This work was a preliminary screening of the appropriate chemical composition for a solution for Ti electropolishing. Different Ti alloys may require different electrolytes, so that a specific work will be carried out in case for specific alloys. The choice of a good electropolishing medium was made based on some morphological features found on the final surface of Ti samples. Optical microscopy was mainly used to investigate the surface at different magnification. This led to a preliminary analysis of the samples, then confirmed or improved by scanning electron microscopy, to investigate the features of the surface, such as for example presence of pitting on the corner of the sample, the amount of micro-smoothing or macro-smoothing, and the grain boundary etching. Solution number 2 gave the best features compared to other solutions; the electrolyte was tested with different concentrations of the composing chemical, as shown in *Table 4.8*.

| Solution | CH <sub>3</sub> COOH | H <sub>2</sub> SO <sub>4</sub> | HF  | Voltage (V) | Current (A) | Time (sec.) | Temperature (°C) |
|----------|----------------------|--------------------------------|-----|-------------|-------------|-------------|------------------|
| N° 6     | 50 %                 | 40%                            | 10% | 70 – 20     | 3           | 60          | 20 – 30          |
| N° 7     | 65%                  | 30%                            | 5%  | 90 – 70     | 3           |             |                  |
| N° 8     | 75%                  | 20%                            | 5%  | 90 – 80     | 3           |             |                  |
| N° 9     | 50%                  | 35%                            | 15% | 60 – 40     | 5           |             |                  |
| N° 10    | 55%                  | 35%                            | 10% | 80 – 50     | 6           |             |                  |

*Table 4.8 The different concentration used from solution number 2 which as tested in Table 4.7.*

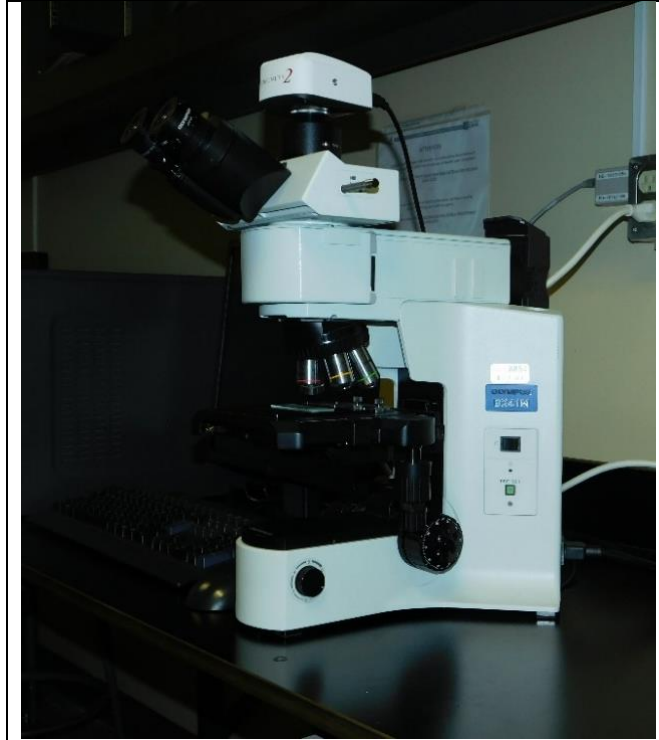
The samples were cleaned as described in section 4.2.1. After the electropolishing process, another 20 mL beaker ultrasound bath with only deionized water was carried out for duration of 15 minutes, to clean the sample from possible acidic residuals.

### 4.3 Characterization

The analysis of the surface morphology and its chemical composition was performed for a better understanding of the surface finish before and after electropolishing. The used characterization methods are the following ones:

#### 4.3.1 Optical microscopy (OM)

Light or optical microscopy is considered as the primary means for scientists and engineers to examine the microstructure of materials. The microstructure of samples was studied with an Olympus BX41M optical microscope (OM) using different magnifications (50X, 100X, 200X, 500X). Optical microscopy is known as a basic tool for microstructural examination of materials including metals, ceramics, and polymers. Reflected-light microscopes are the most commonly used for metallography, [89]. The software used for the acquisition of images was the one provided with the digital camera.

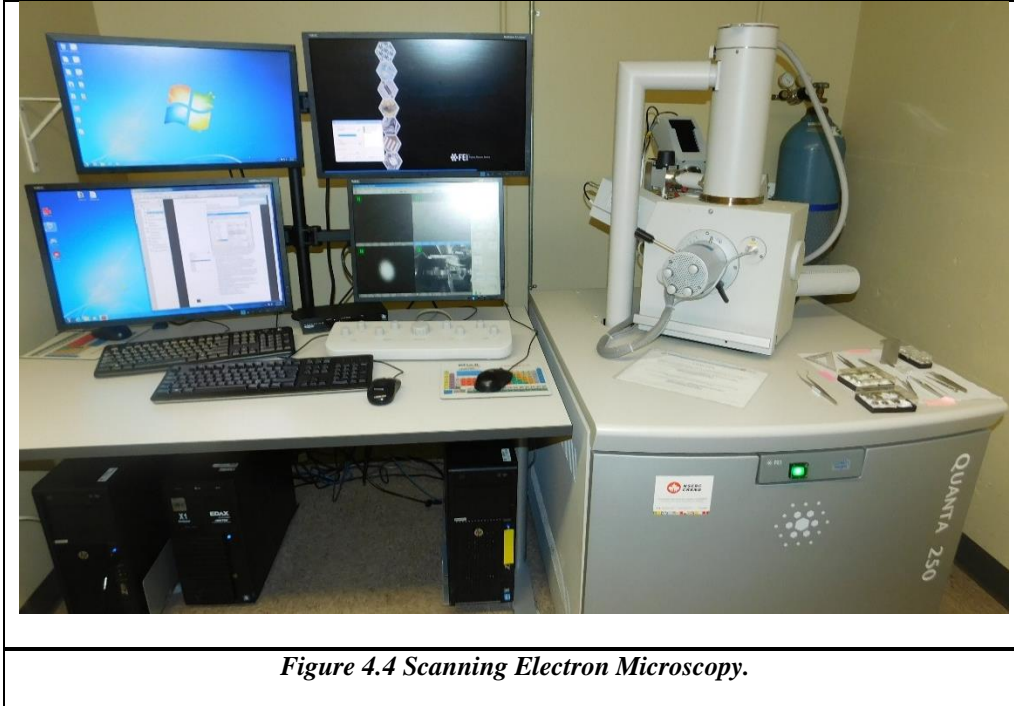


*Figure 4.3 Olympus BX41M optical microscopy.*

#### **4.3.2 Scanning Electron Microscopy (SEM)**

Scanning Electron Microscopy (FEI Quanta 250 Scanning Electron Microscope) with a tungsten filament and an acceleration voltage in the range of 15 - 30 kV was used. Surface structure was observed by different magnifications such as 50X, 100X, 500X, 1000X, and 2000X to evaluate the effect of the electropolishing process on the surface topography. This technique permits to characterize the morphology of the sample surface by electron beam scanning on the material surface. Investigating the surface morphology of the samples. SEM image is formed by a focused electron beam that raster the surface area of a specimen [89]. The software used is a proprietary program (EDAX TEAM) version 2.4, the EDX operating system used is: Microsoft Windows XP Pro - SP3.





*Figure 4.4 Scanning Electron Microscopy.*

### 4.3.3 Atomic Forces Microscopy (AFM)

This technique was used for the observation of the surface topography and studying surface roughness before and after electropolishing at the atomic scale. These analyzes were carried out using an ultra-fine silicon tip with a radius of curvature of 2 nm by using two different scales, 1  $\mu\text{m}$  x 1  $\mu\text{m}$  and 50  $\mu\text{m}$  x 50  $\mu\text{m}$ . The study was done by using Atomic Force Microscopy (Veeco, Woodbury, NY, USA), then the analysis was carried out by supporting software WSxM5.0 Develop version 9.0 providing RMS and  $R_a$  surface roughness, defined by the following equations [90]:

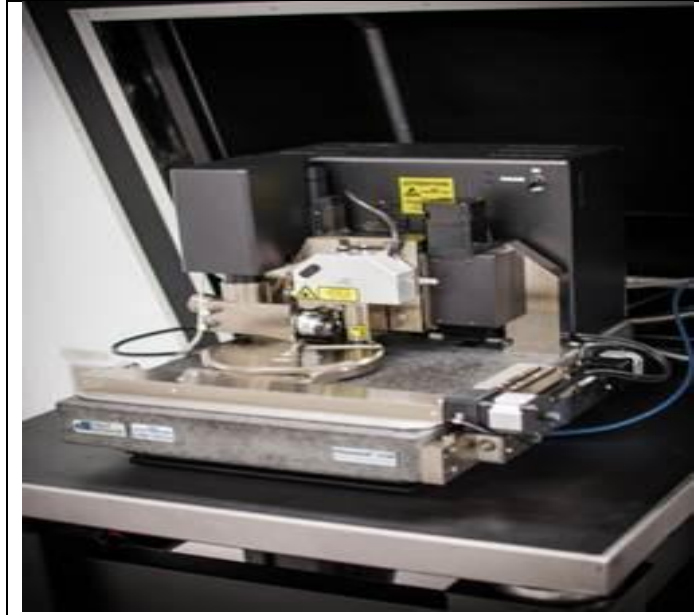
$$RMS = \sqrt{\frac{\sum_{i=1}^N (Z_i - Z_{ave})^2}{N}} \quad \text{Equation [4.1]}$$

$$R_a = \frac{\sum_{i=1}^N |Z_i - Z_{ave}|}{N} \quad \text{Equation [4.2]}$$

where  $z_i$  = vertical distance between the profile height at point i and the average profile line.

$Z_{ave}$  = height of the average profile line.

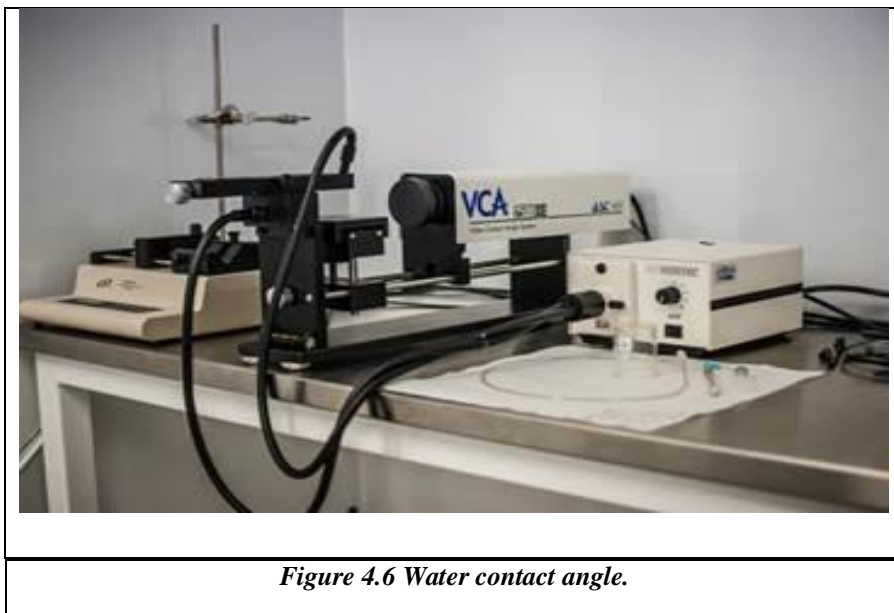
N = total number of points along the control distance.



*Figure 4.5 Atomic Forces Microscopy.*

#### **4.3.4 Contact angle**

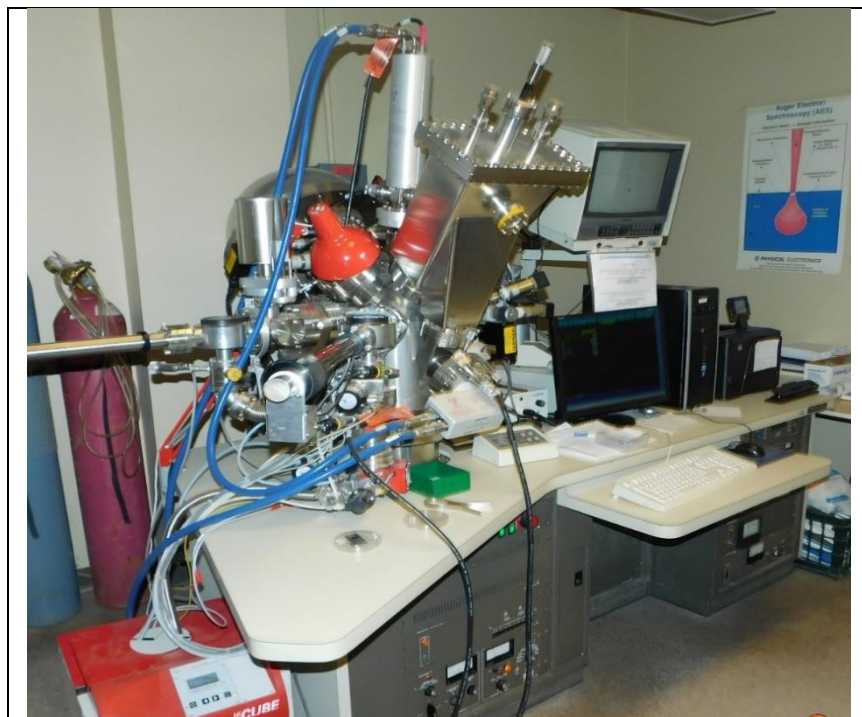
The contact angle technique used to calculate the value of the surface energy. A droplet is dropped on a solid surface. The liquid perimeter, that is the line describing the liquid shape of the droplet base in contact with the solid phase, is in equilibrium: on this liquid perimeter several forces are acting, that is one at the liquid-solid interface, another one at the liquid-gaseous interface and another one at the solid-gaseous interface. The angle formed between the liquid-gaseous and the liquid-solid interfaces,  $\theta$ , is indicative of the surface energy of our system. The material is said to be hydrophobic if  $\theta \geq 90^\circ$  and hydrophilic if  $\theta \leq 90^\circ$ . Contact angle measurements were performed with a VCA-2500 XETM visual system (Billerica Products, Inc., USA, AST Contact Angle). A volume of 3  $\mu\text{L}$  deionized water was used for each measurement, both for L605 and Ti samples. This method has been used to determine the hydrophobic or hydrophilic nature of the surface (wettability) and its energy [91].



#### **4.3.5 X-ray photoelectron spectroscopy (XPS)**

The chemical composition of the surface was investigated by an X-Ray Photoelectron Spectrometer (XPS – PHI 5600-ci spectrometer – Physical Electronics), with a base pressure below  $5 \times 10^{-9}$  mbar. Surveys and depth profiles were acquired at low resolution, using the  $K\alpha$  line of a standard aluminum X-Ray source powered at 400 W ( $K\alpha = 1486.6$  eV). High-resolution spectra (scanning of a defined region around a characteristic line) for C1s, O1s, Co2p<sub>3</sub> and Cr2p<sub>3</sub>, the main components of the surface after electropolishing, were acquired using the  $K\alpha$  line of the magnesium source ( $K\alpha = 1253.6$  eV). Survey spectra were recorded at a detection angle of  $45^\circ$  with respect to the surface plane. [89].

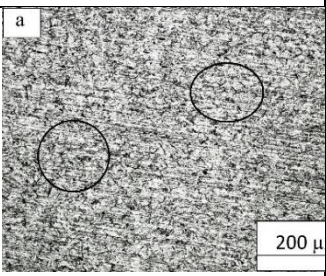
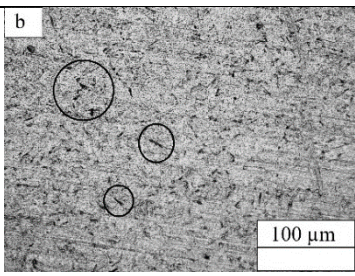
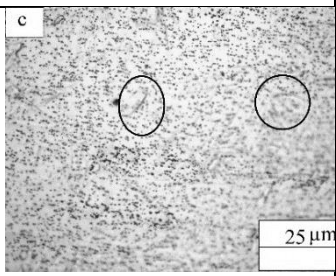
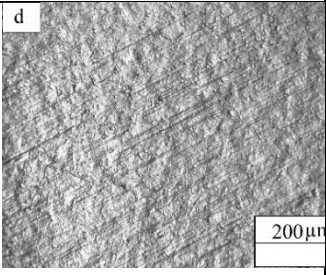
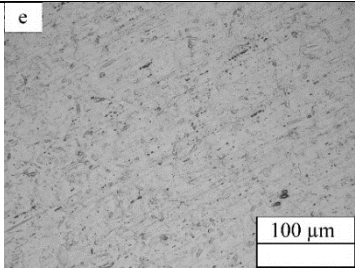
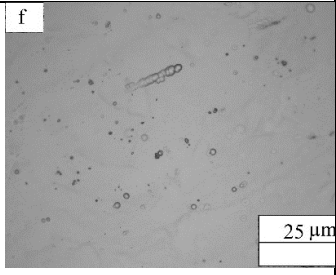
As the stoichiometry of the oxide layer is variable, the oxide layer thickness will be arbitrarily defined as the point where the oxygen signal decreases to half-maximum.



*Figure 4.7 X-ray photoelectron spectroscopy.*

## Chapter 5 Electropolishing of L605: Results and discussion

As already reported in the Materials and methods section, the main solution of electropolishing was composed as follow: 65% H<sub>2</sub>PO<sub>3</sub>, 20% H<sub>2</sub>SO<sub>4</sub>, 10% water, with stable temperature in the range 10 to 25 °C. The current was fixed at 3 A, and the voltage was between 15 and 25 Volt. Table 5.1 shows of as received and electropolished samples using optical microscopy at three different magnifications.

| L605           | 50 X  | 100 X  | 500 X   |
|----------------|---|--|---|
| As-received    |   |   |   |
| Based solution |  |  |  |

*Table 5.1 Optical microscopy images (a-c) as received sample, (d-f) represent respectively samples after electropolishing using the main based solution.*

Some scratching on the surface of as received samples are visible putted in a round circles, probably due to the manufacturing process during the fabrication. The stress and the temperature of the treatment during the hot rolling of the alloy had a relevant role on the structure of surface alloy and may be responsible for the inhomogeneous surface.

On electropolished sample, surface a preferential orientation of polishing is observed, this depends on the position of the two metallic electrodes, they were fixed in a parallel way instead of being perpendicular to each other. The parallel disposition will enhance the dissolution of the ionic metals. It is noticed that some waves caused by the process of dissolution which occurs at the anode, and the high density of pits it is indicative that the electropolishing was effective and it change the surface properties and its structure.

The magnification of 500X shows the presence of carbides. EDAX confirmed that they are chromium and tungsten carbides,  $M_6C_{23}$  [55].

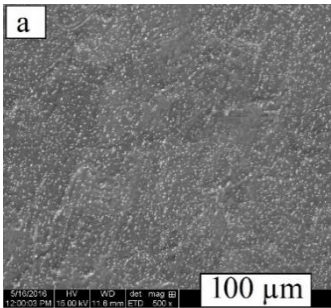
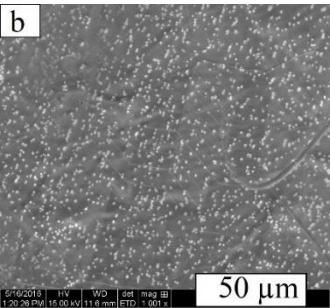
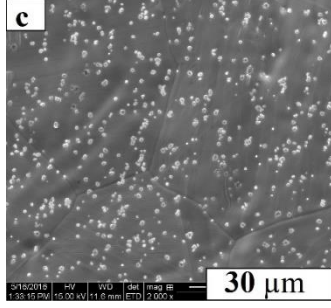
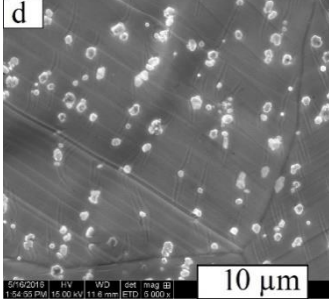
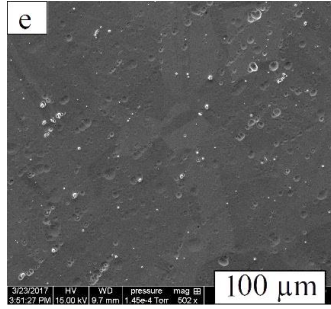
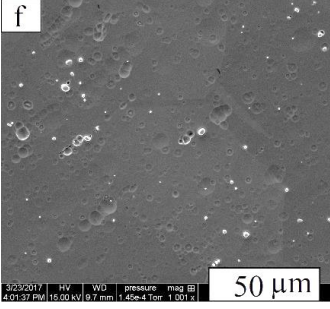
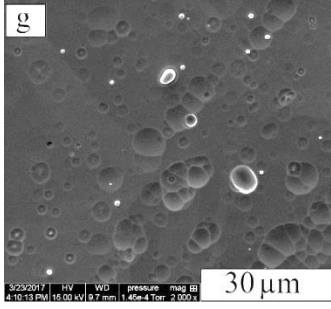
Table 5.2 show results using the electron secondary images by SEM for the as-received samples and the electropolished.

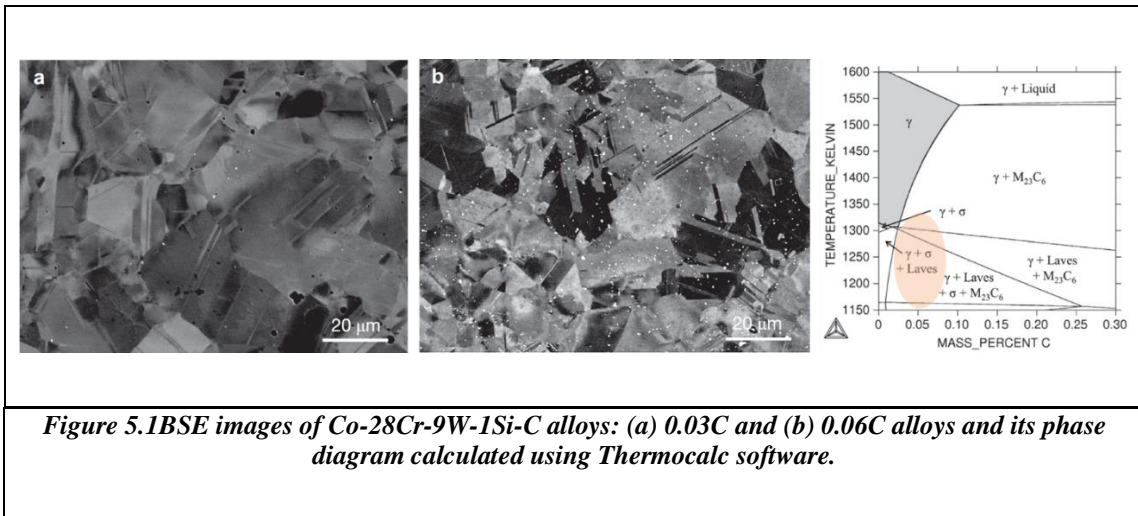
Different types of precipitates are visible on the SEM image. Roundly shaped, they were present mainly along the grains, or in the grain or at twin boundaries, depending on the applied thermomechanical treatment.

SEM analyses show changes in the microstructure and morphology. By secondary electrons images Table 5.2, bright precipitates were discovered in all the surface, predominantly inside the grains before electropolishing process.

This result is quite different from those reported in the literature [57][55]. Normally, bright precipitates as carbides, are found in the grain boundaries due to the presence of elements such as C, Si, and W. These phases can form different phase or intermetallic phases in the Co-Cr alloy. The Laves-phase are harmful in the application that needs a high temperature. They are acceptable for wear-resistance applications [53]. In SEM micrographs pits can be detected. They can be attributed to the detachment from the matrix of different kind of carbides. In general, chromium-rich carbides ( $Cr_7C_3$ ) are darker than the tungsten carbides ( $W_6C$ ), which are brighter, tungsten carbides  $W_6C$  tends to fill the spaces between chromium-rich carbides  $Cr_7C_3$ , by creating a thin film surrounding the chromium-rich carbides [92].

Table 5.2 indicates the presence of precipitates which increase proportionally with the amount of carbon in the Co-28Cr-9W-1Si alloy [93].

| L605  | 500 X   | 1000 X   | 2000 X  | 5000 X   |
|---|---|--|---|--|
| As<br>receive<br>d  |  |  |  |   |
|   | Based<br>solution   |  |  |  |
| <p><i>Table 5.2 Electron secondary images S by SEM of (a-d) as received and (e-h) Electropolished samples using the main based solution at different magnification.</i></p> |   |  |   |  |



The presence of Carbon induces the formation of carbides  $MC$ ,  $M_7C_3$  and  $M_{23}C_6$  and possibly  $M_6C$ , where  $M$  is a metallic element. They appear as bright precipitates in SEM images. The estimated chemical composition of this compounds was confirmed by EDS.

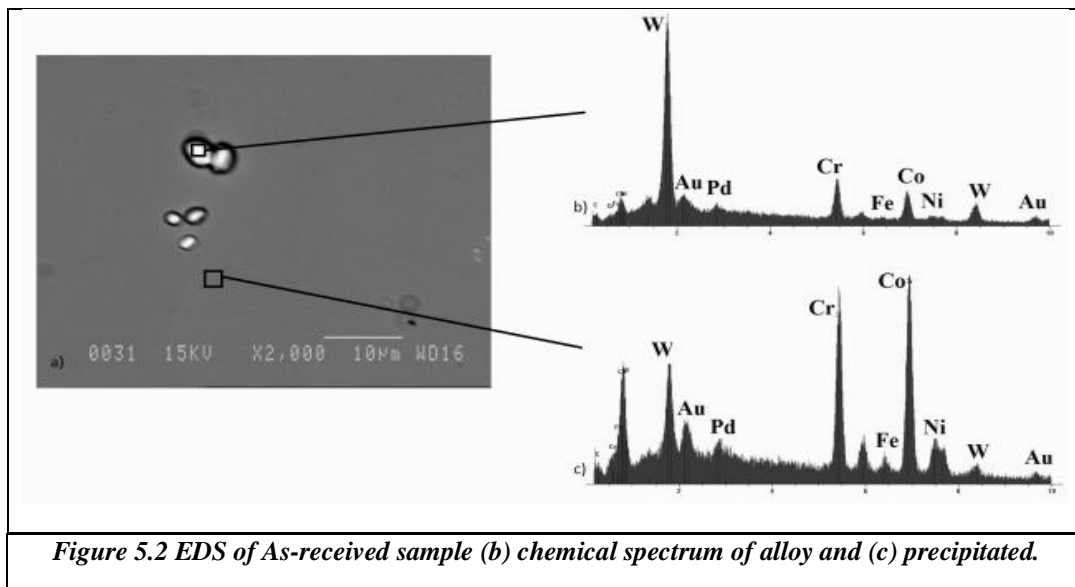




Figure 5.2 shows the EDS spectrum of L605 alloy in order to compare the chemical composition of the matrix and the one of the precipitates. It can be noticed that the spectrum of the bright precipitate showed a higher amount of W than the matrix, supporting the hypotheses that the found precipitates are metallic carbides. The matrix presented also a higher Cr and Co content than the precipitates, where W is dominant.

In general, the alloying elements (Cr, Mo, W, Al) are able to affect the properties of the alloys, especially the crystallographic nature of cobalt, due to their responsibility of the formation of second phases represented by the carbides [94]. Desai et al. [92] found that for cobalt-based alloys an increased size and volume fraction of the present carbides corresponds to an increased abrasive wear resistance. Cobalt base alloys contain a different type of metallic carbides, such as for example chromium-rich  $\text{Cr}_7\text{C}_3$  carbides,  $\text{Cr}_{23}\text{C}_6$ , and a volume of tungsten-rich  $\text{W}_6\text{C}$  carbides. Chromium-rich carbides exist as solid gray material, with high resistance of corrosion, and the ability to kept its strength even under a high temperature [95]. Those properties turn the carbides to an important additive element for the metallic alloys which will improve both wear and corrosion resistance. Pitting due to electropolishing is observed more when the carbides present a finer distribution and size. In general, are used strong acids for electropolishing to dissolve the metal, remove metallic ions, and creates a new protective oxide layer. Hydrofluoric acid is one of the common acids that is used for dissolving oxides and the metallic carbides [96]. The effect of acids on dissolving the carbides is related to the time that the metal has been heated during its finishing process. Longer the metal was heated, higher the time required to dissolve its carbides during electropolishing [96]. For smoother and homogeneous surface, the presence of grain boundaries and carbide are clearly observed. It is clear the electropolishing process removed certain structures which the chemical composition, as confirmed by EDS.

During electropolishing, the newly formed metallic surface is exposed to the chemical electrolyte. The mechanism providing the alternate formation of a salt layer and its detachment leads to the formation of pits and cracks on the surface. The main solution is effective in removing the products that are covering a stent surface. Burr and contaminations

formed during the production, and generally are removed by acids, even when they are produced by welding and heat treatments.

It is clear that the quality of the electropolished surface improved if compared to the one as received specimens was underlined.

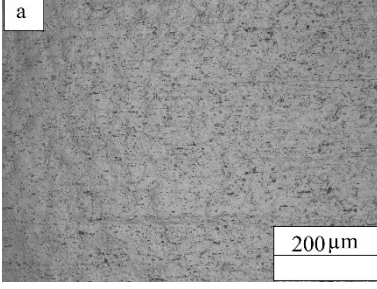
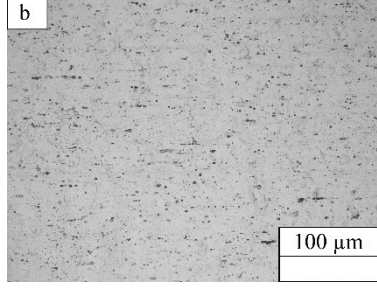
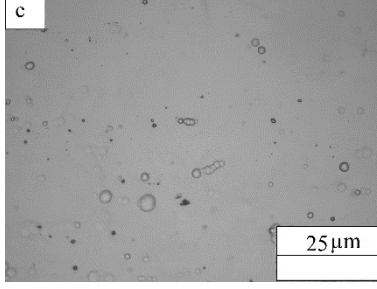
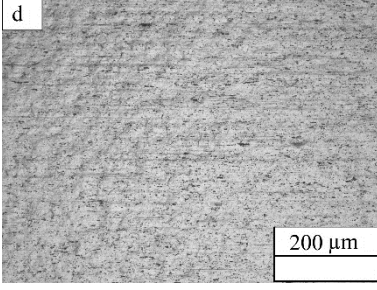
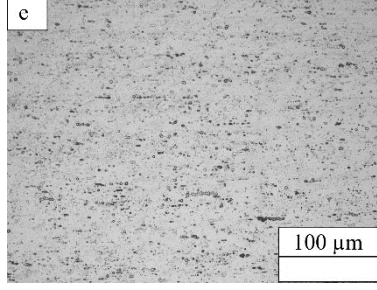
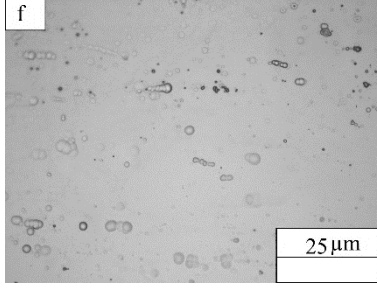
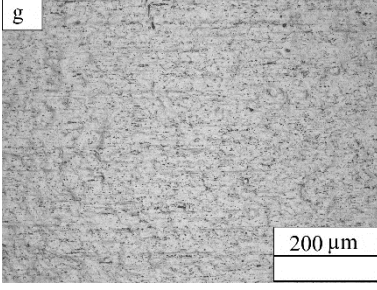
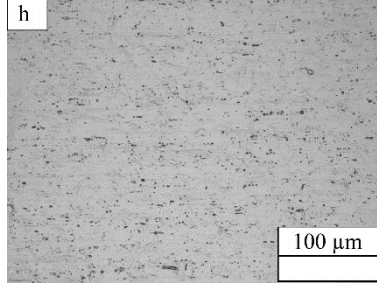
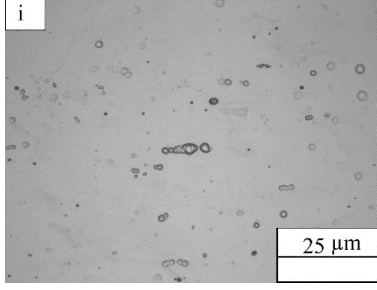
The presence of corrosion induced by the electropolishing process and acid attack, in fact, they result darker in OM, and brighter by SEM with respect to the grains. EDS spectrum of point A in Figure 5.2 shows the presence of O and Fe; Hence, the deposit represented in Figure 5.2 it could be a Fe oxide or hydroxide.

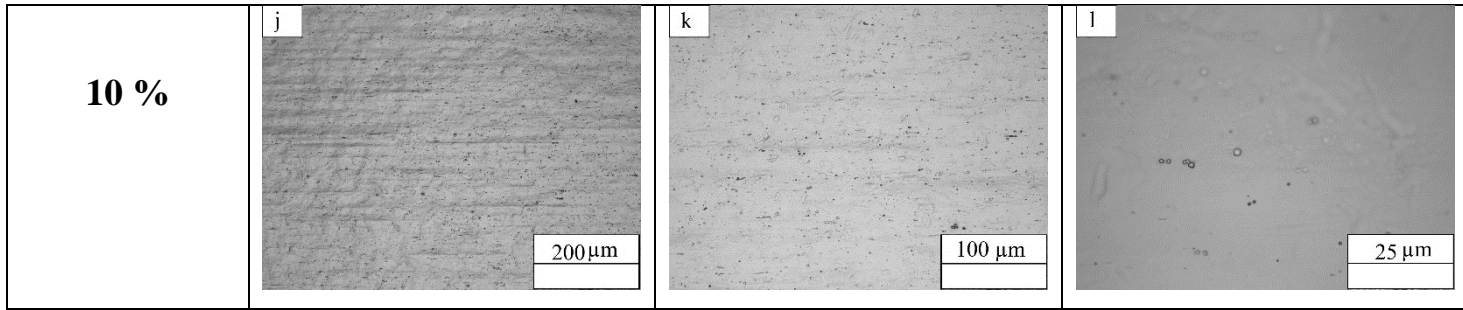
## **5.1 Effect of different amounts of acid addition**

The effect of the presence and the addition of different amounts of acids in the main electrolyte solution was investigated, such as hydrochloric acid (HCl), perchloric acid (HClO<sub>4</sub>), and hydrofluoric acid (HF). Samples were analyzed by optical microscopy and scanning electron microscopy (SEM), to study the morphology as a function of the different components of these electrolytes. They were all used with the same conditions, which means that the temperature was fixed in the range 10 - 25°C, the current also fixed at ~3 A, and the voltage was in the range 15 to 25 V.

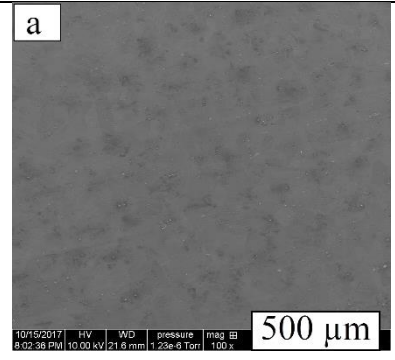
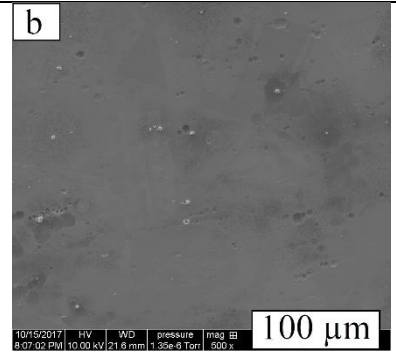
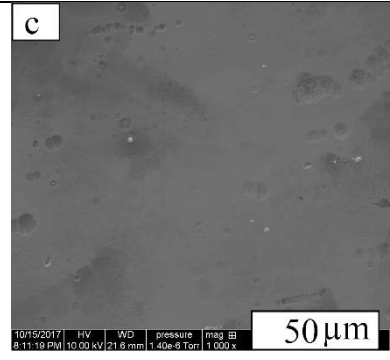
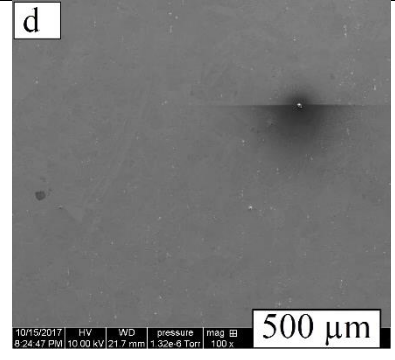
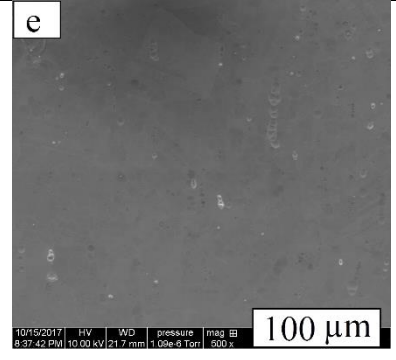
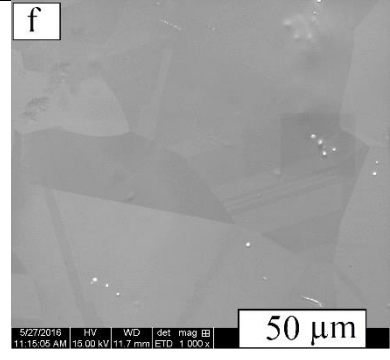
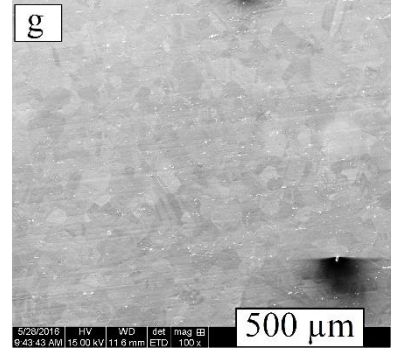
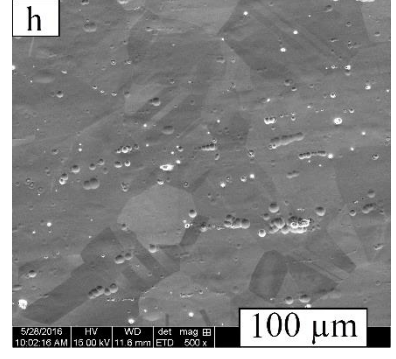
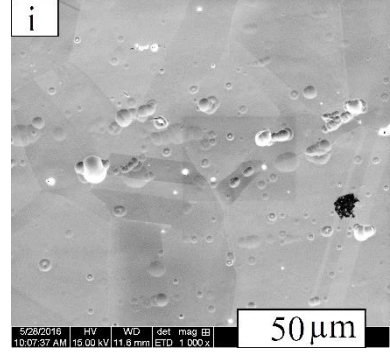
### **5.1.1 Effect of hydrochloric acid**

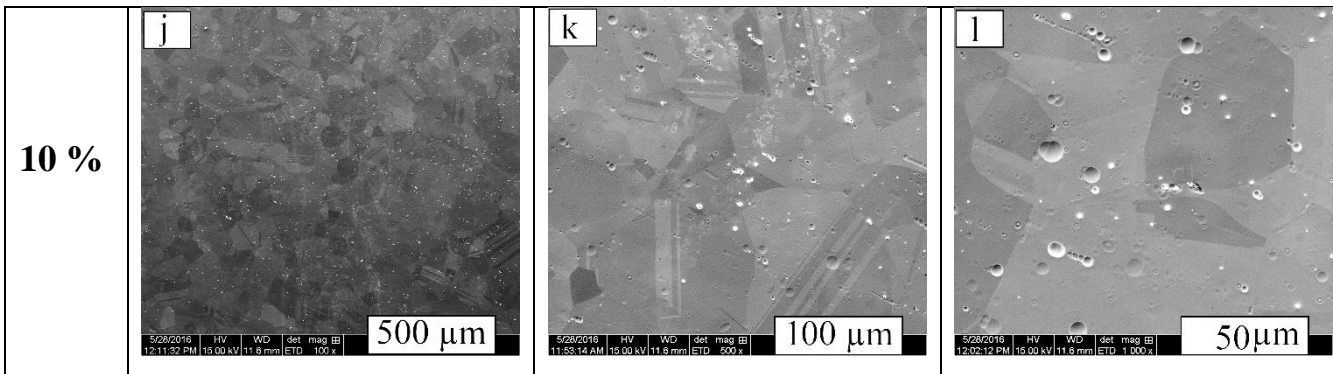
Hydrochloric acid needs to be diluted in water. It reacts with metal, and the outcome of the reaction depends on the chemical composition of the alloy; It can be used for pickling which is an important step to remove oxide and carbides from the metals. Active metals such as chromium and cobalt promote the development of H<sub>2</sub> from the electrolyte while inactive metals cannot remove it [97].

| HCl | 50 X   | 100 X   | 500 X  |
|-----|--|---|--|
| 1%  |   |   |   |
| 3%  |   |   |   |
| 5%  |  |  |  |



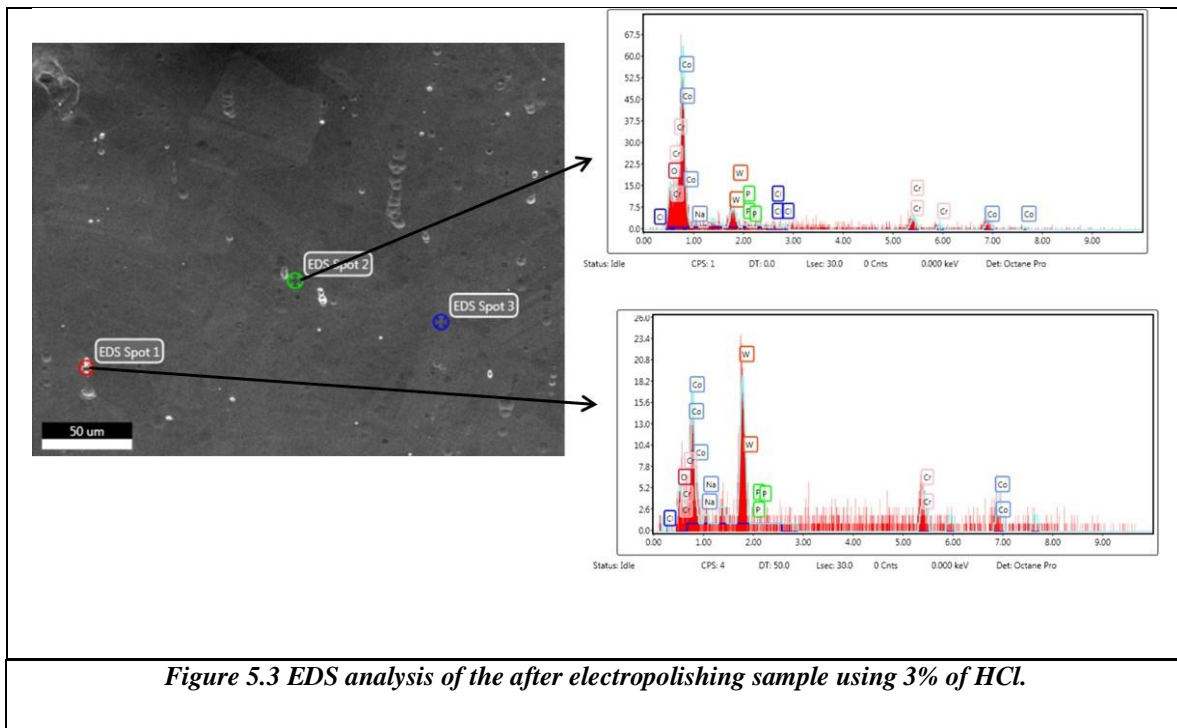
*Table 5.3 Optical microscopy using different addition of hydrochloric acid (a-c) with 1%, (d-f) with 3%, (g-i) with 5%, (j-l) with 10%.*

| HCl | 100 X  | 500 X   | 1000 X  |
|-----|--|---|---|
| 1%  |  <p>10/15/2017 HV 10.00 kV 21.6 mm pressure 1.23e-6 Torr mag 100 x 500 μm</p> |  <p>10/15/2017 HV 10.00 kV 21.6 mm pressure 1.35e-6 Torr mag 500 x 100 μm</p> |  <p>10/15/2017 HV 10.00 kV 21.6 mm pressure 1.40e-6 Torr mag 1,000 x 50 μm</p> |
| 3%  |  <p>10/15/2017 HV 10.00 kV 21.7 mm pressure 1.32e-6 Torr mag 100 x 500 μm</p> |  <p>10/15/2017 HV 10.00 kV 21.7 mm pressure 1.09e-6 Torr mag 500 x 100 μm</p> |  <p>5/27/2016 HV 15.00 kV 11.7 mm det mag 1,000 x 50 μm</p>                    |
| 5%  |  <p>5/28/2016 HV 15.00 kV 11.6 mm det mag 100 x 500 μm</p>                   |  <p>5/28/2016 HV 15.00 kV 11.6 mm det mag 500 x 100 μm</p>                   |  <p>5/28/2016 HV 15.00 kV 11.6 mm det mag 1,000 x 50 μm</p>                   |



**Table 5.4 ES by SEM using different addition of hydrochloric acid (a-c) with 1%, (d-f) with 3%, (g-i) with 5%, (j-l) with 10%.**

In general, during the reaction between an acid and a metal, one or more salts are produced, depending on the type of acid in the reaction. Hydrochloride acid produces chlorides salts which play a role in removing of the ionic metals from the surface. From Table 5.3, it is noticed, the more quantities of HCl added to the electrolytic solution, the fewer carbides are observed in the surface. For this reason, it is supposed that strong acids can dissolve the carbides from the alloy. Table 5.4 gives a better understanding of the changes that occurred in the topography of the surface samples with different addition of HCl. Comparing with OM micrographs, the results using SEM show that, the addition of 1 and 3 % of HCl has not a significant effect on the quantity of carbide on the surface. In the other hand, increasing the addition of HCl up to (5 – 10) % has a significant increase on carbide distribution on the surface. But using the previous high quantity of HCl did not give the expected brilliance to the surface after observing it. Sazou et al.[97] in its study found that mixing hydrochloride acid with phosphoric and sulfuric acid in the electro-dissolution process of a steel, would result in adsorption of the chloride ions on the oxide film that covers the surface, which will lead to increase the presence on carbides on the surface.



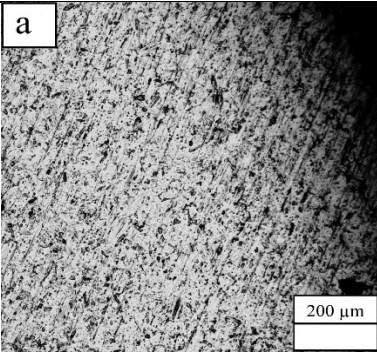
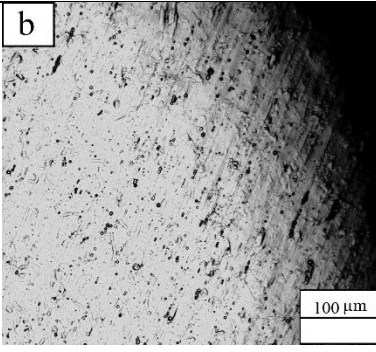
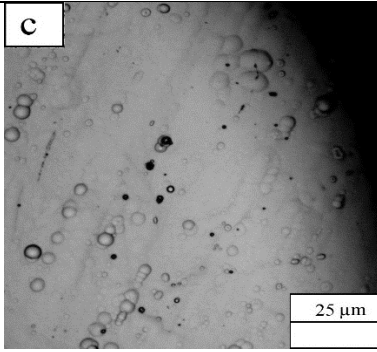
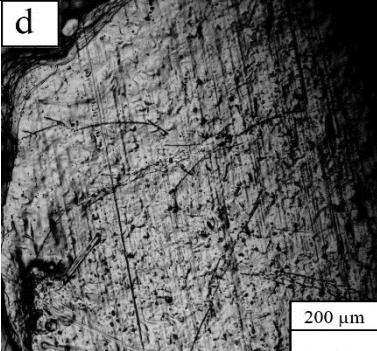
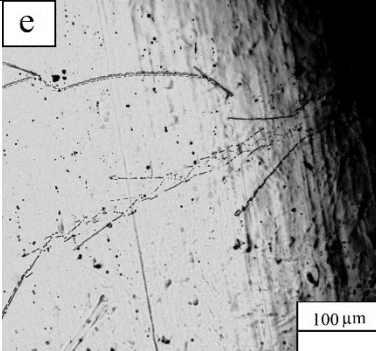
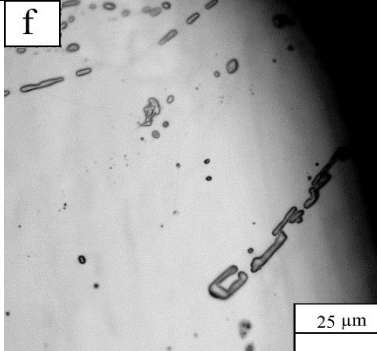
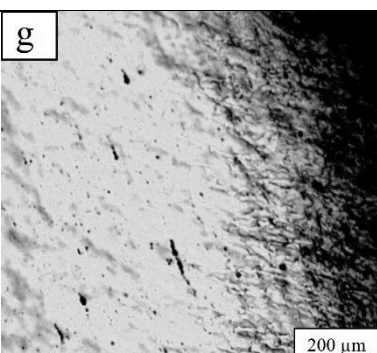
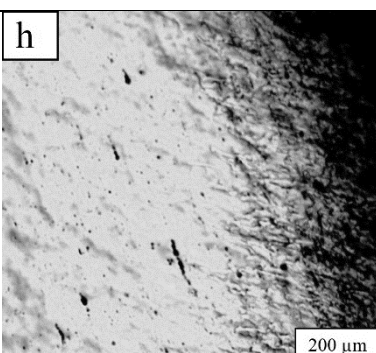
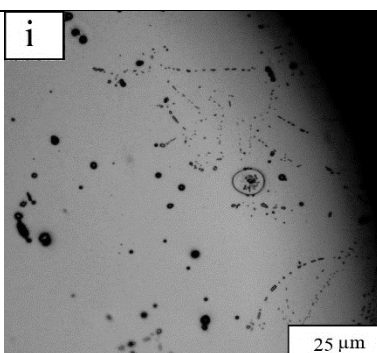
EDS analysis show (spot N°1, Figure 5.3) the identification of tungsten-rich carbides. For example,  $W_6C$  represented with a brighter large white particle formation phenomenon, comparing to the spot N°2 which shows a higher concentration on cobalt. The presence of carbides provides an important degree of wear resistance for the alloy, therefore no pitting was observed [95].

### **5.1.2 Effect of perchloric acid**

Perchloric acid is considered as one of the strongest acids, it is known to be a strong oxidizer at high temperatures, reacting in such a violent way that could lead to explosive mixtures. When it is mixed in aqueous solutions it loses its explosive oxidizing properties; it is very active with metal and it is used during electropolishing process of many metals such as aluminium, titanium, iron [98].

T. Hahn and A. Marder [99] reported the effect of the electropolishing variables, by comparing different quantity of perchloric and chromic acetic acid, in a solution used for electropolishing Cr-Mo-T11 steel, at different concentrations [99]. They concluded that the time has limited effect for the electropolishing when using perchloric acid solution, while the temperature has an important effect. Using a temperature equal to 25°C provide a good electropolished surface, comparing to 2°C, which gives corroded surface and pitting. They found that an increase in the percent of perchloric acid is associated with high current density at a constant voltage. Finally, they conclude that using 7.8% of perchloric acid at 2°C resulted in several pitting regions. Increasing the quantity of perchloric acid also increased the voltage and the current density. Less pitting and corroded region was found by using 5% of perchloric acid.



| <b>HClO<sub>4</sub></b> | <b>50 X</b>  | <b>100 X</b>  | <b>500 X</b>   |
|-------------------------|--|---|--|
| <b>1%</b>               |   |   |   |
| <b>3%</b>               |   |   |   |
| <b>5%</b>               |  |  |  |

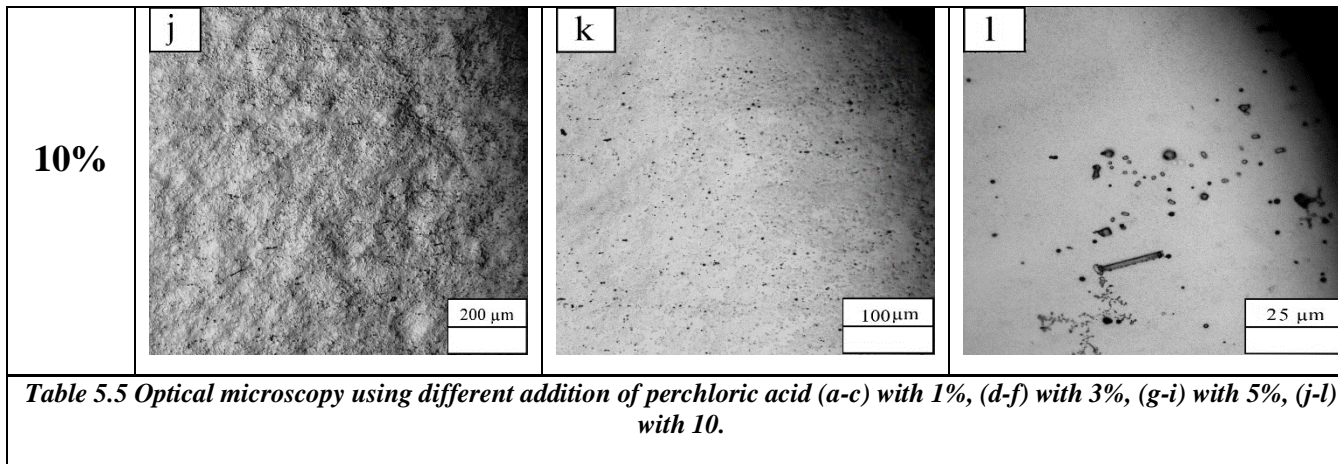
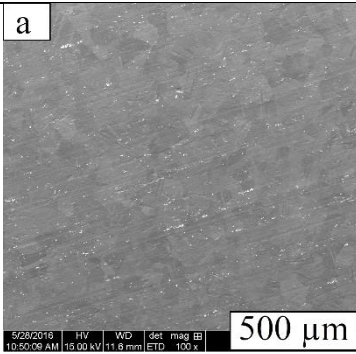
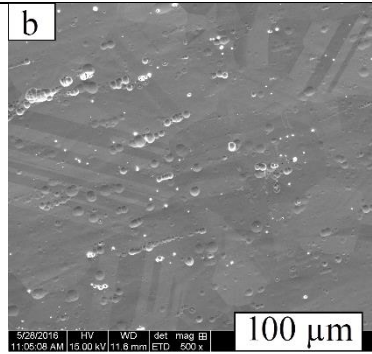
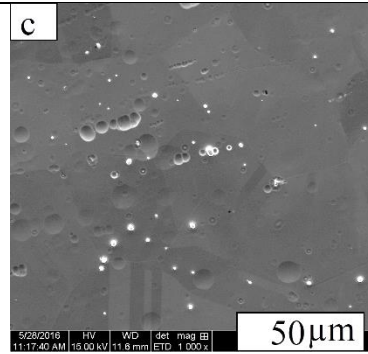
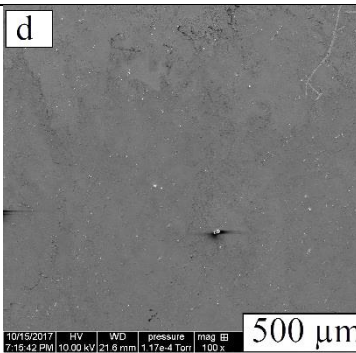
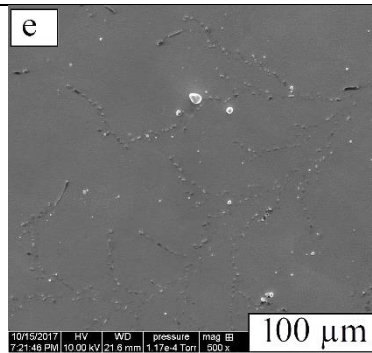
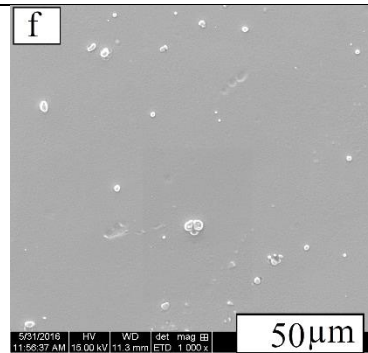
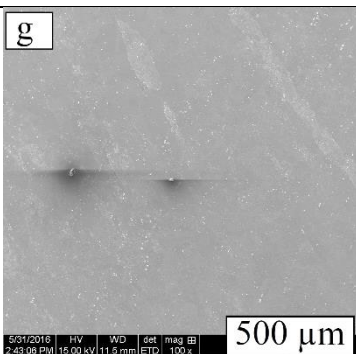
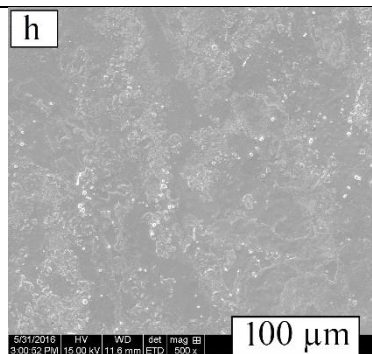
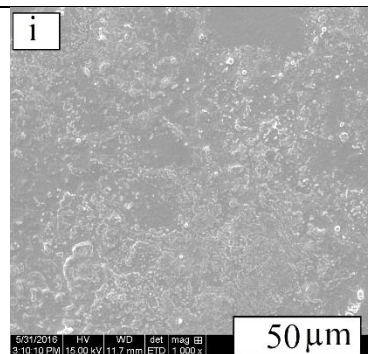
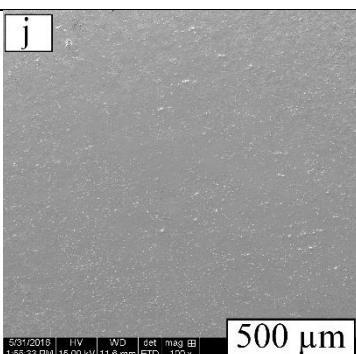
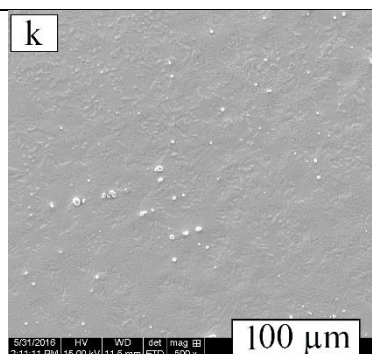
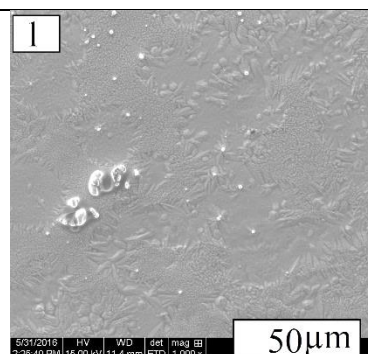


Table 5.5 shows the morphology by OM of the surface attached by different amounts of perchloric acid. Higher is the concentrations of perchloric acid, higher is the corrosion and the pitting. However, carbide particles were still present on the surface after the treatment.

| HClO <sub>4</sub> | 100 X   | 500 X  | 1000 X  |
|-------------------|---|--|---|
| 1%                |    |    |    |
| 3%                |   |   |   |
| 5%                |  |  |  |
| 10%               |  |  |  |

*Table 5.6 SEM micrographs using different addition of perchloric acid (a-c) with 1%, (d-f) with 3%, (g-i) with 5%, (j-l) with 10%.*

Table 5.6 shows SEM micrographs depicting the morphology of the surface after different amounts of perchloric acid. A lot of carbides resulted in presence of 1% and 3% of perchloric acid, but after increasing the concentration to 5 % and 10 %, only some pitting was found on the surface. Different surface textures were found for the different electrolytes. Areas covered with a matt and dark surface was observed after anodic polarization measured in high HClO<sub>4</sub> electrolytes. These areas were less evident than for samples treated with a lower HClO<sub>4</sub> electrolyte. This phenomenon may be the result of the presence of a passive film developed on the surface. Therefore, steel specimens cannot be electrochemically polished in these mixed acids containing HClO<sub>4</sub> higher than 90 vol%. [75]. This result confirms the observation found by T. Hahn and A. Marder [99], adding an elevated quantity of perchloric acid would end by a surface with lots of pitting.

The observation confirms that higher is the concentration of perchloric acid, higher is the presence of carbides, represented in the reported figures by large and dark regions. This observation is coherent results reported in Table 5.4

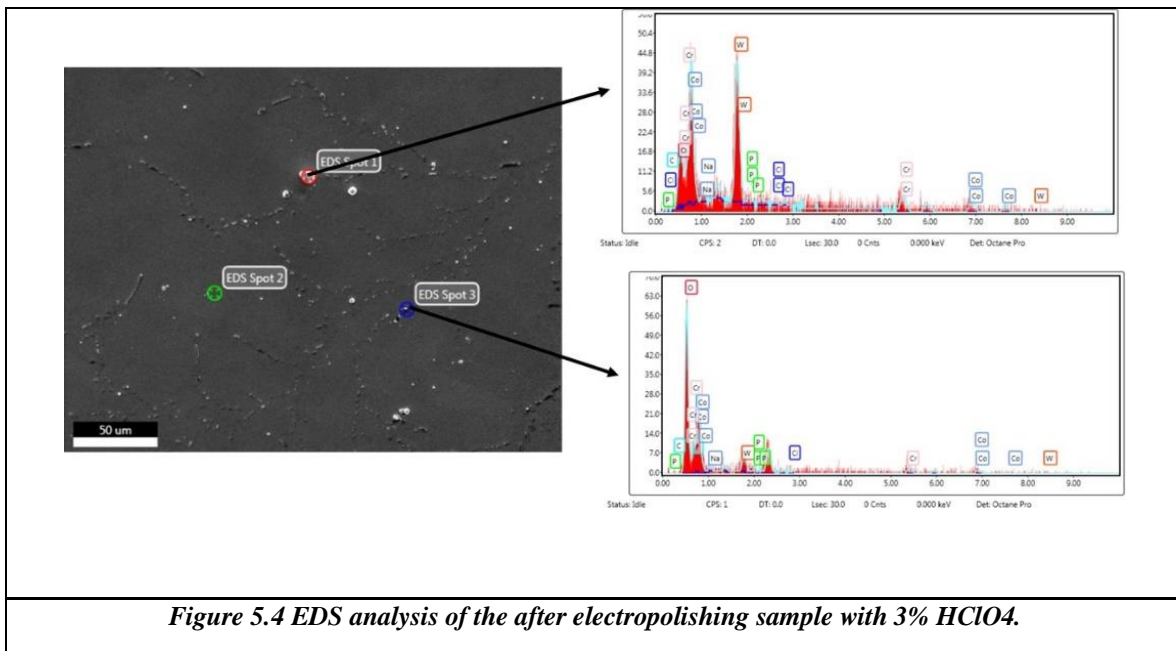
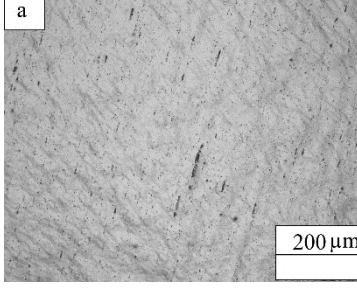
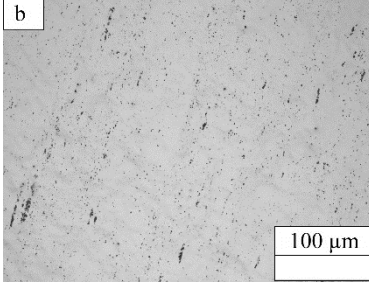
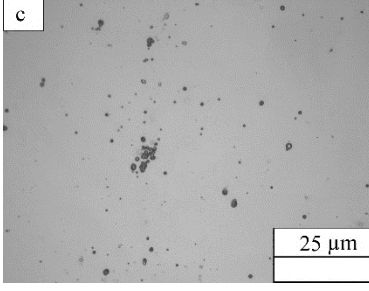
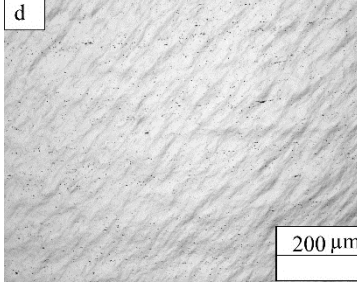
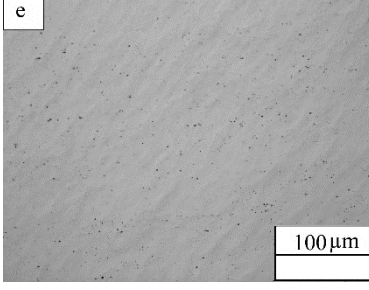
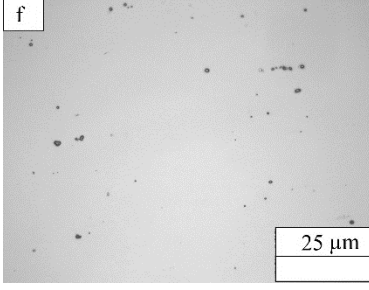
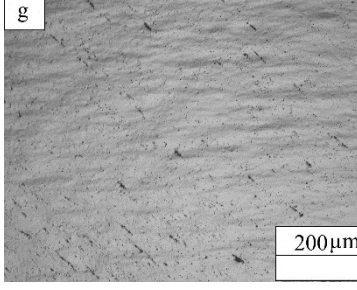
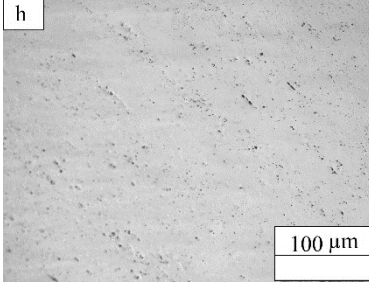
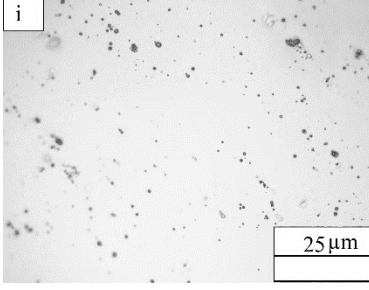
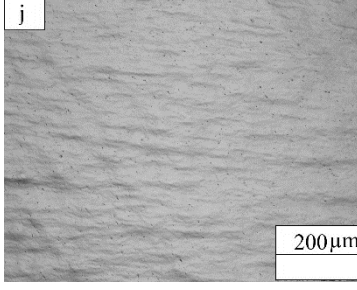
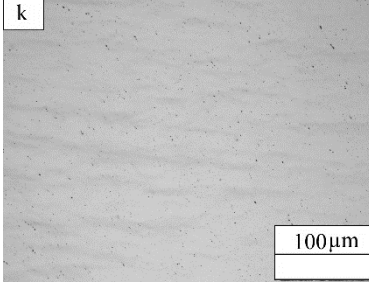
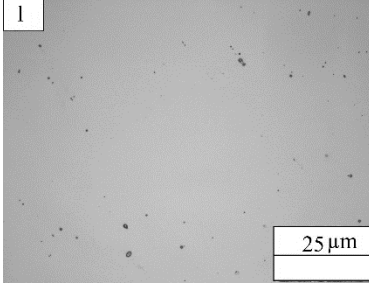


Figure 5.4 shows the EDS result after using 3% of perchloric acid. Possibly, two kinds of carbides are evidenced. An example of the first one is shown in spot N°1. This kind presents a brighter appearance. These particles could be tungsten-rich carbides  $W_6C$ , while the spot N°3 shows a darker region, rich in chromium, which could represent the chromium-rich carbides  $Cr_7C_3$  or  $Cr_{23}C_6$ .

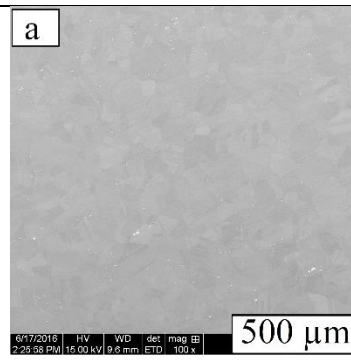
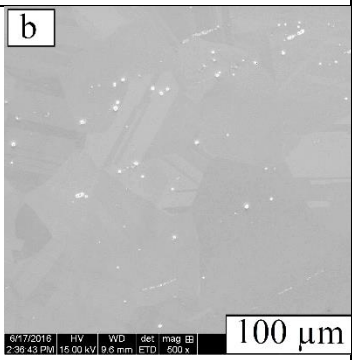
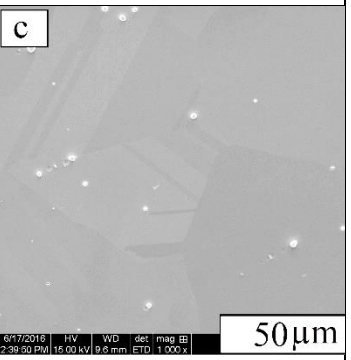
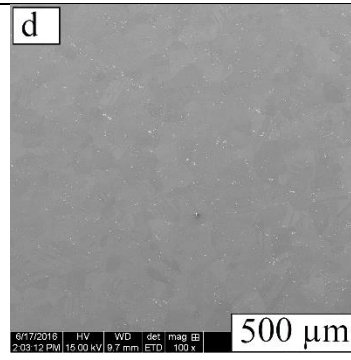
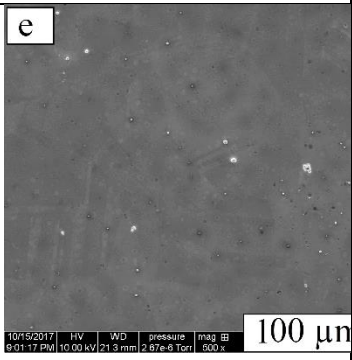
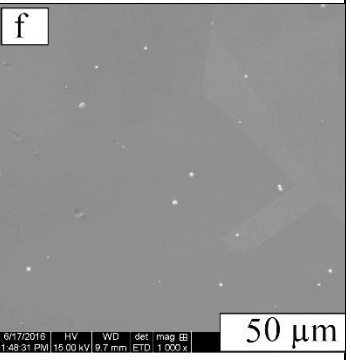
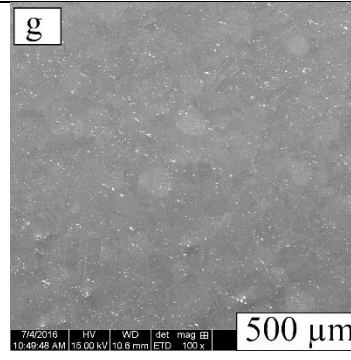
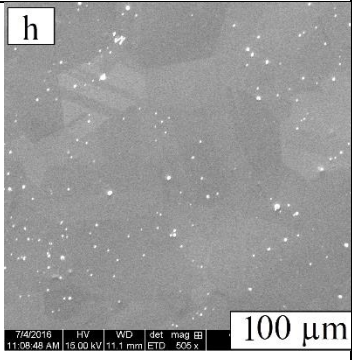
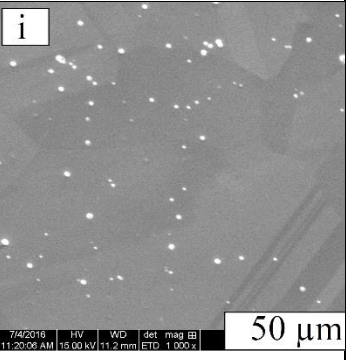
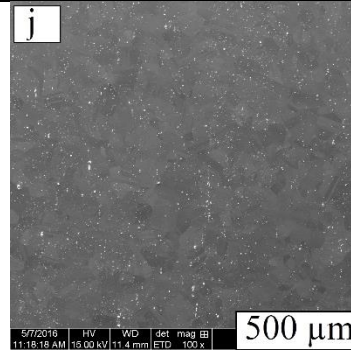
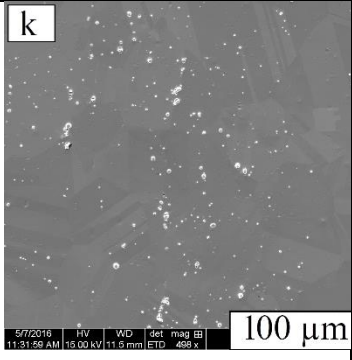
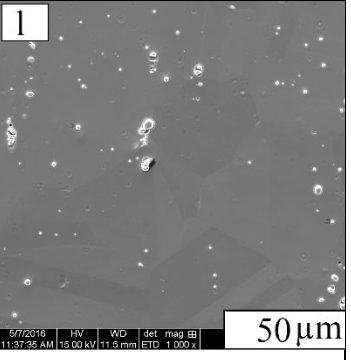
### 5.1.3 Effect of hydrofluoric acid

Hydrofluoric acid represents a solution of hydrogen fluoride (HF) in water and it is known for its extreme reactivity. It is well known to be reactive against oxides, for example, those formed on the surface of metals. [96]. The object of this section was to compare the effect of several electrolytes on the final electropolishing outcome. The electrolytes had the same basic solution, but the same amount of HCl,  $HClO_4$ , and HF was added, and the effect was compared. Table 5.7 Optical microscopy using different addition of hydrofluoric acid (a-c) with 1%, (d-f) with 3%, (g-i) with 5%, (j-l) with 10. represents optical results obtained by microscopy.

The results show a big difference on the sample surface morphology and topography after adding hydrofluoric acid, the surface sample becomes more homogeneous with lots of carbides.

| HF  | 50 X  | 100 X  | 500 X   |
|-----|---|--|---|
| 1%  |    |    |    |
| 3%  |    |    |    |
| 5%  |   |   |   |
| 10% |  |  |  |

*Table 5.7 Optical microscopy using different addition of hydrofluoric acid (a-c) with 1%, (d-f) with 3%, (g-i) with 5%, (j-l) with 10.*

| HF  | 100 X   | 500 X  | 1000 X  |
|-----|---|--|---|
| 1%  |    |    |    |
| 3%  |    |    |    |
| 5%  |   |   |   |
| 10% |  |  |  |

*Table 5.8 ES by SEM using different addition of hydrofluoric acid (a-c) with 1%, (d-f) with 3%, (g-i) with 5%, (j-l) with 10.*

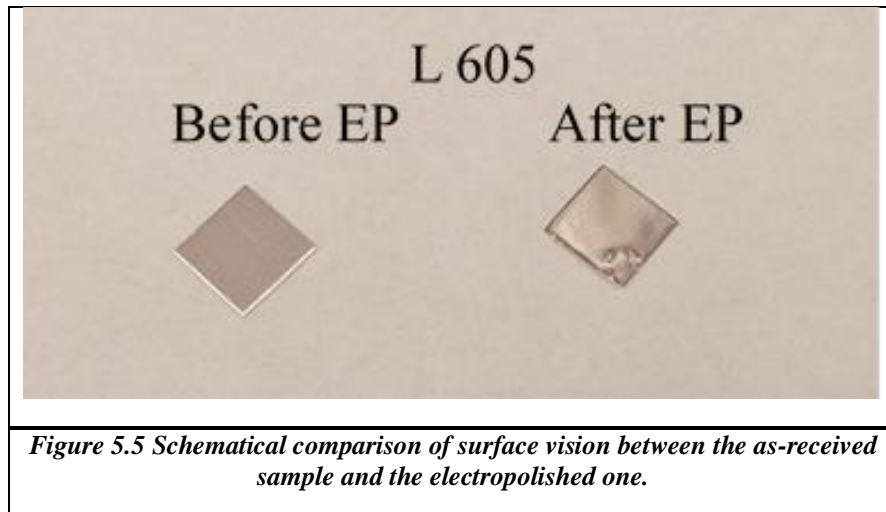
Table 5.8 represents a comparison of the effect of different hydrofluoric amounts in the electrolyte base; micrographs are obtained by SEM. It was obvious that by increasing the amount of hydrofluoric acid, the formation of the pitting was increased. This is related to the aspect that strong acid as hydrofluoric acid, contain fluoride ions which are responsible to increase the conductivity of the chemical electrolyte during the electropolishing, which is an important factor for the dissolution of the metallic ions from the anode (the electropolished workpiece) during the electropolishing process [55].

According to Faraday's Law of Electrolysis represented in the following equation:

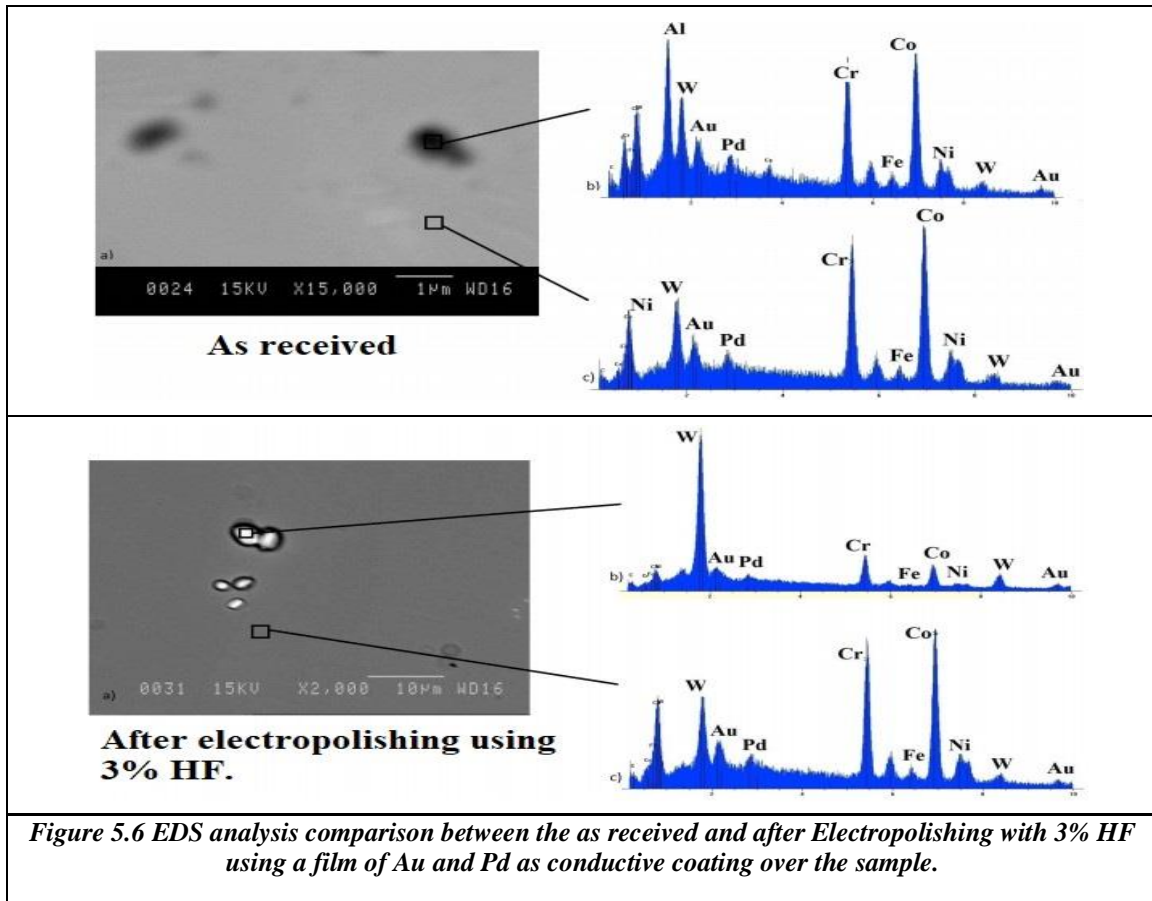
$$W_{loss} = \frac{ItM}{NF} \quad \text{Equation 5.1}$$

the total material loss (the dissolution of the metallic ions) is depending on the applied current through the electrolyte. When the applied current is high, the surface of the metal will lose more metallic ion. As already seen for the polarisation curve (see the section concerning electropolishing) increasing the current increases the sample surface amount pitting, according to the fourth region in the polarisation curve.

Figure 5.5 shows the L605 specimens before and after electropolishing process, it's clear the difference on the surface. The EP surface specimens are very smooth, flat, homogeneous without any scratches. It exhibits an exceptional brightness and luster and good reflectivity, which indicate that electropolishing process is able to improve the quality of metal finishing.







The EDS analyses show a significant change in the surface chemical elemental composition before and after electropolishing process.

Some papers [57] studied the presence of the tungsten-rich carbides after electropolishing. The results in this work showed that the globular carbides that are clearly seen in Figure 5.6 They are principally formed by tungsten and chromium, with some exception, which put in evidence the presence of could be containing some of cobalt and nickel. It is however not clear if these elements belong to the surrounding matrix, rich in Co and Ni.

P. Sojitra performed a study [100] of comparison between three type of characterization of L605 alloys, 1-laser cut stent, 2-acid descaled stent, and 3-electropolished stent. The solution of the electropolished sample was composed of 3% HF, 20% HNO<sub>3</sub>, the rest was deionized water. After the EDS analysis, it was found that the electropolished sample shows a small amount of oxygen due to the oxide film on the surface during the passivation effect of

electropolishing. The EDS results did not show any significant change in the main elemental composition of the stent, even after the descaling process.

A study by A. Karaali [101], on the influence of tungsten on Co-Cr alloy, analyzed different types of alloy with different W contents, and precisely 0.4 wt. %, 4 wt. % and 8 wt. % for the samples W0, W4 and W8 containing different quantities of tungsten between 0,4 and 8 wt.%. using electropolishing solution composed from 10% perchloric acid, 20% ethanol, and 70% butanol, with a potential of 30 V. At the end it was found that increasing content of tungsten decrease the concentration of stacking faults and raise the sigma phase and the fcc phase of cobalt.

The aluminium in the as-received sample represent a precipitate that could be left on sample surface after the finishing process from the company. In fact, the L605 traditional formulation does not contain aluminium. During the washing process, it was not use any kind of acid to remove all the precipitate, which it let to some metallic residues or impurities to stay on the surface of the sample. The reason it was not use the acid, to prevent of having any kind of effect on sample surface, during the electropolishing process.

Similar results were found in this paper [57] after comparing the EDS results, especially for the tungsten-rich particles. After etching of the CoCr semi-finished products used for stent production («mini-tubes») the presence of tungsten rich nodules with an average of diameter up to  $\sim 1 \mu$  was found. EDS analyses on a nodule have identified a high tungsten content.

## **5.2 Roughness analysis by AFM**

The samples surfaces were exanimated using contact and tapping mode AFM. The measurements were carried out on areas of  $1 \times 1 \mu\text{m}^2$  and of  $50 \times 50 \mu\text{m}^2$ . The measurements were performed three times for each of the samples for different areas of reference, to assure the reproducibility of the study.

Table 5.9 compares of roughness analysis for the as-received sample and the electropolished samples after using different quantity of HF in the electrolyte solution. The comparison of the first two images in Table 5.9 (figures a and b) between the as-received sample and the electropolished one, by using the main electropolishing solution without addition of

hydrofluoric acid, it did not show any significant reduction of surface roughness, the  $R_a$  value decreased down to  $\sim 10$  nm. The surface was still not homogeneous, the sample showed some peaks and a lot of grooves were present on its surface. On the other hand, the different addition of hydrofluoric acid (1 vol.%, 3 vol%, 5 vol%, 10 vol%) in Table 5.9 (figures c, d, e, and f) was effective and significant, as the roughness was reduced to less than  $\sim 30$  nm between the as-received sample and the electropolished samples.

The surface topography becomes less rough and more homogeneous by increasing the amount of HF in the solution. In general, low surface roughness is an important factor to avoid bacterial adhesion.

Those results reveal and indicate the efficacy of fluoride ions to remove and dissolving the metallic ions from the anode during the electropolishing process.

From Table 5.9 (d, j) evidenced that adding 3 vol.% of hydrofluoric acid the surface became rougher compared with other HF amounts, such as for example 5 vol. % and 10 vol. % where an increase in roughness was still evident.

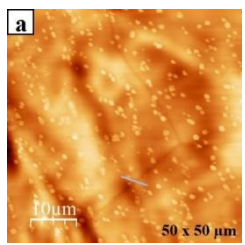
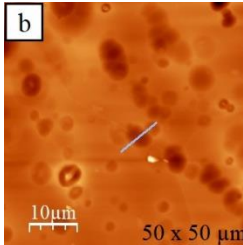
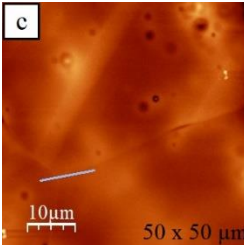
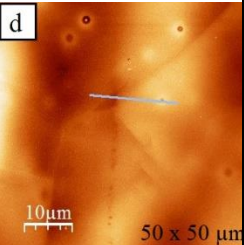
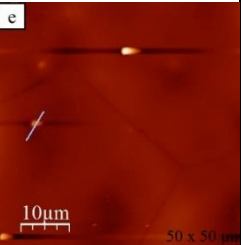
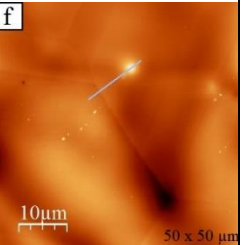
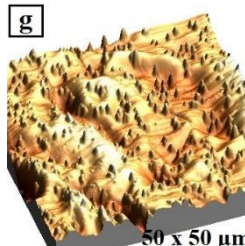
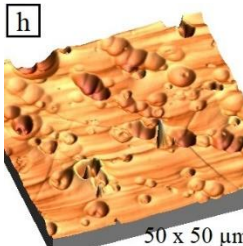
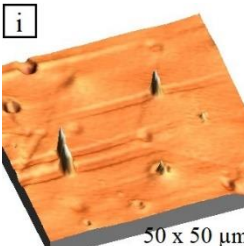
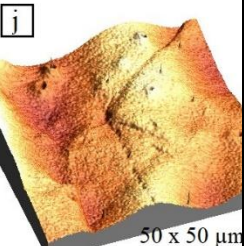
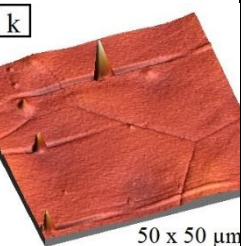
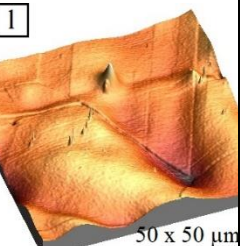
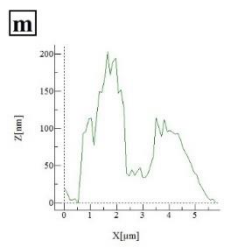
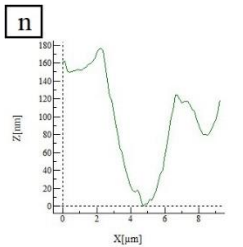
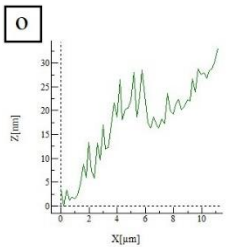
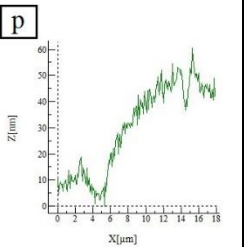
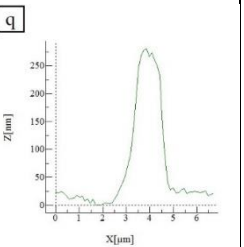
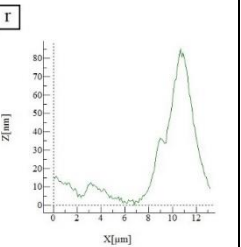
The AFM analysis allowed the analysis of special features of the particles found on the surface AFM images were able to identify lines scan profiles, by calculating two important variables, the RMS (root mean square roughness) and  $R_a$  (roughness average).

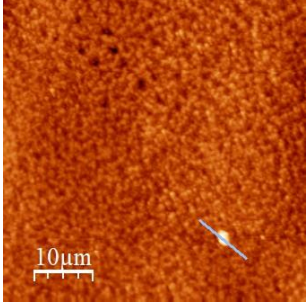
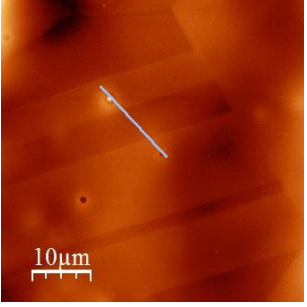
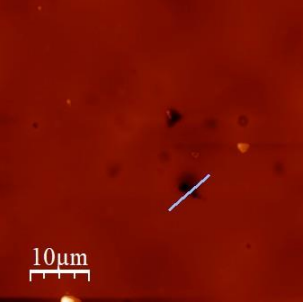
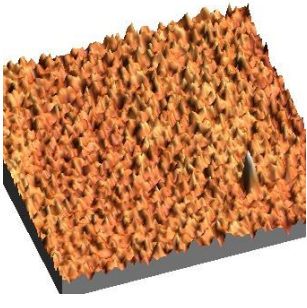

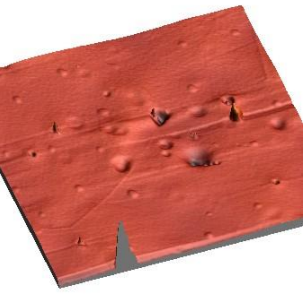
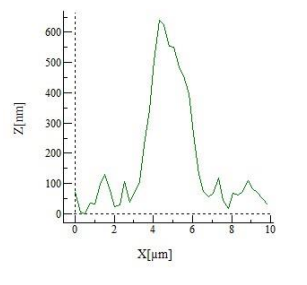
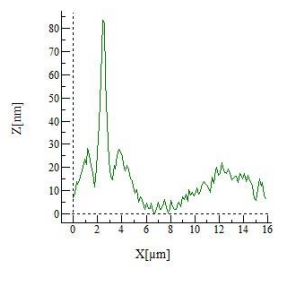
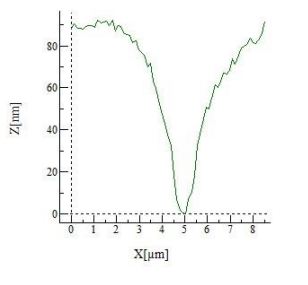
The representative 3-D topographic AFM images, for a scanning area of  $50 \times 50 \mu\text{m}^2$ , of the L605 alloy surfaces can be seen in Table 5.9 (figure g) for as-received sample, Table 5.9 (figure h) for an EP sample using the main solution, and Table 5.9 (figures i, j, k, l) for different EP samples prepared by different addition of hydrofluoric acid.

As a result of AFM images, it was possible to see that the electropolishing was able to dissolve all the peaks and scratches resulting during cold forming.

From the experimental measurements, it was found a lot of difference in surface roughness on the electropolished sample after the addition of different quantities of hydrofluoric acid.

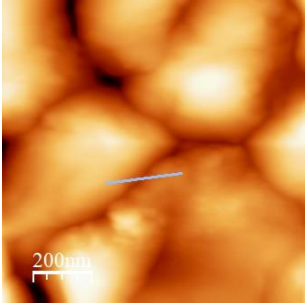
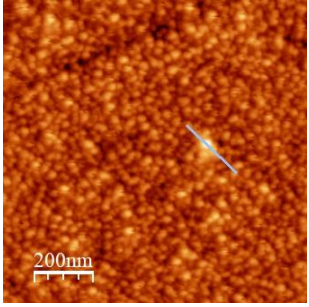
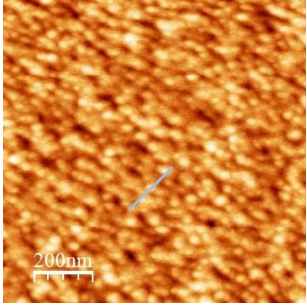
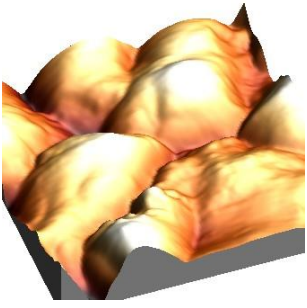
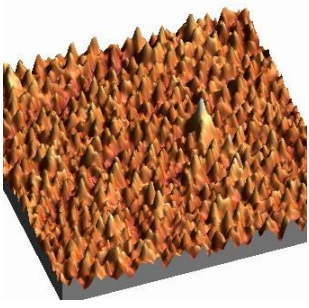
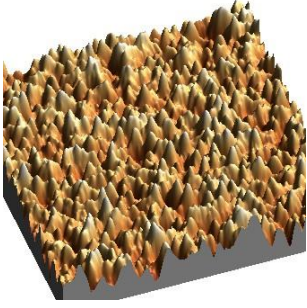
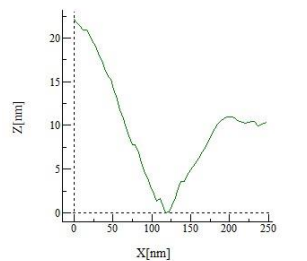
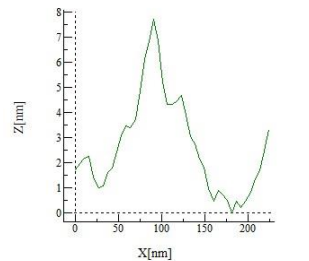
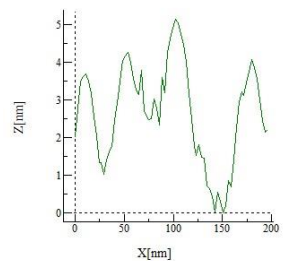
Table 5.10 presents the comparison, for a smaller scale, that is for  $50 \times 50 \mu\text{m}^2$  of the same addition of different acids, chosen among HCl,  $\text{HClO}_4$  and HF, added to the main electropolishing solution, it gives a better understanding of the effect of each electrolyte on the surface topography of the metallic samples.

| As received   | 0%   | 1%  | 3%   | 5%   | 10%  |
|---|--|---|--|--|--|
|    |   |   |   |   |   |
|    |   |   |   |   |   |
|   |  |  |  |  |  |
| RMS: 58.98 nm<br>RA: 43.96 nm   | RMS: 47.12 nm<br>RA: 34.22 nm  | RMS: 23.05 nm<br>RA: 18.26 nm   | RMS: 14.7 nm<br>RA: 12.1 nm  | RMS: 29.79 nm<br>RA: 18.28 nm  | RMS: 18.12 nm<br>RA: 14.34 nm  |
| <i>Table 5.9 Roughness analysis using AFM for the received and electropolished samples, after using a different quantity of HF.</i> |  |   |  |  |  |

| 3 vol. % $HClO_4$<br>(50 x 50 $\mu m^2$ )  | 3 vol. % $HF$<br>(50 x 50 $\mu m^2$ )  | 3 vol. % $HCl$<br>(50 x 50 $\mu m^2$ )   |
|--|--|--|
|   |   |   |
|   |   |   |
|    |  |  |
| RMS: 69.8338 nm<br>RA: 54.5721nm   | RMS: 13.6123nm<br>RA: 10.9268 nm   | RMS: 21.7596 nm<br>RA: 11.2492 nm  |
| <p align="center"><b>Table 5.10 Comparison of surface features for electrolytes with 3 vol. % of <math>HClO_4</math>, <math>HF</math> or <math>HCl</math>.</b></p> |  |  |

The electropolished region by HF and HCl appears smoother and with no trace of grain boundaries, compared to the region electropolished by for the  $HClO_4$  solution; it was evident that the surface morphology showed a higher roughness when  $HClO_4$  was added to the electrolyte, the acid was not able to remove it during the electropolishing process; on the other hand the samples treated with HCl where similar to the one after using the main solution (0 vol. % HF) where pits are present on the surface.

These responses are once again dominated by a single anodic dissolution peak. However, all the dissolution peaks are shifted cathodically. AFM analysis shows high decreasing in surface roughness of surface after electropolishing process when adding hydrofluoric acid.

| <b>3 vol. % <math>HClO_4</math> (<math>1 \times 1 \mu m^2</math>)</b>   | <b>3 vol. % <math>HF</math> (<math>1 \times 1 \mu m^2</math>)</b>                   | <b>3 vol. % <math>HCl</math> (<math>1 \times 1 \mu m^2</math>)</b>                    |
|---|---|---|
|    |    |    |
|   |   |   |
|    |  |  |
| <p>RMS: 11.6851 nm<br/>RA: 9.421 nm</p>   | <p>RMS: 1.0238 nm<br/>RA: 0.8116 nm</p>   | <p>RMS: 1.6482 nm<br/>RA: 1.3288 nm</p>   |
| <p><b>Table 5.11 Comparison of AFM analysis after adding 3% of each acid <math>HClO_4</math>, <math>HF</math>, <math>HCl</math> using a scale of <math>1 \times 1 \mu m</math>.</b></p> |   |   |

### 5.3 Contact angle

Surface wettability is an important factor for the assessment of biomaterial properties. For example, Table 5.12 shows the water contact angle for several L605 samples, with a comparison before and after electropolishing, useful to identify different electropolishing conditions on the wettability of the material. Especially wettability enhances the biocompatibility of the material, affecting the protein adhesion to the surface when the material is immersed in a biological medium. Adherence and absorbance capacity depends on some factors such as the grade of a chemical reaction between the two material, closeness, and contact area [102].

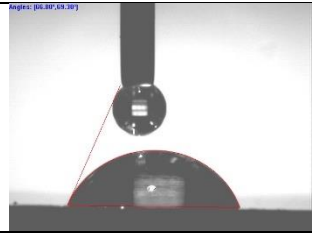

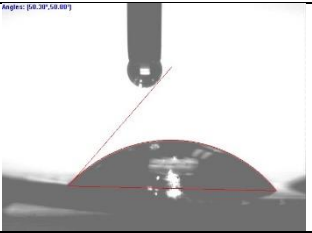
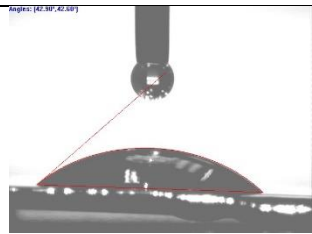

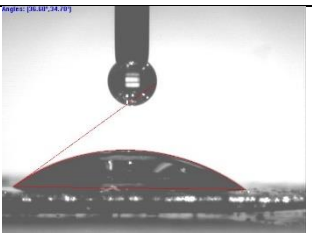
|  |   |  |
|--|---|--|
|    |   |   |
| As received  | 0% HF   | 1% HF  |
|   |  |  |
| 3% HF  | 5% HF   | 10% HF   |
| <i>Table 5.12 Water contact angle for L605 before and after electropolishing with the different addition of hydrofluoric acid.</i> |   |  |

Figure 5.7 shows the water contact angle for L605 before and after electropolishing, generally, the electropolishing turns the sample surface hydrophilic and it increases its wettability.

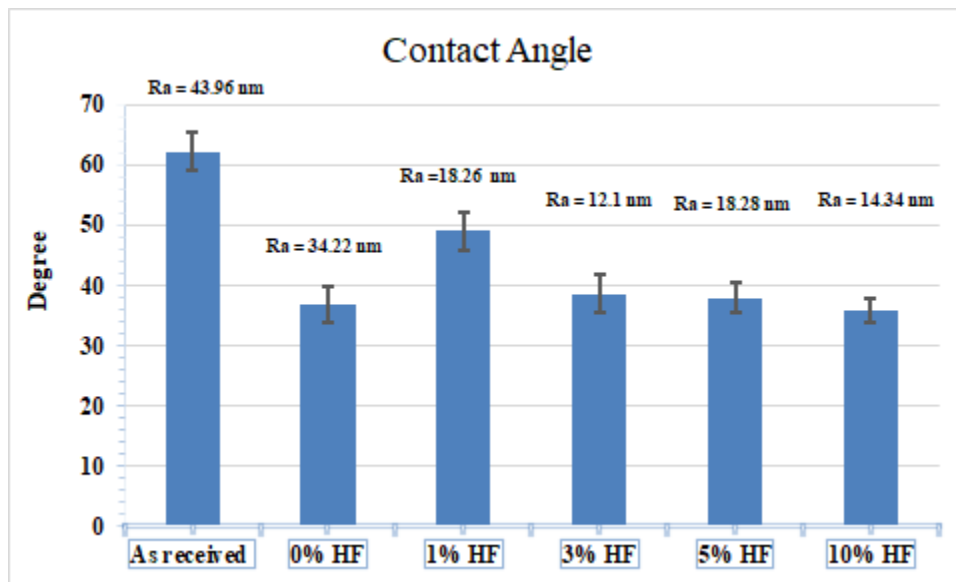


Figure 5.7 The average of contact angle before and after electropolishing of L605 samples.

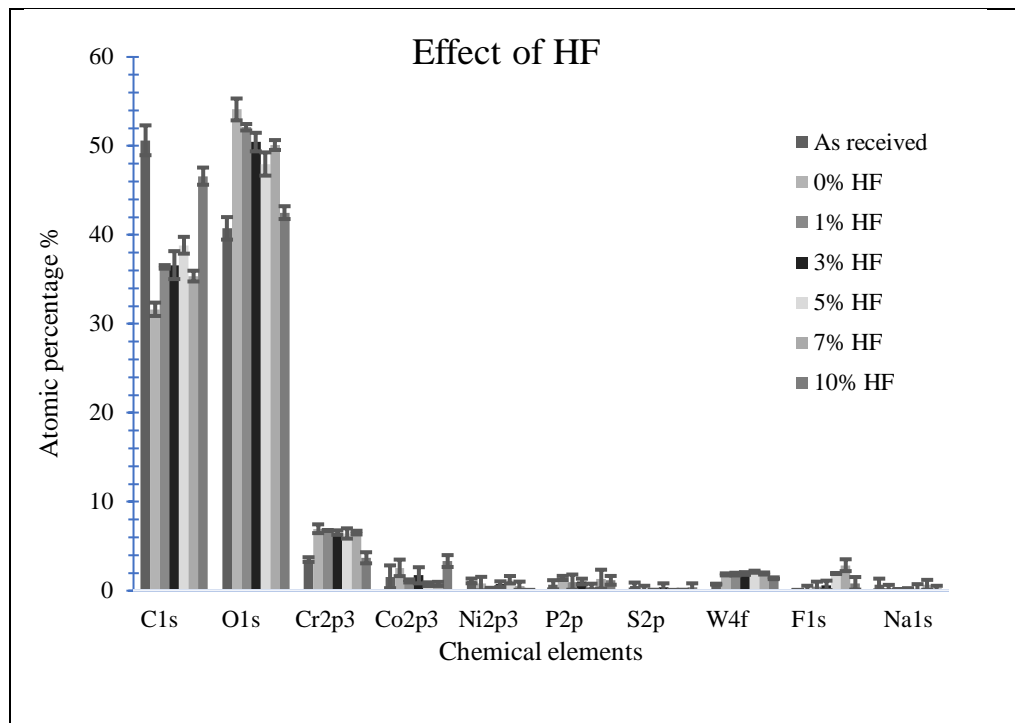


Figure 5.8 XPS surveys describing the effect of different HF amounts on the surface chemical composition.



It is possible from these data that an increase in the fluoride content decreases the metallic content of Co, Cr, and W.

The surface penetration depth of the XPS experiment is in the range of ~5 nm. or in any case limited to a few nanometres because of inelastic collisions and recapture events. However, little detectable O is present on the cleaned surface whereas the O(1s) signal for the exposed sample is very strong.

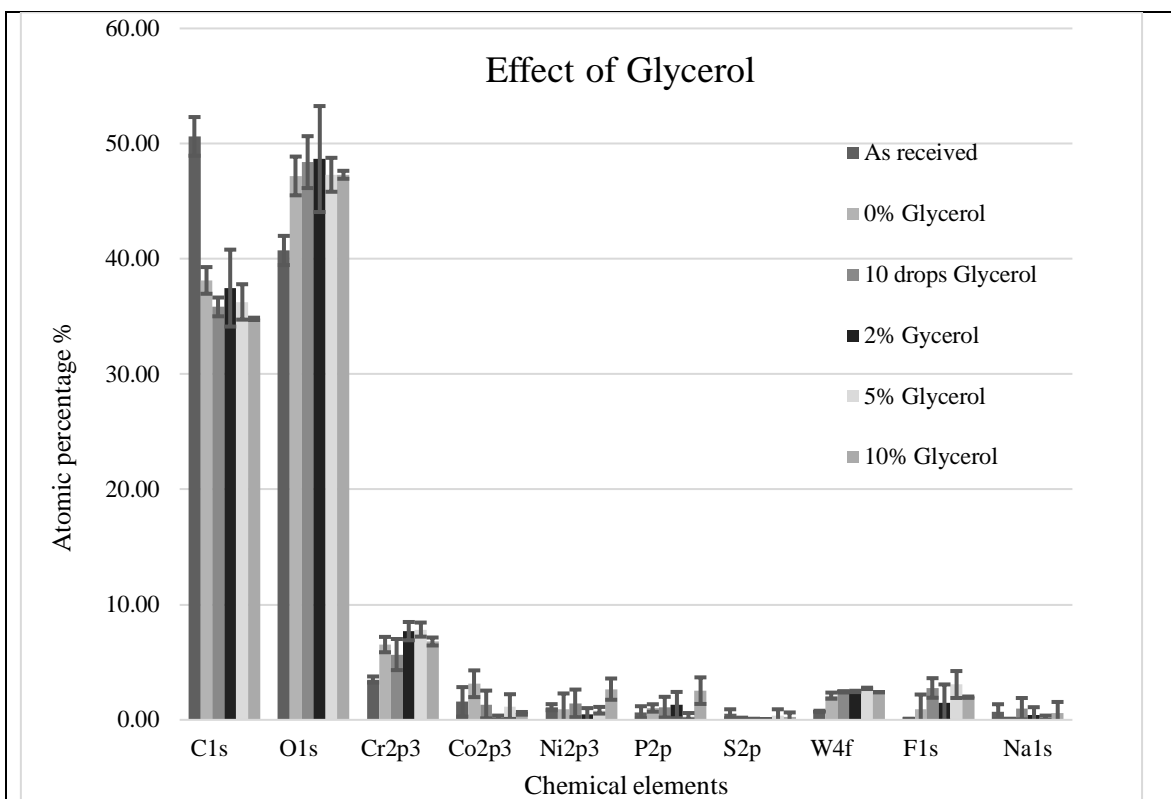
It is noteworthy, however, that some of the observed O(1s) intensity is probably due to adsorbed O containing organics. This is evidenced by a small amount of C also visible (in the C(1s) region) on the surface of the exposed sample.

An interpretation of the onset of the dissolution peak can be related to the breakdown of the oxide film which exposes the underlying metal surface.

It is possible to conclude from XPS measurements that surface oxide formation at the clean steel surface is rapid under aerobic conditions.

Anodic dissolution of metal ions from steel surfaces where the oxide layer was removed in situ was seen to be much faster than at the equivalent alloy surface, where oxide coating was formed and not removed in such an efficient way as for stainless steel. Aggressive proprietary chemical treatments of the steels were successful in removing the oxide from only one of the samples studied here (SS410). The formation and dissolution of a metal oxide passivation layer at the metal–liquid interface is a key feature of the metal dissolution mechanism and one that ultimately determines the quality of the optical finish (i.e. the surface roughness) [103].

The effect of electrolytes containing different amounts of glycerol, in terms of surface chemical composition, is described in the Figure 5.9



*Figure 5.9 XPS surveys describing the effect of different glycerol amounts on the surface chemical composition.*

## 5.4 Mechanical polishing versus electropolishing

Electropolishing cannot be considered as an alternative for mechanical polishing. The difference between those two methods would be easily clear under high magnifications of surface morphology, due the lack of some surface characteristics, that could not be obtained in mechanical polishing.

Mechanical polishing leaves the surface with a lot of abrasion and scratches, and make it flatten. The mechanical polishing is not able to eliminate the particles from the surface, but in some case, particles are embedded in the surface, as the abrasive material is removed from the paper and it sticks to the alloy, such as silicon carbide, diamond, or alumina. The presence of these particles can trigger localized corrosion in preferential points [104].

In the other hand, electropolishing methods produce a featureless surface, it creates a new protective oxide layer, and is able to show the real crystal structure of the metal without deformation that could be formed during the cold working process [105].

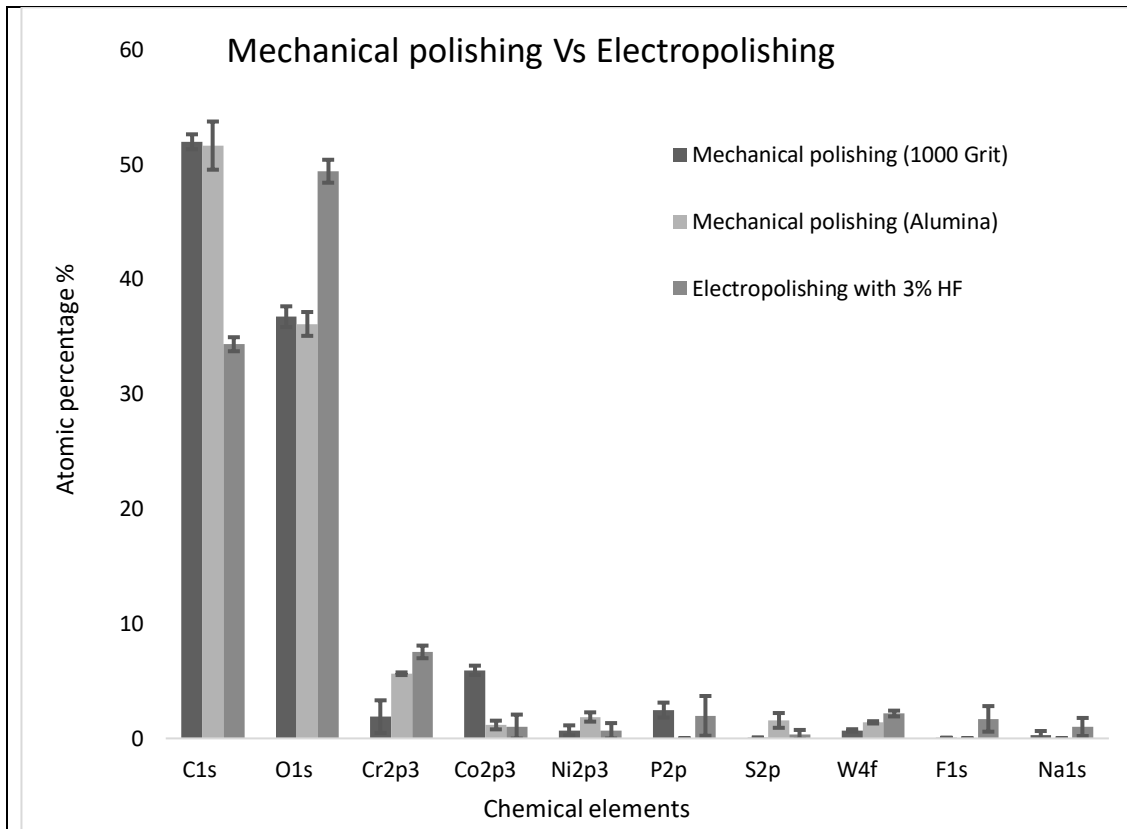
Electropolishing leads to a surface free of contamination and different from the native or the as received one, its able to change the chemical composition of the surface by exposing a new surface to the atmosphere, with the chemical composition of the «bulk» material; the oxidation of the material may make the surface chemical composition vary [106].

The results obtained during the present experiences confirm the previous results, Table 5.13 shows the difference in surface morphology between the mechanical polishing and the electropolishing. The mechanically polished sample has an affected surface from treatment and finishing, resulted by having a lot of inclusions and scratches. The electropolished sample was in general homogeneous and uniform, the grain boundaries were clearly evident, in the same way as the presence of metallic carbides represented by small white precipitates.

Figure 5.10 represents an analysis of the chemical composition of the surface and a comparison between the mechanical polishing and the electropolished surface. Significant differences in surface chemistry are evident, as the surface after electropolishing shows a different chemical composition from the mechanically polished one in particular, the concentration of oxygen and chromium showed a significant increase after electropolishing, while the concentration of carbon decreased after electropolishing.

| <i>L605</i>                       | <i>500 X</i> | <i>1000 X</i> | <i>2000 X</i> |
|-----------------------------------|--------------|---------------|---------------|
| Mechanical polishing 1000 Grit    |              |               |               |
| Mechanical polishing with Alumina |              |               |               |
| Electropolishing with 3% HF       |              |               |               |

*Table 5.13 Comparison between the mechanical polishing (1000 grit, Alumina) and the electropolishing using 3 vol. % of HF.*



*Figure 5.10 XPS analysis and comparison between the mechanical polishing and the electropolishing from chemical point view.*

## 5.5 Conclusions

- The effective addition to the main electrolyte solution was that one constituted by hydrofluoric acid. On the other hand, the addition of perchloric acid was significantly aggressive for the sample surface, which almost presented signs of corrosion.
- The best amount of hydrofluoric acid for L605, in term of surface roughness and final chemical composition, was 3 vol. %, for which the surface was homogeneous and smoother. On the other hand, increasing the amount of hydrofluoric acid increased the pitting formation on the sample surface and corroded its structure.
- The addition of hydrofluoric acid was effective for the decreasing of the sample surface roughness of ~40 nm (from 57 nm to 15 nm).
- The addition of hydrofluoric acid was responsible to change the chemical composition of the surface sample, by decreasing the quantity of carbon and increasing the oxygen, thus increasing the corrosion resistance of the surface.
- The electropolishing process, when the main solution is enriched by HF, turns the sample to be more hydrophilic, by decreasing the water contact angle to ~30° degree.

## Chapter 6 Electropolishing of pure Titanium: Results and discussion

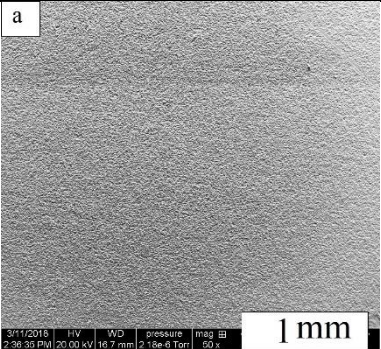
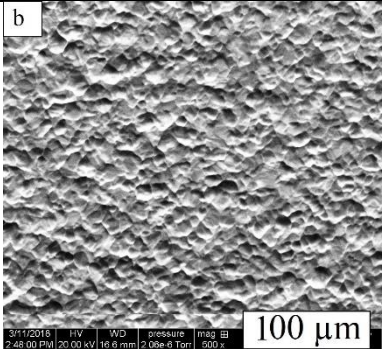
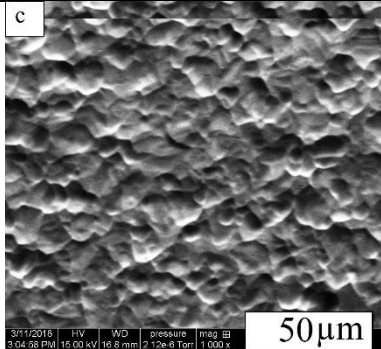
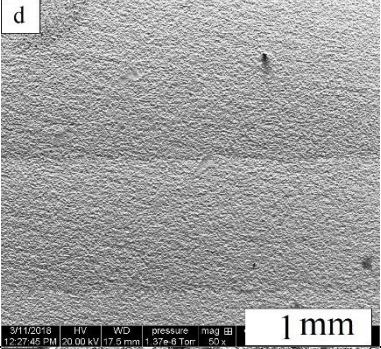
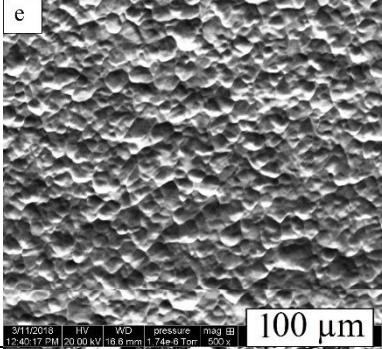
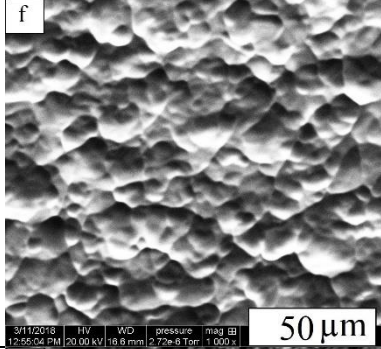
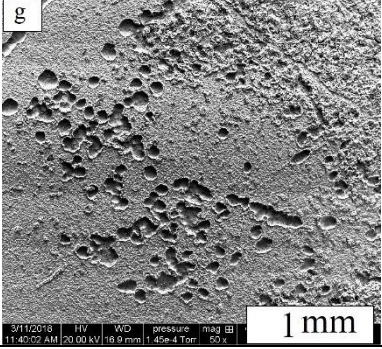
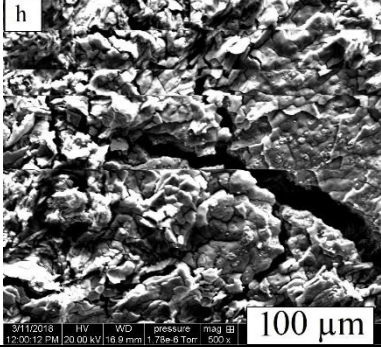
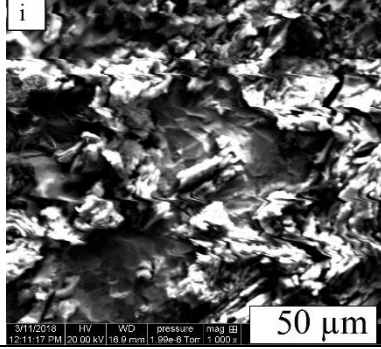
### 6.1 Introduction

It was largely reported [107] that commercially-pure Titanium can be electropolished in electrolytes mainly composed by sulfuric acid and methanol. Other works [108] showed that Ti and Ti-based alloys can be electropolished in electrolytes composed by perchloric acid, methanol and ethylene glycol. The present work compares all these studies to analyze the obtained results in terms of surface finishing for different kinds of solutions.

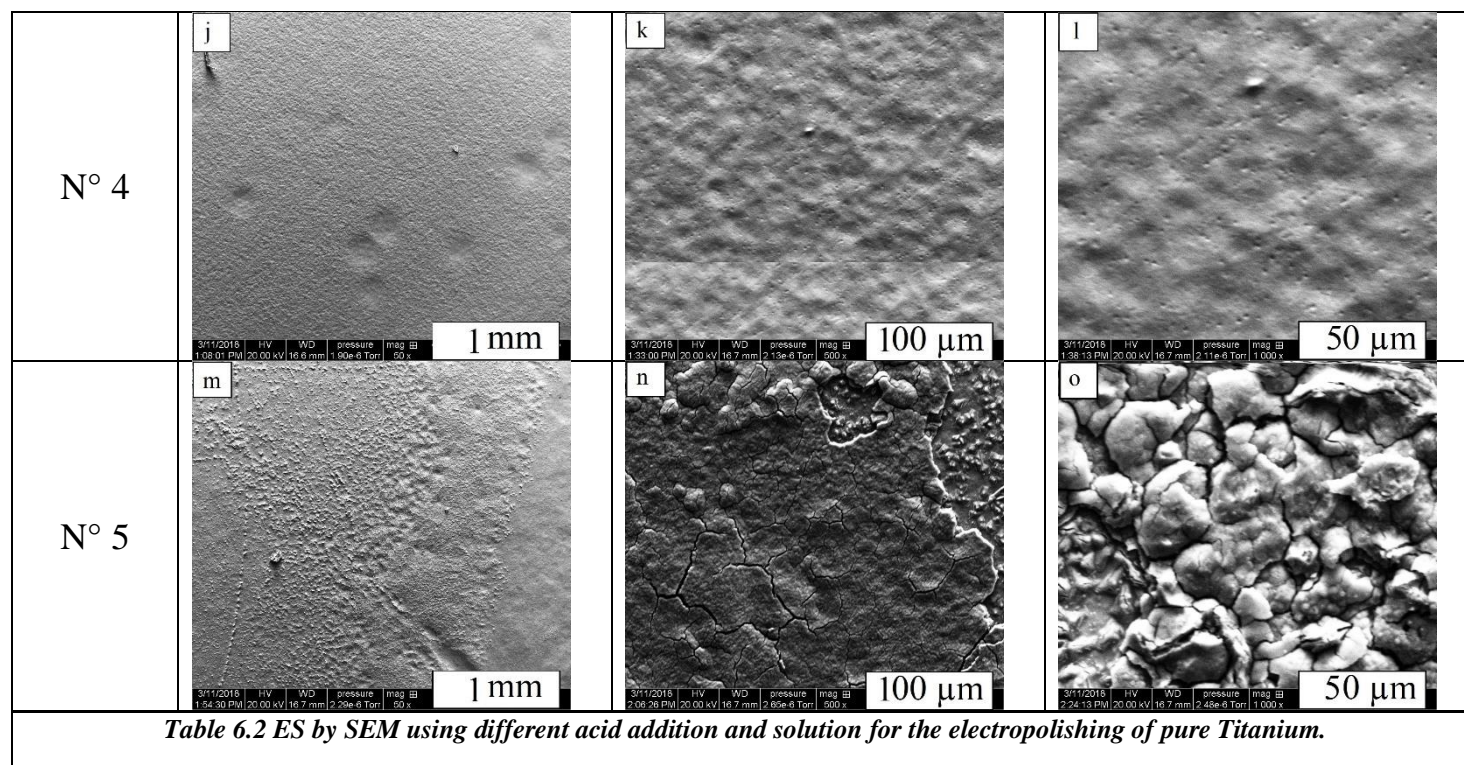
As a first thing, five distinct electrolytes from many studies [107] [108] [88] [109] [110] were compared. Electrolytes contained different amounts and several combinations of H<sub>2</sub>SO<sub>4</sub>, HNO<sub>3</sub>, HF, CH<sub>3</sub>COOH, and HClO<sub>4</sub>, as shown in Table 6.1. This table is a quick reference to the one already presented in chapter 4. The preliminary study for these solutions was mainly carried out by scanning electron microscopy, to understand the surface features introduced by the treatment Table 6.2

| <i>Solutions</i>     | <i>1</i>   | <i>2</i>  | <i>3</i>  | <i>4</i>  | <i>5</i>   |
|----------------------|--|---|---|---|--|
| Chemical composition | 70%<br>(H <sub>2</sub> SO <sub>4</sub> )<br>5% (HNO <sub>3</sub> )<br>5% (HF)<br>20% water | 90%<br>(H <sub>2</sub> SO <sub>4</sub> )<br>5% (HNO <sub>3</sub> )<br>5% HF | 10%<br>methanol<br>70% ethanol<br>20%<br>(HClO <sub>4</sub> ) | 80%<br>(CH <sub>3</sub> COOH)<br>20% (HClO <sub>4</sub> ) | 60% ethanol<br>30% H <sub>2</sub> SO <sub>4</sub><br>10%<br>methanol |

*Table 6.1 Chemical solutions used for electropolishing of pure Titanium. The percentages are in volume.*

| <i>Solution</i> | <i>Magnification</i>   |  |  |
|-----------------|--|--|--|
|                 | <i>50 X</i>  | <i>500 X</i>   | <i>1000 X</i>  |
| N° 1            |  <p>3/11/2018 HV WD pressure mag 2:39:53 PM 20.00 kV 10.7 mm 2.18e-6 Torr 50 x 1 mm</p>   |  <p>3/11/2018 HV WD pressure mag 2:48:00 PM 20.00 kV 10.6 mm 2.06e-6 Torr 500 x 100 μm</p>   |  <p>3/11/2018 HV WD pressure mag 3:04:08 PM 15.00 kV 10.8 mm 2.12e-6 Torr 1,000 x 50 μm</p>   |
| N° 2            |  <p>3/11/2018 HV WD pressure mag 12:22:45 PM 20.00 kV 10.9 mm 1.97e-6 Torr 50 x 1 mm</p>  |  <p>3/11/2018 HV WD pressure mag 12:42:12 PM 20.00 kV 10.8 mm 1.74e-6 Torr 500 x 100 μm</p>  |  <p>3/11/2018 HV WD pressure mag 12:55:02 PM 20.00 kV 10.8 mm 2.22e-6 Torr 1,000 x 50 μm</p>  |
| N° 3            |  <p>3/11/2018 HV WD pressure mag 11:42:02 AM 20.00 kV 10.9 mm 1.45e-6 Torr 50 x 1 mm</p> |  <p>3/11/2018 HV WD pressure mag 12:00:12 PM 20.00 kV 10.9 mm 1.78e-6 Torr 500 x 100 μm</p> |  <p>3/11/2018 HV WD pressure mag 12:11:17 PM 20.00 kV 10.9 mm 1.99e-6 Torr 1,000 x 50 μm</p> |





## 6.2 Preliminary investigations on the effect of the chemical composition of 5 different solutions

Table 6.2 shows the different SEM image by secondary electrons taken after testing the different chemical electrolytes described in Table 6.1. Both solutions n.1 and n.2 contain nitric and hydrofluoric acid. A. Kuhn and coworkers noticed that both previous acids will form  $Ti_2O_3$  on the sample, which is characterized by a low chemical stability and provides only a little protection to the surface [88]. Compared to a  $TiO_2$  oxide layer, which is naturally formed after air exposition,  $Ti_2O_3$  is known to show excellent protective properties. The surface morphology and other structural properties can change according to the formation condition of this layer. A thickness of some nanometers is usual when the  $TiO_2$  layer is formed in atmospheric conditions, for example [88]. This oxide will enhance the corrosion resistance of titanium, but when it is formed at the anode of an electropolishing setup, it could hinder the anodic dissolution and decrease the rate of dissolved ionic metal during the process [107]. Those two solutions produce a relatively flat surface, as it is shown in Table 6.2 (figures a and d). Higher magnification investigations are presented in Table 6.2 (figures b and e) (magnification 500x for the two solutions) and in Table 6.2 (figures c and f) (magnification 1000x for the two solutions). They showed an irregular morphology, due to an irregular corrosion of the surface during the electropolishing process. The two used electrolytes, when the solution is heated by the current, produce noxious vapors, so that a special care was used when the experiments were carried out for these solutions. Moreover, their chemical reactivity was responsible for the corrosion of the metallic parts of the sample holder, which needed to be replaced more often than with the other solutions. Solution n. 3 and n. 4 contained 20 vol. % of perchloric acid. Table 6.2 (figure g), related to a magnification of 50x, shows a severe pit formation; the pits are circular, forming a network, and with a diameter of around  $\sim 100 \mu m$ . A very damaged surface appeared from investigations at higher magnification, respectively shown in Table 6.2 (figure h) (magnification 500x) and in Table 6.2 (figure i) (magnification 1000x). The presented features are compatible not only with the formation of pits, but also with the deposition of a salt layer. On the contrary, the use of solution n. 4 allowed the formation of a homogeneous surface. This was confirmed for all

the magnifications (respectively Table 6.2 figure j, mag. 50x, Table 6.2 figure k, mag. 500x and Table 6.2 figure l, mag. 1000x).

According to Shigolev and coworkers [75], higher amounts of perchloric acid than 40 vol.% is suitable for electropolishing of pure Ti. Several researchers [108][111] highlighted that perchloric acid is suitable for electropolishing of pure Ti, due to its capacity of penetration of the oxidized surface film, thus removing it [108]. The higher the amount of perchloric acids in an electrolytic solution, the higher the electrolyte ability to remove the anodic film. However, it is important to put in evidence that  $\text{HClO}_4$  is a very reactive acid, with a high oxidizing power, so that it should be handled with a lot of care and precautions; for example, it is well known that high amounts of this acid, used together with other chemicals, can increase the risk of explosions, especially if the electrolyte contains organic solvents such as ethanol [108] [112].

Electrolytes 1, 2 and 5 contain sulfuric acids. Huang [107] found that sulfuric acid and ethanol are able to increase the brightening and the leveling of pure Ti surfaces.

For solutions 3 and 5, the surface was full of pitting and quite rough compared to the other surfaces obtained, especially their solutions contain both 10 vol. % of methanol. This solvent is known to increase the localized corrosion and it is responsible for pitting, cracking and stress corrosion [108]. These phenomena are considered dangerous when Titanium is used in long-lasting applications; methanol requires also cautious handling, due to its toxic nature and its low boiling temperature, which explain the natural structure of samples after using this solution [112].

Water was not used in the solutions because sometimes its presence leads to anodic dissolution, which may cause the formation of pitting on the surface of titanium [75], especially when the used amount of water is high. This, in fact, will increase the stability of the titanium surface passive oxide film [75]. On the other hand, other studies showed that using smaller amounts of water has a role in the stabilization of the surface oxide layer [107]. Another study [113] about Ti electropolishing took into account the effects of adding ethanol in an electrolyte composed of ethylene glycol and NaCl. The addition of different amount of ethanol (0, 5, 10, 15, 20, 30 vol. %) was investigated, for an EP voltage of 55 V. A percentage of 20 vol.% ethanol in the solution was effective due to the formation of a quite thick layer of tetrachloride ( $\text{TiCl}_4$ ), which resulted in a good surface mirror-like finishing and a lower

roughness compared to other samples (a  $R_a$  of 2.341 nm was obtained after electropolishing). It was also observed that adding more than > 20 vol.% ethanol resulted in a non-uniform electron exchange between  $Ti^{4+}$  and  $Cl^-$  ions [113]. The chemical reaction of the anode with the electrolyte is described by the following formula:



The diffusion of  $Ti^{4+}$  ions is not uniform, which it will affect the surface. The higher amount of ethanol is present, the thicker the barrier layer becomes, resulting in a decreasing in the ion flux facilitating the pitting reactions [113].

### 6.3 The effect on Ti of several electrolytes composed by $CH_3COOH$ , $H_2SO_4$ , and $HF$ .

| Solution | $CH_3COOH$ | $H_2SO_4$ | $HF$       | Voltage (V) | Current (A) | Time (min) | Temperature ( $^{\circ}C$ ) |
|----------|------------|-----------|------------|-------------|-------------|------------|-----------------------------|
| N° 6     | 50 %       | 40%       | <b>10%</b> | 70 – 20     | 3           | 1          | 20 – 30                     |
| N° 7     | 65%        | 30%       | <b>5%</b>  | 90 – 70     | 3           |            |                             |
| N° 8     | 75%        | 20%       | <b>5%</b>  | 90 – 80     | 3           |            |                             |
| N° 9     | 50%        | 35%       | <b>15%</b> | 60 – 40     | 5           |            |                             |
| N° 10    | 55%        | 35%       | <b>10%</b> | 80 – 50     | 6           |            |                             |

*Table 6.3 Chemical solutions used for electropolishing of pure Titanium with stable conditions.*

Table 6.3 shows the chemical compositions of a group of solutions containing  $CH_3COOH$ ,  $H_2SO_4$ , and  $HF$ . A first solution and its effects on Ti for electropolishing was studied by Guerin [114], who received a patent in 2003 for his invention. The solution is composed of the above-mentioned acids [88]. The present part of this work studies the effect of the different chemical composition of the electrolyte on the final electropolished surface of Ti. For these group of experiments, the current was kept in the range 3 to 6 A, using a voltage in the range 90 to 40 V depending on each solution and its composition; the other parameters used for electropolishing are specified in Table 6.3, which is an extract of the same table in section 4.

Table 6.4 shows the electropolishing effects on a surface of pure Ti, for solutions from 6 to 10. Electrolyte 7 and 9 effects, are evident from the corresponding micrographs in Table 6.4. For every magnification, the presence of a smoothing mechanism is quite evident, and the morphology of the treated surfaces are quite regular, of compared to the other ones. For solution n. 6, an irregular surface is evident, and the presence of pitting can be deduced from high magnification analysis Table 6.4 (figure c). In general, the compositions of these group of electrolytes, composed by hydrofluoric, sulfuric and acetic acids were very effective on the titanium surface in fact, it is well known that HF dissolves the formed oxide layer on the metal surface. Fluoride ions facilitate the attack of the passive layer [75], while sulfuric acid is responsible for the formation of the viscous layer, which is important to improve the electropolishing process [114]. Acetic acid has a low dissociation constant, leading to a better control of the electrochemical process [114]. It was found [115] that increasing the voltage during electropolishing of pure Ti caused the production of hydrogen, decreasing the voltage stability of the electrochemical cell.

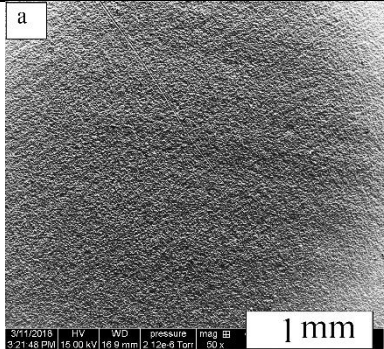
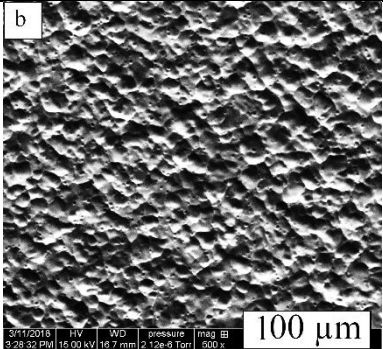
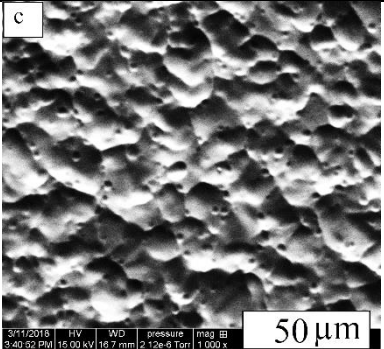
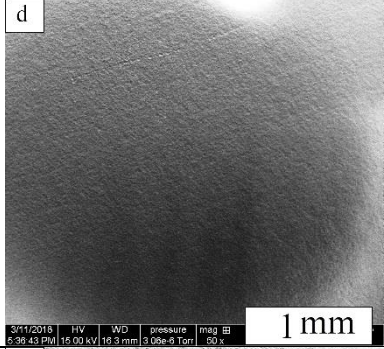
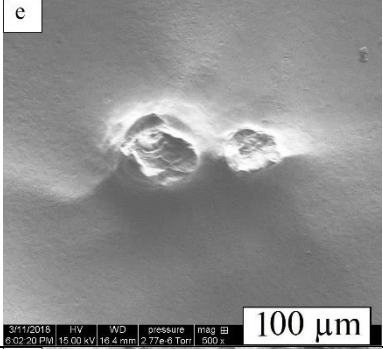
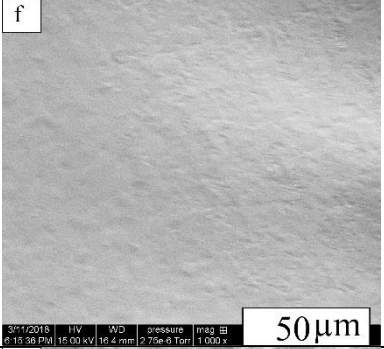
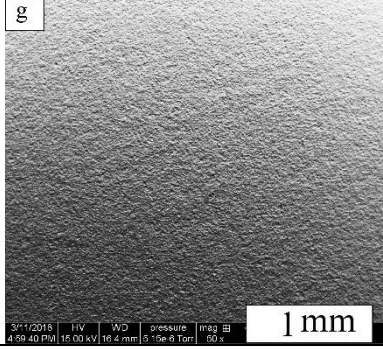
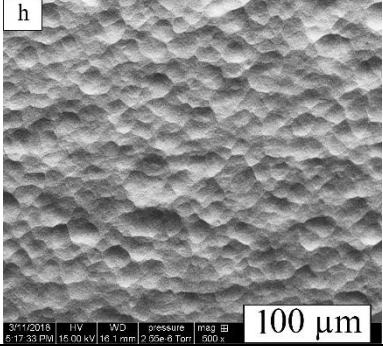
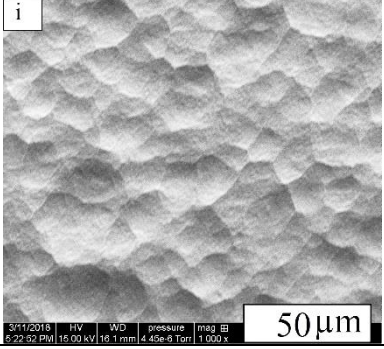
Rokicki [116] compared the chemical composition of the oxide layers between two samples, the first one after mechanical polishing and etched in HF and HNO<sub>3</sub> aqueous solution, and the second one electropolished in the same pure acids. It was found the etched sample had an oxide layer contained mostly Ti<sub>2</sub>O<sub>3</sub>, which did not show any protective properties. On the other hand, the oxide layer of the electropolished sample was mainly composed by TiO<sub>2</sub>, which is known to be stable and to enhance the corrosion resistance of the Titanium [23].

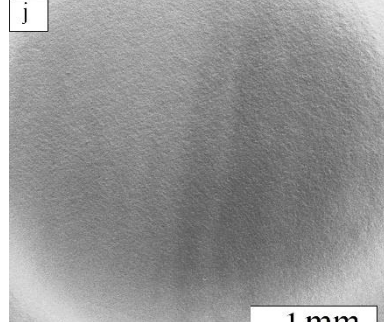
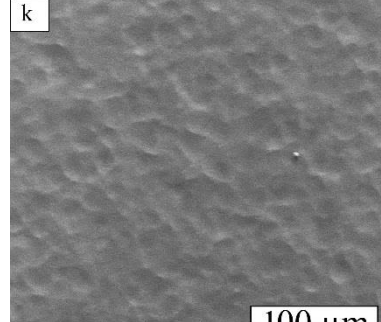
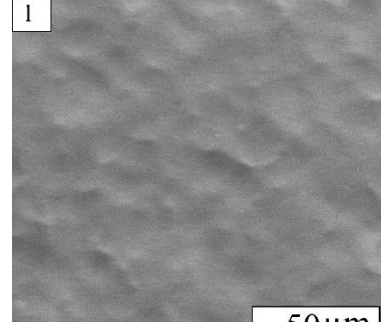
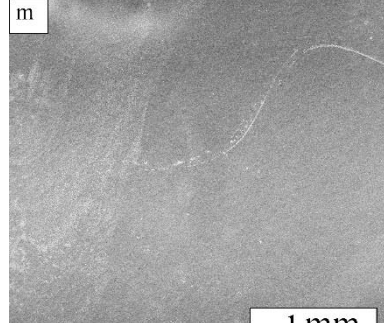
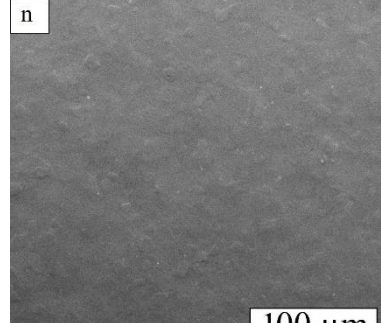
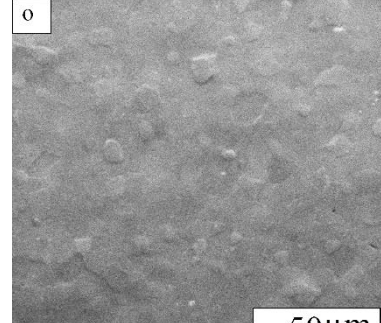
As in this study mechanical polishing was used to prepare the surface, some studies [117] concluded that mechanical polishing is not recommended for titanium alloys used in biomedical applications, due to the possible contamination that could be present on the modified surface, which could trigger phenomena of localized corrosion and uneven surface; this could affect deeply the functionality of the treated piece [117]. On the other hand, other authors suggest to perform both mechanical polishing and electropolishing in order to improve surface quality and to finally obtain a better surface finishing [116].

The effects of solution n. 10 were also studied, in a similar way as for the other electrolytes, the effects are shown in Table 6.4 (figure m) to Table 6.4 (figure o). For the electropolished samples, the surface is quite homogeneous, in Table 6.4 (figure m) (50x magnification) some halos are present; they could be attributed to the dying process, which is not homogeneous

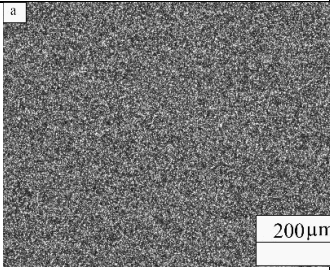
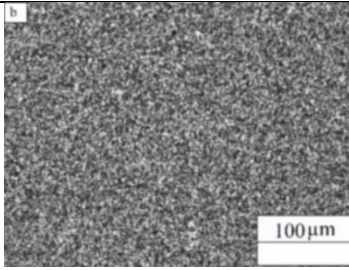
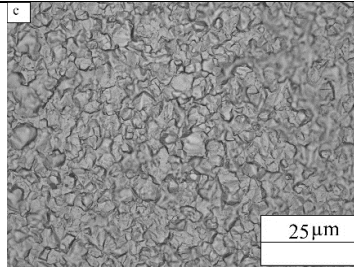
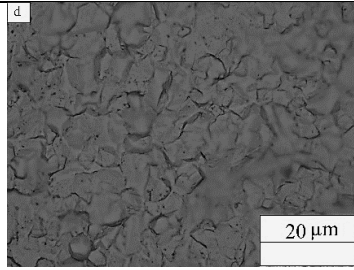
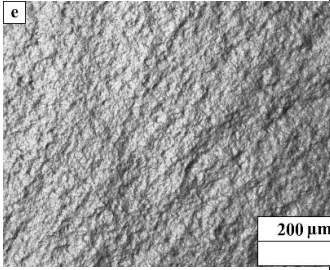
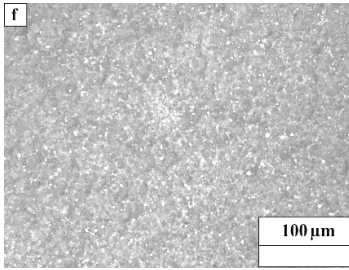
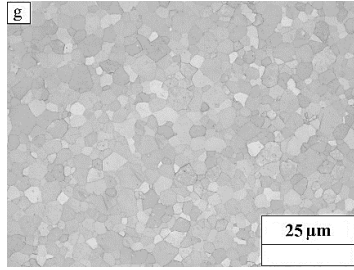
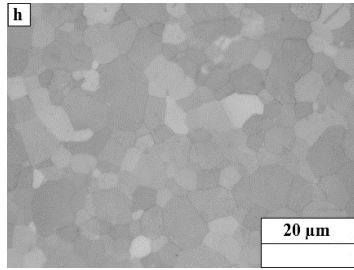
all over the surface. Table 6.4 (figure n) and Table 6.4 (figure o), respectively corresponding to 500x and 1000x magnification, highlight the grain structure of the material; this means that the electrolyte etches with different corrosion rates different grains, and the process is more efficient for some crystallographic orientations. The process is carried out not in optimal conditions.

Table 6.5 shows optical micrographs of a sample before and after electropolishing: the as-received samples are characterized by a rough and irregular surface, while the electropolished ones have a homogeneous, clean, featureless surface, with no pitting. Table 6.6 presents the same study but carried out by SEM.

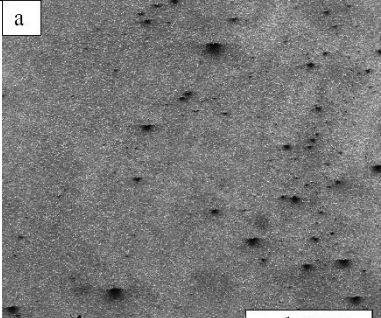
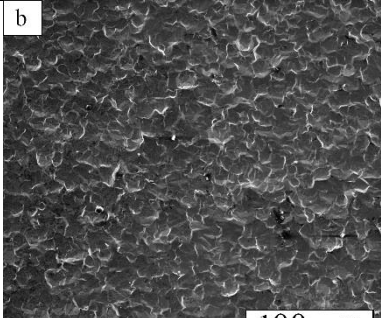
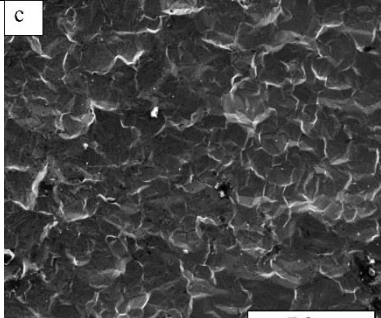
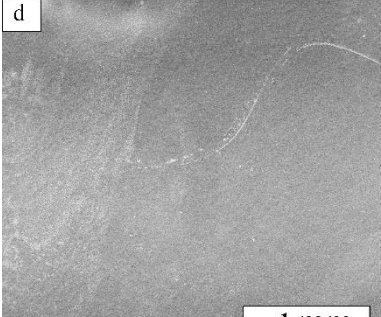
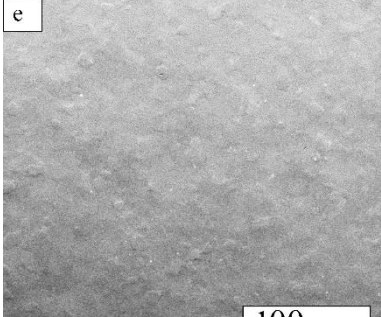
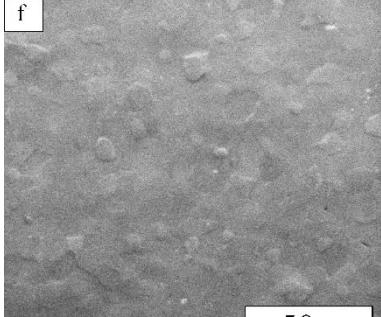
| <i>Solution</i> | <i>50 X</i>   | <i>500 X</i>  | <i>1000 X</i>   |
|-----------------|---|---|---|
| <b>N° 6</b>     |  <p>3/11/2018 HV WD pressure mag 3:21:48 PM 15.00 kV 16.9 mm 2.12e-6 Torr 50 x 1 mm</p>  |  <p>3/11/2018 HV WD pressure mag 3:28:32 PM 15.00 kV 16.7 mm 2.12e-6 Torr 500 x 100 μm</p>  |  <p>3/11/2018 HV WD pressure mag 3:40:52 PM 15.00 kV 16.7 mm 2.12e-6 Torr 1 000 x 50 μm</p>  |
| <b>N° 7</b>     |  <p>3/11/2018 HV WD pressure mag 5:38:43 PM 15.00 kV 16.3 mm 3.00e-6 Torr 50 x 1 mm</p>  |  <p>3/11/2018 HV WD pressure mag 6:02:20 PM 15.00 kV 16.4 mm 2.77e-6 Torr 500 x 100 μm</p>  |  <p>3/11/2018 HV WD pressure mag 6:16:38 PM 15.00 kV 16.4 mm 2.70e-6 Torr 1 000 x 50 μm</p>  |
| <b>N° 8</b>     |  <p>3/11/2018 HV WD pressure mag 4:58:40 PM 15.00 kV 16.4 mm 2.15e-6 Torr 50 x 1 mm</p> |  <p>3/11/2018 HV WD pressure mag 5:17:33 PM 15.00 kV 16.1 mm 2.95e-6 Torr 500 x 100 μm</p> |  <p>3/11/2018 HV WD pressure mag 5:22:52 PM 15.00 kV 16.1 mm 4.45e-6 Torr 1 000 x 50 μm</p> |

|   |  |  |  |
|---|--|--|--|
| <p>N° 9</p>   | <p>j</p>  <p>1 mm</p> <p>3/11/2018 HV 15.00 kV WD 16.3 mm pressure 3.05e-6 Torr mag 60 x</p>  | <p>k</p>  <p>100 μm</p> <p>3/11/2018 HV 15.00 kV WD 16.3 mm pressure 3.00e-6 Torr mag 500 x</p>  | <p>l</p>  <p>50 μm</p> <p>3/11/2018 HV 15.00 kV WD 16.3 mm pressure 2.56e-6 Torr mag 1.000 x</p>  |
| <p>N° 10</p>  | <p>m</p>  <p>1 mm</p> <p>10/17/2017 HV 15.00 kV WD 19.9 mm pressure 2.19e-6 Torr mag 60 x</p> | <p>n</p>  <p>100 μm</p> <p>10/17/2017 HV 15.00 kV WD 19.9 mm pressure 3.35e-6 Torr mag 500 x</p> | <p>o</p>  <p>50 μm</p> <p>10/17/2017 HV 15.00 kV WD 19.9 mm pressure 3.08e-6 Torr mag 1.000 x</p> |
| <p><i>Table 6.4 ES by SEM using different acid addition and solution for the electropolishing of pure Titanium.</i></p> |  |  |  |



| Pure Ti                 | 50 X  | 100 X  | 500 X   | 1000 X  |
|-------------------------|---|--|---|---|
| As received             |  |  |  |  |
| After EP Solution N° 10 |  |  |  |  |

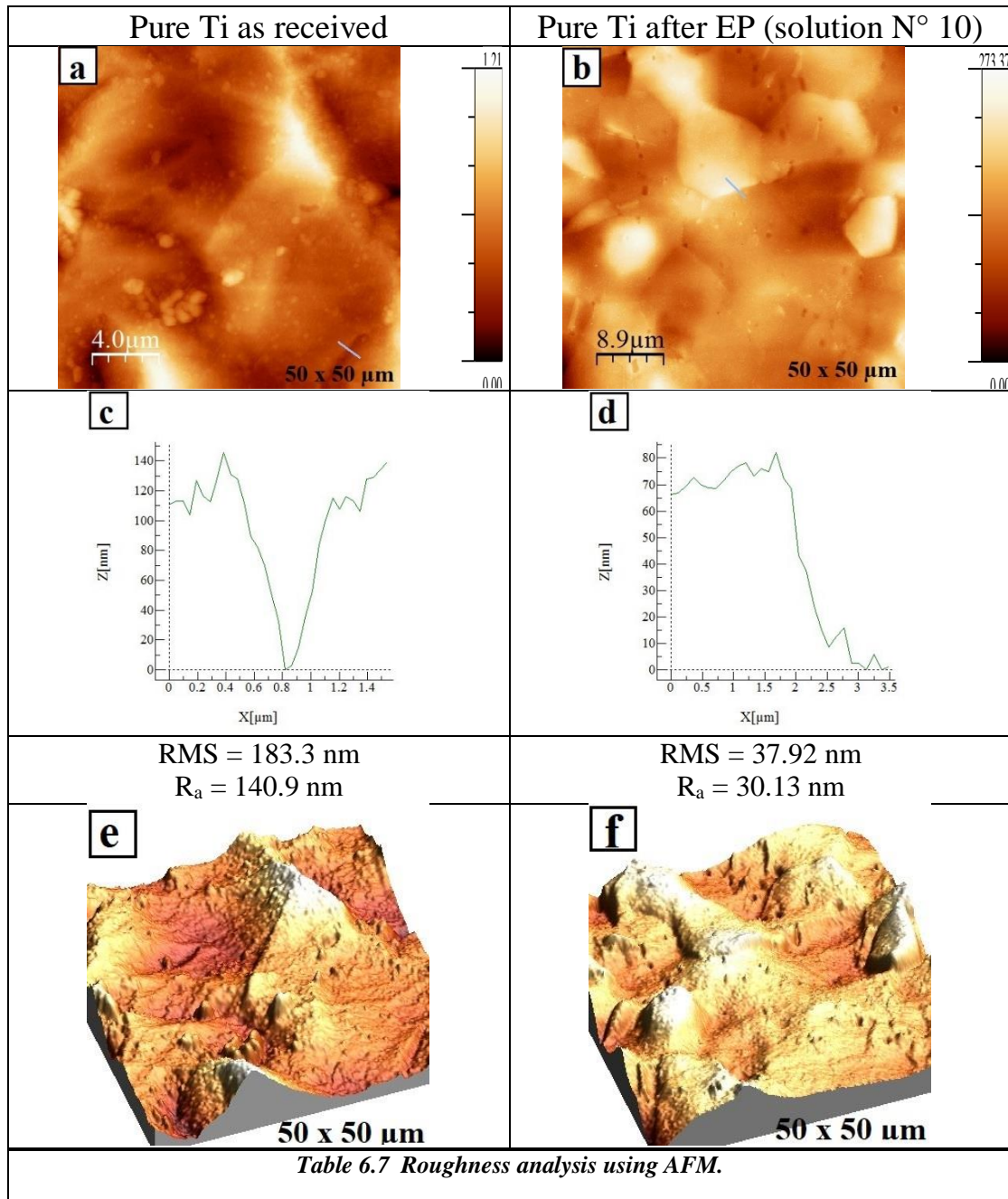
*Table 6.5 Optical microscopy (a-d) as received sample, (e-h) sample after electropolishing using solution N° 10.*

| Pure Ti                 | 50 X   | 500 X  | 1000 X   |
|-------------------------|--|--|--|
| As received             |  <p>10/17/2017 HV WD pressure mag 11:55:27 AM 10.00 kV 20.2 mm 1.18e-6 Torr 50 x 1 mm</p> |  <p>10/17/2017 HV WD pressure mag 12:17:26 PM 10.00 kV 19.9 mm 5.20e-6 Torr 500 x 100 μm</p> |  <p>10/17/2017 HV WD pressure mag 12:45:12 PM 10.00 kV 19.9 mm 4.73e-6 Torr 1,000 x 50 μm</p> |
| After EP Solution N° 10 |  <p>10/17/2017 HV WD pressure mag 1:52:48 PM 15.00 kV 19.9 mm 2.19e-6 Torr 50 x 1 mm</p>  |  <p>10/17/2017 HV WD pressure mag 3:08:18 PM 15.00 kV 19.9 mm 3.33e-6 Torr 500 x 100 μm</p>  |  <p>10/17/2017 HV WD pressure mag 3:28:03 PM 15.00 kV 19.9 mm 3.06e-6 Torr 1,000 x 50 μm</p>  |

*Table 6.6 ES by SEM (a-c) as received sample, (d-f) samples after electropolishing using solution N° 10.*

## 6.4 Roughness analysis by AFM.

According to AFM observation results, the average roughness of the electropolished pure titanium is lower than that one found in the as-received condition. The surfaces represented in the AFM pictures, respectively Table 6.7 (figure a and b), shows the two topographies for respectively an as-received samples and for an electropolished one.



| <b>size<br/>50 x 50<br/>mm<sup>2</sup></b>  | <b>average</b> | <b>standard<br/>deviation</b> |
|---|----------------|-------------------------------|
| <i>As- rec,<br/>RMS</i>   | 693            | 388                           |
| <i>As-rec, R<sub>a</sub></i>  | 556            | 320                           |
| <i>EP, RMS</i>  | 53             | 29                            |
| <i>EP, R<sub>a</sub></i>  | 41             | 23                            |
| <i>Table 6.8 Roughness for different<br/>samples before and after<br/>electropolishing.</i> |                |                               |

The two images represent an image of 50 μm x 50 μm. The roughness range for Table 6.7 (figure a) is 0 -121 nm, while for Table 6.7 (figure b) is 0 -237. Grains are evidenced by the EP treatment of the material, so that even if the average roughness is lowered compared to that one of the as-received condition, the presence of steps between a grain and the other shows the absence of some profile details of the above-mentioned figures are respectively shown in Table 6.7 (figure c and d). A tridimensional rendering of the above-mentioned images is presented respectively in Table 6.7 (figure e and f). Root mean squared roughness (RMS or R<sub>q</sub>) and R<sub>a</sub>, the arithmetic average roughness, are the chosen values for the characterization of the surface features. They are respectively described by the following formulas:

$$R_a = \frac{1}{n} \sum_{i=1}^n |y_i| \quad \text{Equation [6.1]}$$

where  $n$  = number of points whose height is measured, and  $y_i$  = height of the  $i$ -th point.

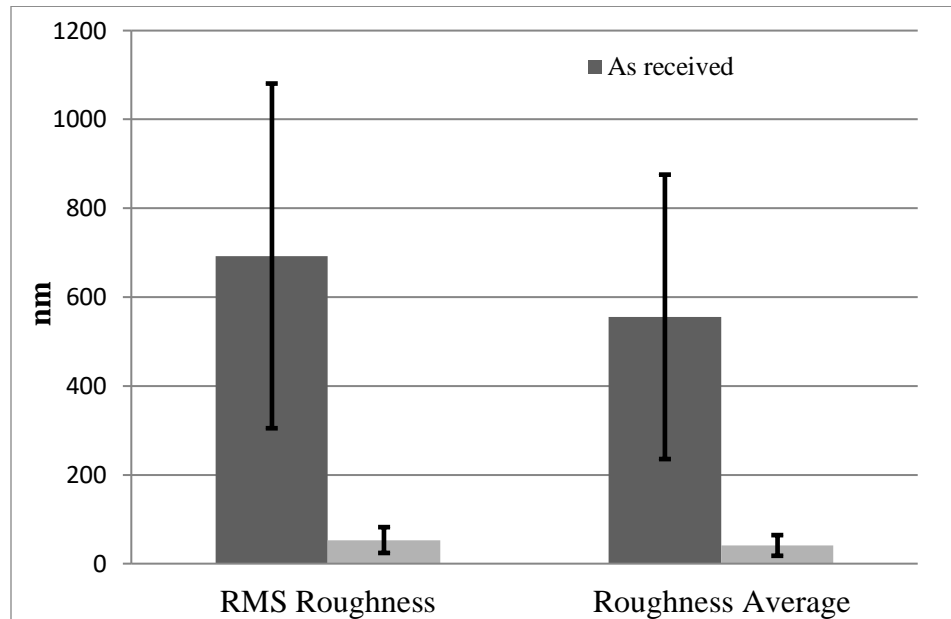
$$R_q = RMS = \sqrt{\frac{1}{n} \sum_{i=1}^n y_i^2} \quad \text{Equation [6.2]}$$

where  $n$  = number of points whose height is measured, and  $y_i$  = height of the  $i$ -th point.

Roughness values are summarized in Table 6.8 RMS for the as-rec sample is 693 ± 388 nm, while R<sub>a</sub> for the same sample is 556 ± 320 nm; for the EP sample, RMS is 53 ± 29 nm, while R<sub>a</sub> is 41 ± 23 nm, in spite of the different etching rates for different grain orientations.

## 6.5 Surface wettability.

In addition to the other surface properties, surface wettability is an important factor for the biomaterial, as in general the hydrophilic materials are biocompatible. This affects the protein absorbance, cell responses and cytocompatibility [118]. Some cells such as epithelial and fibroblasts are able to easily proliferate on smoother surfaces than rougher ones [119].



*Figure 6.1.roughness analysis for as-received and electropolished pure Ti samples.*

Many studies indicated that surface wettability and hydrophilicity are related and depended on the surface roughness. Kubiak et al [118] concluded during their experience on stainless steel that surface roughness has big influence on the wetting properties of the materials. He found that the contact angle decreases in a material with smaller roughness limit. On the other hand, the contact angle is larger for materials with the highest roughness area. Chemical composition and roughness can contribute to the surface energy of the material; the increase of surface roughness does not correspond to a linear increase of the surface energy. Different kinds of roughness (macro-, micro- and nano-roughness) has different effects on surface energy.


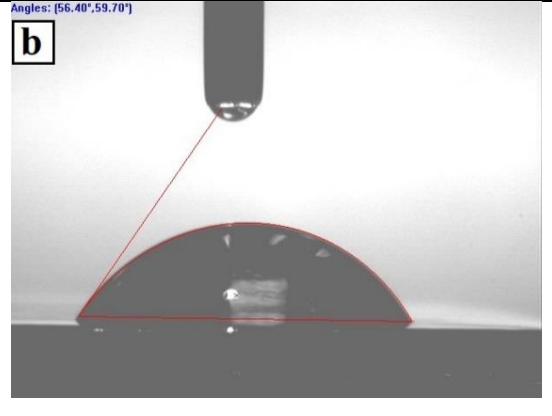
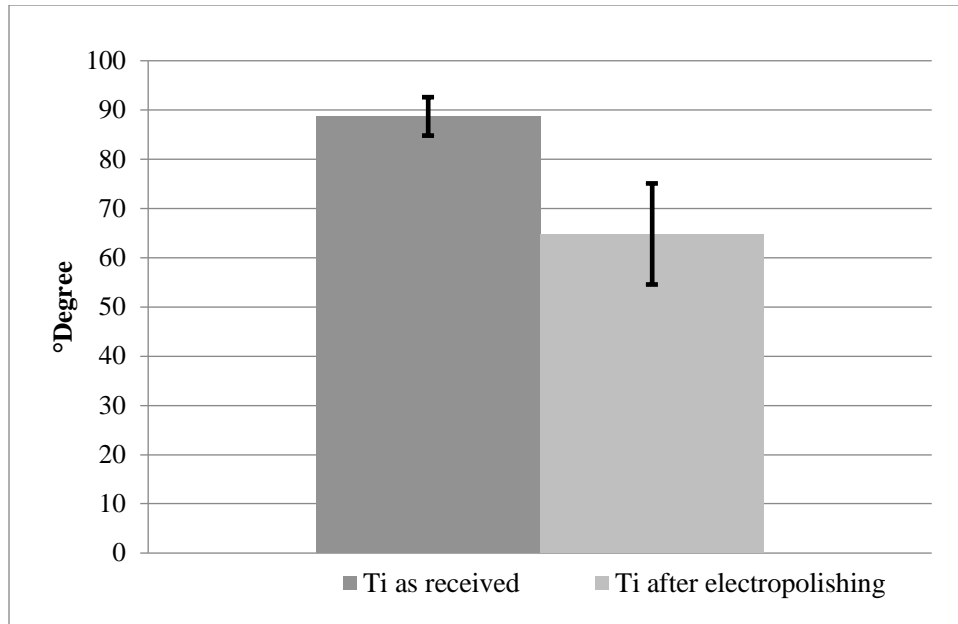
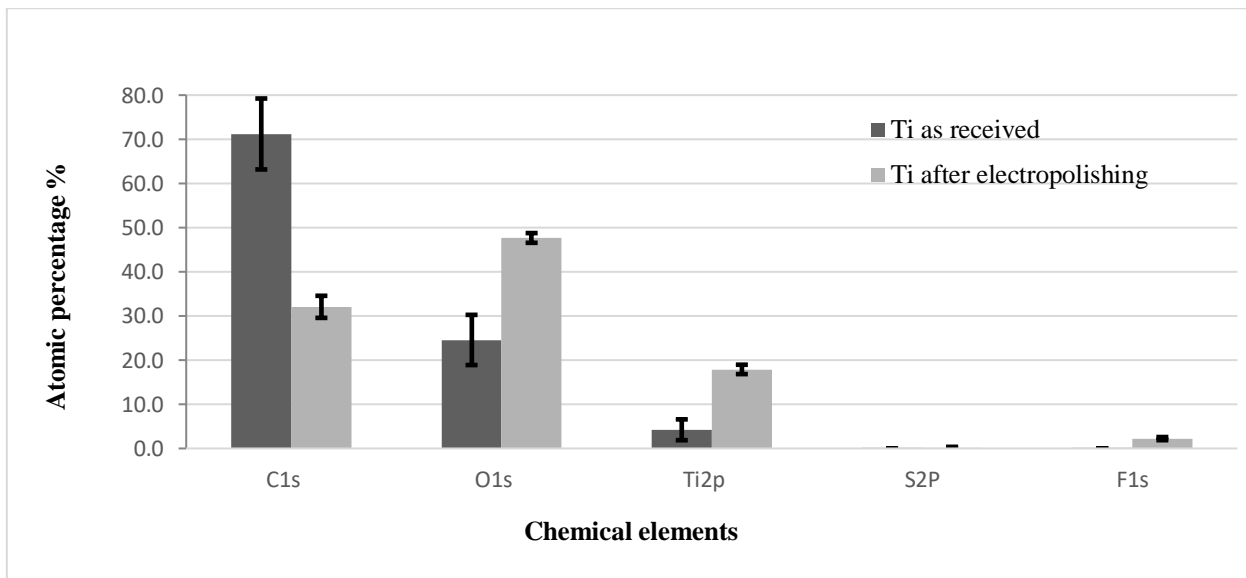
|   |  |
|---|--|
|  |  |
| Pure Ti as received   | Pure Ti after EP (solution N° 10)  |
| <i>Table 6.9 water contact angle before and after electropolishing.</i>           |  |

Figure 6.1 and Figure 6.2 confirm the conclusion of Kubiak et al [118]. As received samples showed higher roughness and a contact angle value in the range  $82^{\circ} - 92^{\circ}$ . The electropolishing process was responsible for a smaller contact angle and become more hydrophilic, corresponding to a lower surface roughness. The hydrophilicity is related also with the surface energy which controls the liquid absorbability on the surface, and the rate of bacterial adhesion on the material [120]. Generally, the contact angle range related to the spreading of drops on the material surface increases with higher roughness surfaces [121]. Kilpadi and coworkers [119] studied the effect of pure Titanium passivation and its effects on surface energy. Titanium surfaces with higher roughness show a greater contact angle (lower wettability) than a surface with lower roughness. Babilas and coworkers [122] found that the anodic dissolution of Ti-15Mo alloy, that is the application of an electropolishing process to this alloy, increases the wettability of its surface. He compared the effect of using two different voltage treatments; using a high voltage of 80 V the surface presented the lowest value of contact angle of  $85.4^{\circ}$ . For another treatment performed at 60 V, the sample increased the contact angle value up to  $97.5^{\circ}$ . Lower contact angles for pure titanium were obtained after passivation in nitric acid; for this reason, it was possible to conclude that the surface wettability is not related just with the topography and morphology of surface, but it is connected to its chemical composition.



*Figure 6.2 Average contact angle for as received and electropolished Ti.*

## 6.6 Chemical composition of the surface by XPS.



*Figure 6.3 Chemical composition of the surface before and after electropolishing.*

After electropolishing, the metallic dissolution processes taking place at the anode can remove the outer layer of the metal; all the surface modification of the material, for example,

created during mechanical polishing, are affected and finally a new surface is created. Electropolishing will create a new layer of titanium oxide on the material surface, with new surface properties that will be different from the core of the metal. This surface structure and composition affect the electrochemical activity, by sometimes reducing the corrosion resistance of the metal [115].

In the other hand, creating this new oxide layer will enhance the corrosion resistance, and increase the percentage of bonded oxygen on the surface, and decreasing the presence of carbon, as shown by the results of XPS surveys in Figure 6.3

## 6.7 Conclusions

- Sulfuric, hydrofluoric, perchloric, nitric, and acetic acid are the main acids used in electrolytes for Ti electropolishing. Several solutions were investigated and adapted to the laboratory setup, to study the effect of the chemical composition on the material. Our study was mainly focused on the effect of different HF concentrations on the surface properties of pure titanium, and it was demonstrated that using 10 vol. % of HF improved the topography and homogeneity of pure titanium.
- The electrolytic solution composed of  $\text{H}_3\text{COOH}$ ,  $\text{H}_2\text{SO}_4$  and HF provided a satisfying result in terms of roughness and surface morphology of pure titanium.
- The presence of hydrofluoric acid decreases the pitting, making the surface more homogenous, and creating an oxide layer of  $\text{TiO}_2$  that enhance the corrosion resistance of pure Titanium. The enhancement of corrosion resistance was related to the smoothing effect of the solution and to the newly formed oxide layer.
- The electropolishing decreases the roughness of the sample at about ~ 50 nm, against a roughness of around ~ 600 nm for the as-received material.
- The electropolishing process makes the sample more hydrophilic, by decreasing the water contact angle from ~90° to around ~65°.
- The electropolishing was responsible for changing the chemical composition of the surface, by decreasing the quantity of carbon and increasing the oxygen, probably bonded to Ti because of the oxide formation; high-resolution studies are however required, to better understand the chemical nature of the surface.



## **General conclusions**

Stents are small metallic meshes that are implanted in narrowed blood vessels to restore blood flow and to avoid a heart attack or stroke.

Electropolishing is a pre-treatment step applied to stents, its control the chemical and the physical properties of the surface, by modifying the surface morphology, removing surface inhomogeneities, or previous processing residuals. At the end of electropolishing process, the metal would have a new homogeneous surface, covered with a uniform and amorphous oxide layer, generally with a very low roughness. Those news properties obtained by electropolishing, make the metals more compatible with the human body and its biologic liquids.

The electropolishing process is described by some parameters, for example, the current, the voltage, the composition of the electrolytic solutions and the temperature of the electrolyte. By controlling those parameters led to understand the condition of electropolishing, which it will reflect positively on the surface properties of the metal itself.

It was found that the lower bath temperature, decrease the electropolishing rate proportionally. Increasing electropolishing time would decrease surface roughness of metals, with an increase in the contact angle.

Different approaches have been evaluated to reduce the restenosis rate and thinning of stent strut was shown to be the most satisfactory method. To be able to reduce strut thickness, while maintaining the required longitudinal and the radial strength of a stent, new alloys with superior mechanical properties are needed such as cobalt-based alloys, stainless steel, or titanium and its alloys.

This research is aimed to study the influence of different electropolishing parameters on the final features of a Co-Cr alloy and on pure Titanium.

The current study and experiences were engaged to investigate the acid concentration (which affect strongly the surface finish), and the effect of different strong acidic addition on the electrolytic bath and the surface characteristics and biocompatibility of electropolished Co-Cr alloy, and pure titanium alloy.

The mains result that was concluded in this research:

- Sulfuric, hydrofluoric, phosphoric, are the main acids used in electrolytes for cobalt-based alloys (L605) electropolishing, while the mains acids used for electrolytes of pure Titanium electropolishing were sulfuric, hydrofluoric, perchloric, nitric, and acetic acid.
- Controlled electropolishing was found at a lower quantity of hydrofluoric acid for Co-Cr alloy (3%), and a higher one for pure Titanium alloy (10%), depending on each structure of metals.
- The presence of hydrofluoric acid decreases the pitting, making the surface more homogenous, for both alloy (cobalt-based alloys (L605), and pure Titanium).
- In general, the electropolishing decreases the roughness of the sample at about ~ 30 nm, for L605 and about ~ 50 nm for pure Titanium alloy.
- The electropolishing was responsible for changing the chemical composition of the surface in both alloys, by decreasing the quantity of carbon and increasing the oxygen.

## Bibliography:

- [1] “Cardiovascular diseases (CVDs),” *World Health Organization*, 2015. [Online]. Available: <http://www.who.int/mediacentre/factsheets/fs317/en/>.
- [2] “Atherosclerosis,” *American Heart Association*, 2018. [Online]. Available: [https://watchlearnlive.heart.org/CVML\\_Player.php?moduleSelect=athero](https://watchlearnlive.heart.org/CVML_Player.php?moduleSelect=athero).
- [3] J. Berry and L. Adam, “what is plasma,” *University of Rochester*, 2016. [Online]. Available: <https://www.urmc.rochester.edu/encyclopedia/content.aspx?ContentTypeID=160&ContentID=37>.
- [4] T. Taylor, “Cardiovascular system,” *Innerbody.*, 1999. [Online]. Available: <http://www.innerbody.com/image/cardov.html>.
- [5] E. Michel, “Recouvrement à base de dextrane pour applications médicales.” Université Laval \_ Université Paris XIII, 2016.
- [6] “Structure of arteries veins and capillaries.” 2006. [Online]. Available: <https://www.purposegames.com/game/structure-of-arteries-veins-and-capillaries>.
- [7] Cardiovascular Center University of Michigan., “Heart surgery information For patients and their families,” Michigan, 2015.
- [8] I. B. Wilkinson and C. M. McEniery, “Arteriosclerosis: Inevitable or self-inflicted?,” *Hypertension*, vol. 60, no. 1, pp. 3–5, 2012.
- [9] A. Manuscript, W. Blood, and C. Count, “Novel mediators and biomarkers of thrombosis.” *Natl. institutes Heal.*, vol. 49, no. 18, pp. 1841–1850, 2009.
- [10] G. Piazza, B. Hohlfelder, and S. Z. Goldhaber, *Handbook for venous thromboembolism*. 2015.
- [11] W. Geerts, “Central venous catheter-related thrombosis,” *Hematology*, vol. 2014, no. 1, pp. 306–311, 2014.
- [12] G. A. Mackay, Judith, Mensah, “Types of cardiovascular diseases,” *Atlas Hear. Dis. Stroke*, pp. 18–19, 2004.
- [13] “Understanding cardiovascular diseases,” *Open education*, 2016. [Online]. Available: <http://www.open.edu/openlearn/ocw/mod/oucontent/view.php?printable=1&id=2613>.
- [14] “Risk factors for heart disease.” 2016. [Online]. Available: <http://www.immilife.com/risk-factors-for-heart-disease.html>.
- [15] “Coronary angioplasty and stenting.” *Michigan Medicine*. [Online]. Available: <https://medicine.umich.edu/dept/cardiac-surgery/patient-information/adult-cardiac-surgery/adult-conditions-treatments/coronary-angioplasty-stenting>.
- [16] “Common heart disease drugs,” *Web MD*, 2005. [Online]. Available: <https://www.webmd.com/heart-disease/common-medicine-heart-disease-patients#1>.
- [17] J. Iqbal, J. Gunn, and P. W. Serruys, “Coronary stents: Historical development, current status and future directions,” *Br. Med. Bull.*, vol. 106, no. 1, pp. 193–211, 2013.
- [18] L. Bax, A. J. Woittiez, H. J. Kouwenberg, and E. Buskens, “Stent placement in patients with atherosclerotic renal artery stenosis and impaired renal function,” *Ann. Intern. Med.*, vol. 150, p. 12, 2009.
- [19] H. Hara, M. Nakamura, J. C. Palmaz, and R. S. Schwartz, “Role of stent design and coatings on

- restenosis and thrombosis,” *Adv. Drug Deliv. Rev.*, vol. 58, no. 3, pp. 377–386, 2006.
- [20] Central Georgia Vein Center, “What you need To know about a heart stent.,” 2017. [Online]. Available: <http://centralgaheart.com/need-know-heart-stent/>.
- [21] S. Deb, H. C. Wijeyesundera, D. T. Ko, H. Tsubota, S. Hill, and S. E. Fremes, “Coronary artery bypass graft surgery vs percutaneous interventions in coronary revascularization: A systematic review,” *JAMA - J. Am. Med. Assoc.*, vol. 310, no. 19, pp. 2086–2095, 2013.
- [22] “Coronary artery bypass graft surgery,” *johns Hopkins medicineopkins medicine*, 2014. [Online]. Available: [https://www.hopkinsmedicine.org/healthlibrary/test\\_procedures/cardiovascular/coronary\\_artery\\_bypass\\_graft\\_surgery\\_92,P07967](https://www.hopkinsmedicine.org/healthlibrary/test_procedures/cardiovascular/coronary_artery_bypass_graft_surgery_92,P07967).
- [23] W. Simka *et al.*, “Electrochemical polishing of Ti-13Nb-13Zr alloy,” *Surf. Coatings Technol.*, vol. 213, pp. 239–246, 2012.
- [24] C. Brozek *et al.*, “A  $\beta$ -titanium alloy with extra high strain-hardening rate: Design and mechanical properties,” *Scr. Mater.*, vol. 114, pp. 60–64, 2016.
- [25] A. R. Chatterjee and C. P. Derdeyn, “Stenting in Intracranial Stenosis: Current Controversies and Future Directions,” *Curr. Atheroscler. Rep.*, vol. 17, no. 8, 2015.
- [26] R. Reejsinghani and A. S. Lotfi, “Prevention of stent thrombosis: Challenges and solutions,” *Vasc. Health Risk Manag.*, vol. 11, pp. 93–106, 2015.
- [27] T. Hanawa, “Materials for metallic stents,” *J. Artif. Organs*, vol. 12, no. 2, pp. 73–79, 2009.
- [28] G. Mani, M. D. Feldman, D. Patel, and C. M. Agrawal, “Coronary stents: A materials perspective,” *Biomaterials*, vol. 28, no. 9, pp. 1689–1710, 2007.
- [29] R. A. Schatz, “A view of vascular stents,” *Circulation*, vol. 79, no. 2, pp. 445–457, 1989.
- [30] J. Choi and N. S. Wang, “Metals for Biomedical Applications,” *Biomed. Eng. – From Theory to Appl.*, pp. 411–430, 2011.
- [31] F. City, “Stent Tubing : Understanding the Desired Attributes,” *Mater. Inf. Soc.*, no. September, 2003.
- [32] W. P. T. Liberte *et al.*, “Intravascular Ultrasound Results From the NEVO ResElution-I Trial,” *ahajournals*, 2011.
- [33] L. Immunology and P. Catalogue, “Product Catalogue,” *Immunology*, pp. 1–23, 2009.
- [34] P. K. Bowen *et al.*, “Biodegradable Metals for Cardiovascular Stents: From Clinical Concerns to Recent Zn-Alloys,” *Adv. Healthc. Mater.*, vol. 5, no. 10, pp. 1121–1140, 2016.
- [35] J. Shabto, “Bioabsorbable Coronary Stents,” *Dartmouth Undergrad. J. Sci.*, pp. 14–16, 1977.
- [36] I. P. Prevention, C. R. Document, and B. A. Techniques, “Surface Treatment of Metals and Plastics,” *Animals*, no. August, 2006.
- [37] M. Kulkarni, A. Mazare, P. Schmuki, and A. Igljč, “Biomaterial surface modification of titanium and titanium alloys for medical applications,” *Nanomedicine*, pp. 111–136, 2014.
- [38] A. J. García, “Surface Modification of Biomaterials,” *Princ. Regen. Med.*, pp. 663–673, 2011.
- [39] M. Moravej and D. Mantovani, “Biodegradable metals for cardiovascular stent application: Interests and new opportunities,” *Int. J. Mol. Sci.*, vol. 12, no. 7, pp. 4250–4270, 2011.
- [40] H. Hermawan, “Conception, développement et validation d’alliages métalliques dégradables utilisés en chirurgie endovasculaire.,” Université Laval, 2009.

- [41] M. Peuster *et al.*, “A novel approach to temporary stenting: degradable cardiovascular stents produced from corrodible metal—results 6-18 months after implantation into New Zealand white rabbits.,” *Heart*, vol. 86, no. 5, pp. 563–569, 2001.
- [42] M. Moravej, “Développement et validation des matériaux métalliques pour stents cardiovasculaires biodégradables par dépôt électrolytique.,” Université Laval, 2011.
- [43] J. Han *et al.*, “Superplasticity in a lean Fe-Mn-Al steel,” *Nat. Commun.*, pp. 8–13, 2017.
- [44] P. Zartner, R. Cesnjevar, H. Singer, and M. Weyand, “First successful implantation of a biodegradable metal stent into the left pulmonary artery of a preterm baby,” *Catheter. Cardiovasc. Interv.*, vol. 66, no. 4, pp. 590–594, 2005.
- [45] Q. Chen and G. A. Thouas, “Metallic implant biomaterials,” *Mater. Sci. Eng. R Reports*, vol. 87, pp. 1–57, 2015.
- [46] G. K. Levy, J. Goldman, and E. Aghion, “The Prospects of Zinc as a Structural Material for Biodegradable Implants — A Review Paper,” *Metals (Basel)*, pp. 1–18, 2017.
- [47] J. H. Qiu, “Passivity and its breakdown on stainless steels and alloys,” *Surf. Interface Anal.*, vol. 33, no. 10–11, pp. 830–833, 2002.
- [48] T. Hanawa, “A comprehensive review of techniques for biofunctionalization of titanium,” *J. Periodontal Implant Sci.*, vol. 41, no. 6, pp. 263–272, 2011.
- [49] K. Otsuka and X. Ren, “Physical metallurgy of Ti-Ni-based shape memory alloys,” *Prog. Mater. Sci.*, vol. 50, no. 5, pp. 511–678, 2005.
- [50] D. Lawrence and L. Madamba, “The effect of surface treatment on nickel leaching from nitinol.,” San Jose State University, 2013.
- [51] Y. Zhou, M. Li, Y. Cheng, Y. F. Zheng, T. F. Xi, and S. C. Wei, “Tantalum coated NiTi alloy by PIIID for biomedical application,” *Surf. Coatings Technol.*, vol. 228, no. SUPPL.1, pp. 2–6, 2013.
- [52] A. Fattah-Alhosseini, F. R. Attarzadeh, S. Vafaeian, M. Haghshenas, and M. K. Keshavarz, “Electrochemical behavior assessment of tantalum in aqueous KOH solutions,” *Int. J. Refract. Met. Hard Mater.*, vol. 64, pp. 168–175, 2017.
- [53] V. 2 ASM International Handbook, “Properties and selection: Nonferrous alloys and special-purpose materials,” *ASM Met. Handb.*, vol. 2, p. 1300, 1990.
- [54] A. Marti, “Cobalt-base alloys used in bone surgery,” *Injury*, vol. 31, pp. D18–D21, 2000.
- [55] H. Aihara, “Surface and biocompatibility study of electropolished Co-Cr alloy L605,” San Jose State University, 2009.
- [56] M. Nishioka, Y. Yamabe, K. Hisatsune, and H. Fujii, “Influence of polishing of denture base resin and metal surfaces on wettability with water and saliva.,” *Dent. Mater. J.*, vol. 25, no. 1, pp. 161–5, 2006.
- [57] P. Poncin, C. Millet, J. Chevy, and J. Proft, “Comparing and optimizing Co-Cr tubing for stent applications,” *Mater Process. Med. Devices Conf.*, pp. 25–27, 2004.
- [58] M. Geetha, A. K. Singh, R. Asokamani, and A. K. Gogia, “Ti based biomaterials, the ultimate choice for orthopaedic implants - A review,” *Prog. Mater. Sci.*, vol. 54, no. 3, pp. 397–425, 2009.
- [59] S. Wernick and S. Wernick, “Electrolytic Polishing and Bright Plating of Metals,” p. 1960, 1960.
- [60] S. Wernick and S. Wernick, “Electrolytic Polishing and Bright Plating of Metals.,” *J. Electrodepositors’ Tech. Soc.*, vol. 9, pp. 139–153, 1934.
- [61] F. I. Metz, “Electropolishing of metals,” p. 170, 1960.

- [62] J. Swain, "The 'then and now' of electropolishing," *Surface World*. pp. 32–36, 2010.
- [63] E1558-09, "Standard guide for electrolytic polishing of metallographic specimens.," *ASTM Int.*, vol. 9, no. Reapproved 2014, pp. 1–13, 2009.
- [64] Hydraulic & Pneumatic., "Electropolishing for hydraulics & pneumatics." [Online]. Available: <http://www.ableelectropolishing.com/industry-solutions/hydraulic-pneumatic/>.
- [65] S. Trigwell and G. Selvaduray, "Effect of surface treatment on the surface characteristics of AISI 316L stainless steel," 2005.
- [66] R. Of and T. H. E. Fundamental, "The electrodeposition of precious Metals.," *Current*, vol. 18, pp. 829–834, 1973.
- [67] LaurensvanLieshout, "Electropolishing process," *wikipedia*. [Online]. Available: [https://upload.wikimedia.org/wikipedia/commons/2/24/Electropolishing\\_principle.png](https://upload.wikimedia.org/wikipedia/commons/2/24/Electropolishing_principle.png).
- [68] J. Toušek, "Electropolishing of metals in alcoholic solution of sulphuric acid," *Electrochim. Acta*, vol. 22, no. 1, pp. 47–50, 1977.
- [69] A. Chandra, M. Sumption, and G. S. Frankel, "On the mechanism of niobium electropolishing," *J. Electrochem. Soc.*, vol. 159, no. 11, pp. C485–C491, 2012.
- [70] G. Yang, B. Wang, K. Tawfiq, H. Wei, S. Zhou, and G. Chen, "Electropolishing of surfaces: theory and applications," *Surf. Eng.*, vol. 33, no. 2, pp. 149–166, 2017.
- [71] R. Kirchheim, K. Major, and G. Tiflg, "Diffusion and Solid-Film Formation during Electropolishing of Metals," *J. Electrochem. Soc.*, vol. 128, no. 5, pp. 1027–1034, 1981.
- [72] D. Kopeliovich, "Diffusion layer," *Subst. Technol.*
- [73] "Nernst diffusion layer," *Substech*. [Online]. Available: [http://www.substech.com/dokuwiki/lib/exe/fetch.php?cache=cache&media=diffusion\\_layer.png](http://www.substech.com/dokuwiki/lib/exe/fetch.php?cache=cache&media=diffusion_layer.png).
- [74] G. Yang, B. Wang, K. Tawfiq, H. Wei, S. Zhou, and G. Chen, "Electropolishing of surfaces: theory and applications," *Surf. Eng.*, 2017.
- [75] O. Piotrowski, "The Mechanism of Electropolishing of Titanium in Methanol-Sulfuric Acid Electrolytes," *J. Electrochem. Soc.*, vol. 145, no. 7, p. 2362, 1998.
- [76] Y. Fovet, J. Gal, and F. Toumelin-chemla, "Influence of pH and fluoride concentration on titanium passivating layer : stability of titanium dioxide," *Talanta*, vol. 53, pp. 1053–1063, 2001.
- [77] R. R. and K. R. Tadeusz Hryniewicz1, *Biomaterials Science and Engineering*. <http://creativecommons.org/licenses/by-nc-sa/3.0/>, 2011.
- [78] P. Related, "Theory of the oxidation of metals," 1949.
- [79] T. P. Hoar, D. C. Mears, and G. P. Rothwell, "The relationships between anodic passivity, brightening and pitting," *Corros. Sci.*, vol. 5, no. 4, pp. 279–289, 1965.
- [80] A. Dzyuba and L. D. Cooley, "Combined effects of cold work and chemical polishing on the absorption and release of hydrogen from SRF cavities inferred from resistance measurements of cavity-grade niobium bars," *Supercond. Sci. Technol.*, vol. 27, no. 3, 2014.
- [81] R. P. Frankenthal, "The effect of surface preparation and of deformation on the pitting and anodic dissolution of Fe-Cr alloys.," vol. 8, no. September 1967, 1968.
- [82] C. Madore and D. Landolt, "Electrochemical micromachining of controlled topographies on titanium for biological applications," *J. Micromechanics Microengineering*, vol. 7, no. 4, pp. 270–275, 1997.

- [83] Rolled alloys Canada, “L605.” [Online]. Available: <https://www.rolledalloys.ca/alloys/cobalt-alloys/l605/en/>.
- [84] Rolled alloys Canada, “CP titanium Grade 2.” [Online]. Available: <https://www.rolledalloys.ca/alloys/titanium-alloys/cp-3-gr-2/en/>.
- [85] “ELMA Elmasonic 1.5 Gal tabletop ultrasonic cleaner, P60H.” 2015. [Online]. Available: [https://www.sonicleaners.com/store/p104/ELMA\\_Elmasonic\\_1.5\\_Gal\\_Tabletop\\_Ultrasonic\\_Cleaner%2C\\_P60H.html](https://www.sonicleaners.com/store/p104/ELMA_Elmasonic_1.5_Gal_Tabletop_Ultrasonic_Cleaner%2C_P60H.html).
- [86] Adapted courtesy of Stephanie Colvey Photography, “Photos of Electropolishing system,” 2017. .
- [87] S. K. Sudheer, D. Kothwala, S. Prathibha, C. Engineer, A. Raval, and H. Kotadia, “Laser microfabrication of L605 cobalt-chromium cardiovascular stent implants with modulated pulsed Nd:YAG laser,” *J. Micro/Nanolithography, MEMS MOEMS*, vol. 7, no. 3, p. 33012, 2008.
- [88] A. Kuhn, “The electropolishing of titanium and its alloys,” *Met. Finish.*, vol. 102, no. 6, pp. 80–86, 2004.
- [89] Y. Leng., *Materials Characterization: Introduction to Microscopic and Spectroscopic Methods.*, Second Edi. Wiley-VCH Verlag GmbH & Co. KGaA., 2013.
- [90] E. S. Gadelmawla, M. M. Koura, T. M. A. Maksoud, I. M. Elewa, and H. H. Soliman, “Roughness parameters,” *J. Mater. Process. Technol.*, vol. 123, no. 1, pp. 133–145, 2002.
- [91] T. S. Meiron, A. Marmur, and I. S. Saguy, “Contact angle measurement on rough surfaces,” *J. Colloid Interface Sci.*, vol. 274, no. 2, pp. 637–644, 2004.
- [92] V. M. Desai, C. M. Rao, T. H. Kosel, and N. F. Fiore, “Effect of carbide size on the abrasion of cobalt-base powder metallurgy alloys,” *Wear*, vol. 94, no. 1, pp. 89–101, 1984.
- [93] Y. Chen *et al.*, “Effects of sigma phase and carbide on the wear behavior of CoCrMo alloys in Hanks’ solution,” *Wear*, vol. 310, no. 1–2, pp. 51–62, 2014.
- [94] Y. Bedolla-Gil and M. A. L. Hernandez-Rodriguez, “Tribological behavior of a heat-treated cobalt-based alloy,” *J. Mater. Eng. Perform.*, vol. 22, no. 2, pp. 541–547, 2013.
- [95] A. D. B. Gingell, H. K. D. H. Bhadeshia, D. G. Jones, and K. J. A. Mawella, “Carbide precipitation in some secondary hardened steels,” *J. Mater. Sci.*, vol. 32, no. 18, pp. 4815–4820, 1997.
- [96] J. B. Headridge and R. A. Chalmers, “The applications of hydrofluoric acid and fluorides in analytical chemistry,” *C R C Crit. Rev. Anal. Chem.*, vol. 2, no. 4, pp. 461–490, 1971.
- [97] D. Sazou, K. Michael, and M. Pagitsas, “Intrinsic coherence resonance in the chloride-induced temporal dynamics of the iron electrodisolution-passivation in sulfuric acid solutions,” *Electrochim. Acta*, vol. 119, pp. 175–183, 2014.
- [98] A. Trummal, L. Lipping, I. Kaljurand, I. A. Koppel, and I. Leito, “Acidity of Strong Acids in Water and Dimethyl Sulfoxide,” *J. Phys. Chem. A*, vol. 120, no. 20, pp. 3663–3669, 2016.
- [99] T. S. Hahn and A. R. Marder, “Effect of electropolishing variables on the current density-voltage relationship,” *Metallography*, vol. 21, no. 4, pp. 365–375, 1988.
- [100] P. Sojitra, C. Engineer, A. Raval, D. Kothwala, and A. Jariwala, “Surface Enhancement and Characterization of L-605 Cobalt Alloy Cardiovascular Stent by Novel Electrochemical Treatment,” *Biomaterials*, vol. 23, pp. 55–64, 2009.
- [101] A. Karaali, K. Mirouh, S. Hamamda, and P. Guiraldenq, “Microstructural study of tungsten influence on Co-Cr alloys,” *Mater. Sci. Eng. A*, vol. 390, no. 1–2, pp. 255–259, 2005.
- [102] Ş. Țălu, S. Stach, B. Klaić, T. Mišić, J. Malina, and A. Čelebić, “Morphology of Co-Cr-Mo dental alloy

- surfaces polished by three different mechanical procedures,” *Microsc. Res. Tech.*, vol. 78, no. 9, pp. 831–839, 2015.
- [103] A. P. Abbott, G. Capper, K. J. McKenzie, A. Glidle, and K. S. Ryder, “Electropolishing of stainless steels in a choline chloride based ionic liquid: an electrochemical study with surface characterisation using SEM and atomic force microscopy,” *Phys. Chem. Chem. Phys.*, vol. 8, no. 36, p. 4214, 2006.
- [104] “Electropolishing,” *Delstar metal finishing*. [Online]. Available: <https://www.delstar.com/electropolishing>.
- [105] C. Kaufmann, G. Mani, D. Marton, D. Johnson, and C. M. Agrawal, “Long-term stability of self-assembled monolayers on electropolished L605 cobalt chromium alloy for stent applications,” *J. Biomed. Mater. Res. - Part B Appl. Biomater.*, vol. 98 B, no. 2, pp. 280–289, 2011.
- [106] M. Haïdopoulos, S. Turgeon, C. Sarra-Bournet, G. Laroche, and D. Mantovani, “Development of an optimized electrochemical process for subsequent coating of 316 stainless steel for stent applications,” *J. Mater. Sci. Mater. Med.*, vol. 17, no. 7, pp. 647–657, 2006.
- [107] C. A. Huang, F. Y. Hsu, and C. H. Yu, “Electropolishing behavior of pure titanium in sulfuric acid-ethanol electrolytes with an addition of water,” *Corros. Sci.*, vol. 53, no. 2, pp. 589–596, 2011.
- [108] N.-S. Peighambaroust and F. Nasirpouri, “Electropolishing behaviour of pure titanium in perchloric acid–methanol–ethylene glycol mixed solution,” *Trans. IMF*, vol. 92, no. 3, pp. 132–139, 2014.
- [109] W. Wu, X. Liu, H. Han, D. Yang, and S. Lu, “Electropolishing of NiTi for improving biocompatibility,” *J. Mater. Sci. Technol.*, vol. 24, no. 6, pp. 926–930, 2008.
- [110] S. A. Shabalovskaya, G. C. Rondelli, A. L. Undisz, J. W. Anderegg, T. D. Burleigh, and M. E. Rettenmayr, “The electrochemical characteristics of native Nitinol surfaces,” *Biomaterials*, vol. 30, no. 22, pp. 3662–3671, 2009.
- [111] A. Teixeira, “Development of an Electropolishing Method for Titanium Materials,” Concordia University, 2011.
- [112] C. A. Huang, W. Lin, and S. C. Lin, “The electrochemical polishing behaviour of P/M high-speed steel (ASP 23) in perchloric-acetic mixed acids,” *Corros. Sci.*, vol. 45, no. 11, pp. 2627–2638, 2003.
- [113] D. Kim, K. Son, D. Sung, Y. Kim, and W. Chung, “Effect of added ethanol in ethylene glycol-NaCl electrolyte on titanium electropolishing,” *Corros. Sci.*, 2015.
- [114] S. Kong, F. Application, and P. Data, “( 12 ) United States Patent,” vol. 2, no. 12, pp. 12–15, 2011.
- [115] W. Simka, M. Kaczmarek, A. Baron-Wiecheć, G. Nawrat, J. Marciniak, and J. Zak, “Electropolishing and passivation of NiTi shape memory alloy,” *Electrochim. Acta*, vol. 55, no. 7, pp. 2437–2441, 2010.
- [116] R. Rokicki, W. Haider, and T. Hryniewicz, “Influence of sodium hypochlorite treatment of electropolished and magnetoelectropolished nitinol surfaces on adhesion and proliferation of MC3T3 pre-osteoblast cells,” *J. Mater. Sci. Mater. Med.*, vol. 23, no. 9, pp. 2127–2139, 2012.
- [117] K. Tajima, M. Hironaka, K.-K. Chen, Y. Nagamatsu, H. Kakigawa, and Y. Kozono, “Electropolishing of CP Titanium and Its Alloys in an Alcoholic Solution-based Electrolyte,” *Dent. Mater. J.*, vol. 27, no. 2, pp. 258–265, 2008.
- [118] K. J. Kubiak, M. C. T. Wilson, T. G. Mathia, and P. Carval, “Wettability versus roughness of engineering surfaces,” *Wear*, vol. 271, no. 3–4, pp. 523–528, 2011.
- [119] D. V. Kilpadi, J. J. Weimer, and J. E. Lemons, “Effect of and dry heat-sterilization on surface energy and topography of unalloyed titanium implants,” *Colloids Surfaces A Physicochem. Eng. Asp.*, vol. 135, no. 1–3, pp. 89–101, 1998.



- [120] M. A. Shafique, R. Ahmad, and I. U. Rehman, "Study of wettability and cell viability of H implanted stainless steel," *Mater. Res. Express.*, 2018.
- [121] K. J. Kubiak and T. G. Mathia, "Influence of roughness on contact interface in fretting under dry and boundary lubricated sliding regimes," *Wear*, vol. 267, no. 1–4, pp. 315–321, 2009.
- [122] D. Babilas *et al.*, "On the electropolishing and anodic oxidation of Ti-15Mo alloy," *Electrochim. Acta*, vol. 205, pp. 256–265, 2016.